Rao Arsalan Khushnood

High Performance Self Compacting Cementitious Materials Using Carbonaceous Nano/Micro Inerts

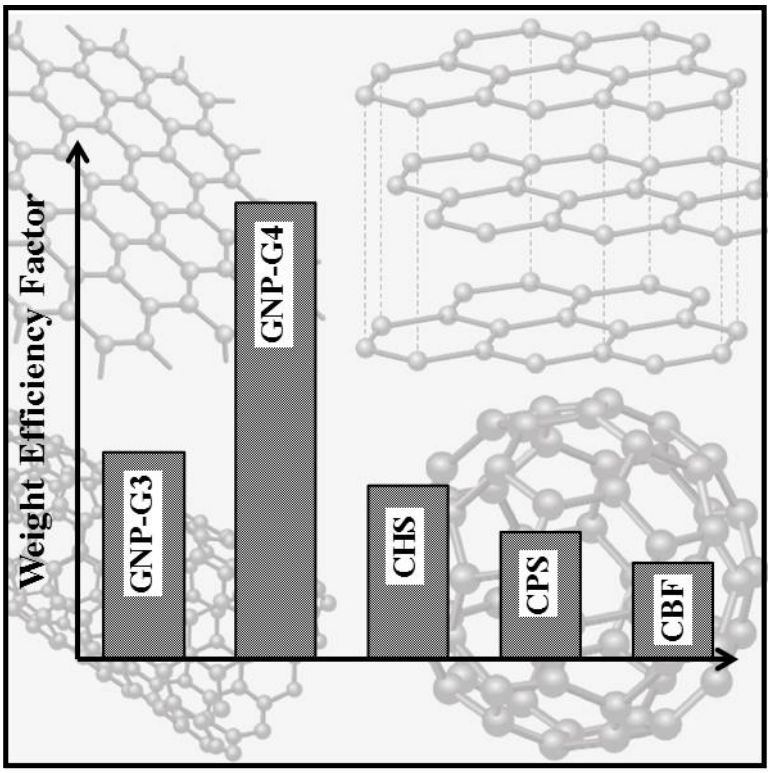

Dottorato di Ricerca in Ingegneria delle Strutture
Politecnico di Torino

Rao Arsalan Khushnood

High Performance Self-Compacting Cementitious Materials Using Nano/Micro Carbonaceous Inerts

Tesi per il conseguimento del titolo di Dottore di Ricerca
XXVII Ciclo (2012 - 2013 - 2014)

Dottorato di Ricerca in Ingegneria delle Strutture
Politecnico di Torino

Dicembre 2014

Dottorato di Ricerca in Ingegneria delle Strutture
Politecnico di Torino, Corso Duca degli Abruzzi 24, 10129 Torino, Italy

Tutori: Prof. Giuseppe Andrea Ferro, Prof. Jean-Marc Tulliani

Coordinatore: Prof. Alberto Carpinteri

Dedicated
To my parents
and my homeland

Acknowledgements

I am grateful to Almighty Allah, the most beneficent, the most merciful, whose blessings gave me the strength and courage to complete this research work.

I express my gratitude and sincere thanks to Professor Giuseppe Andrea Ferro (Department of Structural, Geotechnical and Building Engineering - DISEG) and Associate Professor Jean-Marc Tulliani (Department of Applied Science and Technology - DISAT) for graciously providing me their kind encouragement, untiring guidance and able supervision throughout the research work reported in the thesis.

I am pleased to thank Associate Prof. Matteo Pavese (DISAT, Politecnico di Torino) for providing me with the graphene nano platelets and for his continuous guidance in exploring the most suitable dispersion scheme. I am grateful to Dr. Pravin Jagadale (DISAT, Politecnico di Torino) for his constant support and guidance concerning synthesis and characterization of the nano/micro carbonized inerts. I would like to pay my gratitude to Assoc. Prof. Patrizia Savi (Department of Electronics and Telecommunication – DET, Politecnico di Torino) for her guidance and help in the analysis of electrical properties of cement composites. I would also like to thank all the laboratory staff, especially Marco Costanzo Alessio and Pietro Paolo Provenzano of DISEG, for their help and cooperation in the laborious testing. I would also like to thanks Dr. Guastella Salvatore (DISAT) for FESEM and EDX analysis and Dr. Mauro Giorcelli (DISAT) for Raman analysis of the carbonized inerts.

I also offer my deepest feelings of gratitude to all of my friends and colleagues specially Sajjad Ahmed, Lucciana Restuccia and Lili Zhou for their physical and moral support as well as encouragement which contributed a lot in making this entire research tenure healthy, motivating and enjoyable. I am much thankful to my father (late) and my mother whose love and prayers made me able to successfully finish my doctorate dissertation.

I would like to acknowledge the PhD study grant provided by Higher Education Commission (HEC), Pakistan under the project of HRDI-UESTPs (Ref no. HRDI-UESTPs/HEC/2012/36).

Summary

Cementitious materials are commonly and extensively used worldwide by construction industry for various types of infrastructures. Despite of their exceptional strength in compression they still possess limited tensile strength and tensile strain capacity. Different types of fibers have been investigated since last fifty decades to reinforce the cementitious matrix against tensile failures and to impart ductility. The size of the reinforcing fillers has diminished from macro to micro and now even to the nano scale with the recent advancements in nanotechnology. Due to exceptional intrinsic properties and large aspect ratio, carbon nanotubes have been successfully investigated as a reinforcing filler to modify the mechanical strength, fracture toughness, electrical and electromagnetic wave absorbing properties of cementitious composites. However the problems associated with its effective dispersion and bonding with the host material limit its widespread applications on large scale.

To overcome the aforementioned issues concerning the dispersion and bonding of nano reinforcing materials with the host matrix, graphene nano sheets were explored for the first time as a reinforcing agent for high performance cementitious matrices. Graphene sheets are free form entanglement problems and therefore need comparatively lesser energy for proper dispersion. Due to very high specific surface area and large aspect ratio in comparison with carbon nanotubes, they are much capable to develop strong interfacial bond with the host medium. In the commercialization of these nano carbon particles filled cementitious composites, another major concern would be the related expenses. Therefore in parallel, research work was also done to explore the cost effective alternatives for the production of carbon nano/micro particles to be used for modifications or improvements in the properties of cement matrices. In recent wok by Prof. G. Ferro's research team it has been explored that carbon nano particles produced from coconut shells can be effectively used to improve the mechanical strength and fracture toughness of cementitious composites with limited dispersion issues (G. Ferro et al. 2014, 2015). To continue with the productive research concerning the cost effective production of carbon nano particles for high performance cementitious composites, bio-wastes in the form of bagasse fibers, hazelnut shell and peanut shell were investigated. These particular types of agricultural wastes were selected keeping in view their economic availability and excellent conversion efficiency via pyrolysis. The present work encompasses complete characterization of the

investigated materials, detailed study on their dispersion ability in water and the cement matrix, entire mechanical characterization of reinforced cementitious composites at varying proportions as well as their electromagnetic wave absorption properties in 0.2-10 GHz of frequency range.

It was determined that graphene nano-platelets can be uniformly dispersed in water as well as in the cementitious matrix without any addition of separate dispersant or surfactant or stabilizing agent. It was found that even at a very low content of addition, remarkable improvements in the mechanical strength and fracture toughness can be attained. The optimum content of addition for the grade 4 graphene nano-platelets was found as 0.08 wt% providing with a significant increase of 89% and 29% in compressive and flexural strengths along with 115% improved fracture toughness. Similarly the carbonized particles produced for bio-waste were found quite effective in modifying the mechanical performance of cementitious composites. Maximum enhancement by 139% and 88% in flexural and compressive strength were attained on 0.2 wt % addition of nano/micro carbonized particles produced from peanut shell with an increase of 69% in the fracture toughness as well. Microstructural investigations evidenced the proper homogeneous dispersion of GNPs and NMCPs throughout the cementitious matrix along with their efficient filling action to refine the pore-structure of resultant cementitious composite. The phenomena of crack bridging, crack deflections, crack contouring and crack branching were observed in scanning electron micrographs revealing the mechanism behind the remarkable improvements of mechanical properties achieved in the present research.

A novel cost effective material in the form of cement composites containing carbonized agricultural residue (comprising CPS and CHS) was proposed for shielding against electromagnetic waves. The investigated material was found much efficient for electromagnetic interference shielding applications, providing the advantage of better dispersion, simple manufacture at a much lower cost (cost saving > 85%) compared to the corresponding carbon nanotubes based cement composite material.

Table of Contents

List of Tables

List of Figures

List of Notations/Abbreviations

A_{dB}	Absorption loss
CBF	Carbonized Bagasse Fibers
CFRC	Carbon Fibers Reinforced Cementitious Composites
CH	Calcium Hydro-oxide
CHS	Carbonized Hazelnut Shell
CMOD	Crack Mouth Opening Displacement
CNFs	Carbon Nano Fibers
CNTs	Carbon Nano Tubes
CPS	Carbonized Peanut Shell
CS	Carbonized Shell
CSH	Calcium Silicate Hydrate
dB	Decibels
E	Modulus of Elasticity
E	Real permittivity
ε'	Imaginary permittivity
EDX	Energy-dispersive X-ray
EMI-SE	Electromagnetic Interference Shielding Effectiveness
FESEM	Field Emission Scanning Electron Microscope
F_{max}	maximum vertical Force in third-point bending test
FPZ	Fracture Process Zone
F_t	Tensile strength of composite
G_f	Fracture energy
GNPs	Graphene Nano Platelets
GNP_3	Grade 3 Graphene Nano Platelets
GNP_4	Grade 4 Graphene Nano Platelets
H	height of the specimen excluding notch length
HPC	High Performance Concrete
HPCC	High Performance Cementitious Composites
HPMC	High Performance Mortar Composites
HRWRA	High Range Water Reducing admixture
HS	Hazelnut shell
IPD	Inter Particle Distance
ITZ	Interfacial Transition Zone

L	span length for flexure test
L_{ch}	Characteristic length
M_{dB}	Multiple reflections loss
MIP	Mercury Intrusion Porosimetry
MWCNTs	Multi-walled Carbon nanotubes
NMCPs	Nano/Micro carbonized particles
NRCC	NCPs Reinforced Cementitious Composites
OPC	Ordinary Portland Cement
P_c	Percolation threshold
PP	Polypropylene
PS	Peanut shell
PVA	Poly-Vinyl Alcohol
R_{dB}	Reflection loss
S	span length
SCC	Self-Compacting Concrete
SCM	Self-Consolidating Mortar
SCP	Self-Consolidating Paste
SPS	Sodium Polynaphthalene Sulfonate
SWCNTs	Single-walled Carbon nanotubes
TGA	Thermo-Gravimetric Analysis
TI	Toughness Index
W	width of the specimen
Σmax	Modulus of rupture
Z_o	Characteristic Impedance
Z_m	Material Impedance

Chapter 1. Introduction

1.1 Background

Concrete is the second most consumable material after water in this global Era. Its production and utilization is increasing day by day with the advent of urban environment in the entire world. An estimated consumption of concrete was 21-31 billion tonnes in 2006 (contains 2.54 billion tonnes of cement) compared to less than 2-2.5 billion tonnes in 1950 (200 million tonnes of cement) ("Recycling Concrete" 2009). Along with enhanced annual production there are a lot of advancements made concerning the performance of concrete. The performance of concrete can be technically expressed in terms of better consistency in green state; relatively high strength and deformation in hardened state; improved durability and good aspect of structure during its service life.

The term 'high performance concrete' defines the concrete that can perform efficiently against the assigned job. This type of concrete perfectly adapts itself according to the desired functionality or tailors itself as per the requirements. It is not essential that high performance concrete would have high ultimate strength, increased deformation, low heat of hydration, better frost resistance and reduced permeability at the same time but it must be nearly ideal for the selected application. Without any doubt, the first and foremost characteristic property of high performance concrete is its high compressive strength, but some other requirements have to be satisfied, otherwise a more narrow term would be correct: 'high strength concrete' (Andrzej 2009).

Besides number of advancements in terms of strength, mobility and durability, concrete still exhibits quasi-brittle nature of failure. Based upon constituent materials, it has the ability to absorb very high compressive stresses (>200MPa ultimate strength) but generally possess a low resistance in tension and ultimately a limited bending strength. High performance concrete (HPC) possess more brittle nature in comparison with ordinary concrete. As reported by Gettu et al. (Gettu, Balant, and Karr 1990), when there is an increase in the strength, there is little increase in the values of fracture energy and fracture toughness much lesser than the strength. Also the effective size of fracture process zone diminishes consequently reducing the shielding against crack tip with an ultimate addition to the brittleness of the specimen or structure. It was found that an increase in compressive strength of 160 percent causes more than twice increase in the brittleness number. A

graphical comparison of the fracture properties of HPC and the ordinary concrete is presented in Figure 1.1.

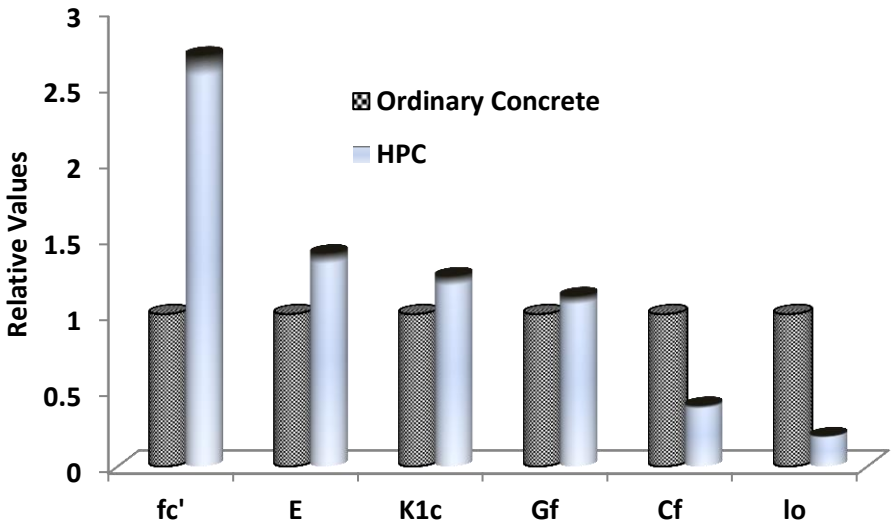

Figure 1.1 Comparison of mechanical properties of ordinary concretes and high performance concrete (relative values), after Gettu et al. (Gettu, Balant, and Karr 1990)

With the recent developments in construction especially in terms of high rise buildings and long span bridges, there is a stringent demand of concrete possessing enhanced mechanical properties particularly improved strength and toughness. As the brittle mechanical behaviour is the major issue in concern, therefore toughness improvement is the major goal to achieve for concrete. For the sake of this stance fibres have been added to concrete for more than a decade to improve its fracture properties. The effects of fibres on the mechanical response depend on their volume, aspect ratio, strength and bondage with the adjacent matrix (Brandt 1995). The influence on the fracture properties of cement composites varies also with the type of fibres because some fibres reduce the workability of concrete. Naaman et al (Naaman and Reinhardt 2003) introduced high performance fiber reinforced cement composites (HPFRCC), reinforced in such a way that they possess the excellent effects of strain hardening (tension) and deflection hardening (bending) as explained in Figure 1.2. Proper distribution of fibres inside the matrix is most important to attain requisite fracture properties; very small and very well dispersed fibres significantly enhance the overall mechanical response of cement composites (Brandt 1995). A lot of research was done and even in progress now with the advent of nanotechnology concerning the multistate reinforcements to resist cracks at micro, meso and macro scales. Parant et al (Parant, Pierre, and Maou 2007) successfully analyzed the performance of

multi scale fibre reinforced cement composites (MFRCC) containing micro fibres or steel wool, straight meso fibres of 5mm length and twisted macro fibres of approx. 30mm. He found the concept of multistage reinforcement very well suited for cementitious materials from the mechanical and durability perspectives. Use of cellulose fibres at micro and nano scales were also investigated with the similar objectives (Peters et al. 2010).

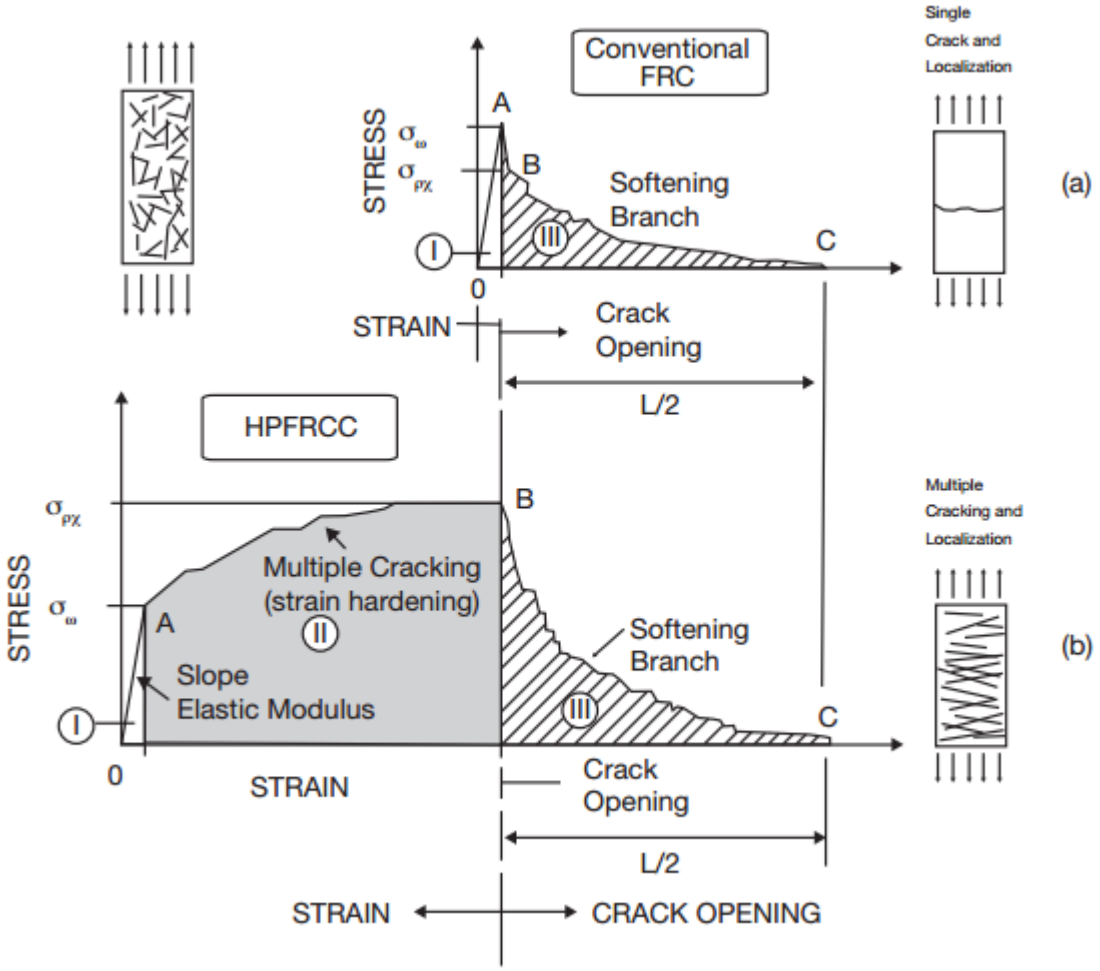

Figure 1.2 Comparison of typical stress-strain response in tension of HPFRCC with conventional FRCC (reproduced on permission (Naaman and Reinhardt 2003)**)**

Recent advancements in nanotechnology have opened new ways in the form of nano scale particles or fibers that could be effectively used as reinforcements to restrict the formation and propagation of nano/micro sized cracks. The nano scale reinforcements are much more effective for cementitious materials in comparison with conventional steel bars/fibers at millimeter scale, because they have the ability to restrict nano sized cracks at their very initial stages and thus control them to develop into micro sized cracks. Nano silica particles were investigated by Jo et al (Jo et al. 2007) and were found quite suitable

in improvement of mechanical strength with limited or no increase in fracture toughness. The nano silica particles are spherical in shape and possess high specific surface area of 300 m^2/g. The increase in mechanical strength on addition of nano silica particles is due to nucleation effect that promotes cement hydration, and the filling action as the size of nano silica particle is comparable to the size of gel pore in cement matrix. However, due to lower aspect-ratio, nano-silica particles lack the ability to control micro-cracks development from nano-size cracks, thus provide little increase in post crack toughness.

In comparison with spherical shaped nano silica particles, carbon nanotubes (CNTs) can be regarded as single dimensional tubes of high aspect ratios. The diameter of CNT's varies between 1-3nm in case of single walled CNTs (SWCNTs) while it generally lies between 5-50 nm for multi walled CNTs (MWCNTs). Since the length of CNTs can be in centimeters therefore they possess much higher aspect ratio of exceeding 1000. Along with large aspect ratio, CNTs exhibit extraordinary mechanical strength and elastic modulus on the order of GPa and TPa respectively. These characteristics render CNTs ideal nano scale reinforcement for cementitious materials to improve mechanical strength and fracture toughness. However the inclusion of CNTs in cementitious composites is a complex phenomenon and sometimes yields quite contrasting results. Some researchers have found that the addition of CNTs results in limited improvement of mechanical properties or in some cases even deterioration in mechanical performance was reported. The main associated reasons were the poor dispersion of CNTs within the cement matrix and weak bondage in between CNTs and the host matrix. Due to strong Van der Waal's forces CNTs tend to agglomerate and in case of poor dispersion such agglomerates act as defective sites to promote the fracture instead of controlling it. Saez et al (Sáez de Ibarra et al. 2006) reported that the efficient dispersion of CNTs by means of expensive surfactants can result in attaining the desired mechanical performance of cement/CNTs composites.

Besides effective dispersion, the second major problem that restricts the efficiency of CNTs in the cement matrix is related with the bondage in between CNTs and the adjacent cement matrix. Since CNTs exhibit tubular structure therefore reduced interfacial contact area is available as the outer face shields the inner face of the tube from being contacted with the adjacent matrix (Pan et al. 2011). Due to lackness in the interfacial contact, strong connection is not established which ultimately reduces the reinforcing efficiency of CNTs in the cementitious materials. Cwirzen et al. (Habermehl-Cwirzen, Penttala, and Cwirzen 2008) reported that MWCNTs added into the cement matrix along with a quality surfactant did not increase any of the mechanical strength and fracture toughness, even though well dispersion was attained. This can be associated with poor bonding in between CNTs and cement matrix that causes CNTs to be pulled out from the cement matrix on the application of tensile stresses.

To overcome issues concerning the dispersion and bonding of nano reinforcing materials with the host cementitious matrix, graphene nano-platelets (GNPs) were investigated for the first time in conjunction with cement. GNPs also comprise SP^2 carbon atoms like CNTs with an exceptional mechanical properties (Rafiee et al. 2009). They possess an intrinsic strength varying between 60-130 GPa and young's modulus of 1TPa (Kuilla et al. 2010). They are free from entanglement problem as associated with the use of nanotubes therefore need little effort to get easily dispersed within the host matrix. Graphene is a single atom thick flat sheet of carbon atoms (Lee et al. 2008). Its planar structure provides significant interfacial contact area (top and bottom) to develop strong connection with the host material. It also possesses the aspect ratio of more than 2000 and specific surface area of approximately 2600 m^2/g which is much more in comparison to conventional CNTs (Collins, Lambert, and Duan 2012a). In a recent research on graphene/epoxy composites it has been proved that graphene outperforms CNTs for establishing strong connection with the host material resulting in the improvement of overall fracture behavior (Rafiee et al. 2009).

Since the cost of production is the limitation on widespread application of graphene in cementitious materials so in parallel with the work of graphene it has been tried to explore cost effective reinforcing materials at nano/micro scale for enhancing the fracture properties of high performance cementitious materials. In recent work by Ferro et al (G. Ferro et al. 2015) it has been reported that carbonized particles from coconut shells can effectively improve fracture toughness of cement mortar. Adopting similar pyrolyzing regime with a few modifications, carbonized particles were prepared from bagasse fibre, hazelnut shell and peanut shell. These particular types of agricultural wastes were selected keeping in view their economic availability as well as the excellent conversion efficiency via pyrolysis (Ferreira et al. 2015; Huff, Kumar, and Lee 2014; Nisamaneenate et al. 2014; E. Pu and Pu 1999).

Since the addition of carbon as reported in case of CNTs reinforced matrices doesn't only influence the structural parameters but also imparts some positive impact on the microstructure, porosity as well as electrical and electromagnetic properties of the host cementitious material (H. K. Kim, Nam, and Lee 2014; Konsta-Gdoutos, Metaxa, and Shah 2010c; Metaxa et al. 2012; Nam, Kim, and Lee 2012; Nien and Huang 2010; Son et al. 2008). Therefore, in order to have a detailed analysis of the investigated nano/micro carbon reinforcements on the behavior of high performance cementitious materials, a study on electromagnetic interference shielding effectiveness of plain and reinforced cementitious formulations was also conducted. So that the overall effectiveness of the material may be stated in the conclusion phase with strong evidences as well as throughout brightened and darkened phases of the research may be successfully explored.

1.2 Nano/Micro Carbonaceous Inerts

The nano/micro carbon particles investigated as a reinforcing medium for cementitious materials are briefly introduced in this section.

1.2.1 Graphene Nano Platelets (GNPs)

The word graphene comes from Greek word graphein, which means 'to write' that was one of the earliest uses of this material. Graphene is a two-dimensional single-atom thick membrane of carbon atoms arranged in a honeycomb crystal (Raza 2012). Bilayer graphene is also an important material having unique electronic and transport properties. Monolayer and bilayer graphene nano structure is shown in Figures. 1.3 & 1.4 respectively.

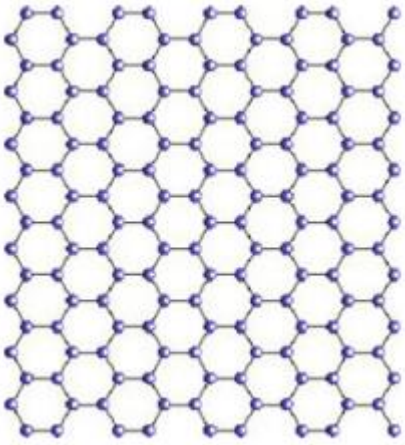

Figure 1.3 Monolayer Graphene (Raza 2012)

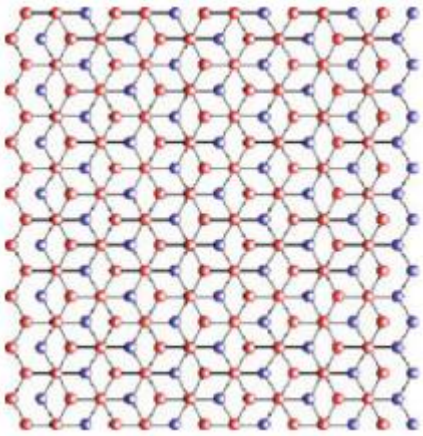

Figure 1.4 Bilayer Graphene (Raza 2012)

GNPs are ideal reinforcing materials bearing unique electrical, mechanical and thermal properties. It is one of the strongest materials known per unit weight. The theoretical Young's modulus of an individual sheet is 1060 GPa. The theoretical surface area of individual graphite sheet is 2630–2965 m^2/g (Viculis et al. 2005). Due to very large surface area and a high aspect ratio, GNPs are much favourable as mechanical reinforcement and forming conductive network in composites with low filler content.

GNPs are free from entanglement problem which is very common in case of CNTs and CNFs. Because of their smaller longitudinal dimension in comparison with nanotubes and nano fibres, they exhibit the property of establishing an excellent conductive network in a cement or polymer composite, which is extremely sensitive to damage. Based on literature

(Collins, Lambert, and Duan 2012a; Hilding et al. 2003; W. Yu et al. 2010) a comparison between the properties of GNPs and CNTs is given in Table 1.1:

Table 1.1 Properties of GNPs and CNTs (Alkhateb et al. 2013; Collins, Lambert, and Duan 2012b; Hilding et al. 2003)

Property	Unit	GNPs	CNTs
Elastic Modulus	TPa	1 (in plane)	~1 for SWNT,~ 0.3-1 for MWNT
Strength	GPa	10-20	50-500 for SWNT, 10-60 for MWNT
Resistivity	μΩcm	50 (in plane)	~5-50
Dimensions		Dia 1-20 μm Thickness 1-30 nm	Diameter: 0.75~3nm for SWNTs, 2~30nm for MWNTs. Length: 1~50μm for SWNTs, 0.1~50μm for MWNTs
Surface Area	m^2/g	2630	>400
Aspect Ratio		50-900	~500

Recently most of researchers are focused on investigating its utilization in polymer composites (Kuilla et al. 2010; Pan et al. 2011; Rafiee et al. 2009). However nothing has been reported so far in the literature concerning its use in conjunction with cement to form multifunctional GNPs reinforced cement based composites. Keeping in view the outstanding performances GNP reinforced polymer and epoxy composites their utilization with cement as a reinforcing agent has been explored in the present work.

1.2.2 Carbonized Particles Produced from Agricultural Residue

To explore cost effective alternative for the production of carbon particles to be used as a reinforcing medium for cementitious materials; bio-waste in the form of bagasse fiber, hazelnut shell and peanut shell was investigated.

1.2.2.1 Bagasse Fibers

Bagasse is a solid residue that left behind after the extraction of juice from sugarcane to be used for sugar and ethanol production. Another type of residue associated with the sugarcane production is the leaves that are left in agricultural fields during sugarcane harvesting. These dried leaves are named as sugarcane trash and their production ranges from 6-8 tons in a unit hector of sugarcane crop. Generally sugarcane trash is burnt in the fields which produces fly ash, severely damages soil microbial diversity and raises

environmental concerns. Among sugarcane-producing countries, Brazil is the top producer, with 653 million tons of sugarcane in 2014, followed by India and China (UNICA 2014). Generally, 280 kg of humid bagasse is generated from 1 ton of sugarcane. Pandey et al.(Pandey et al. 2000) reported that 50% of SB is used for energy generation within the plant and the rest remains unused in the environment. Therefore, the bioconversion of leftover bagasse into value-added products may have sustainable economic and strategic benefits.

1.2.2.2 Hazelnut Shell

Hazelnut is also getting renowned all over the world especially because of its vast usage in many chocolate and ice-cream flavors. Food and agricultural production statistics of United Nations reported that the world's hazelnuts production was about 0.91 million metric tons in year 2012, with major part coming from Turkey and Italy about 70% and 20% of its production respectively (FAOSTAT-Food and Agriculture Organization n.d.).

1.2.2.3 Peanut Shell

Peanut is one of the most popular and magnificently consumed dry fruit all over the world especially in China and India that are ranked as its top two producers. According to the latest survey of United States Department of Agriculture (USDA) world total production of peanuts is almost 40 million metric tons with more than 60% contributions from China and India (USDA-Foreign Agriculture Service n.d.). Both hazelnut and peanut generate considerable amount of residues in form of their shells with little to no specific value. Therefore it is important to look for ways to manage and utilize this bio-waste beneficially.

Figure 1.5 Raw bagasse fiber (a), hazelnut shell (b) and peanut shell (c)

Bagasse fiber, Hazelnut shell and peanut shell yield high content of bio char on carbonization (Ferreira et al. 2015; Huff, Kumar, and Lee 2014; Nisamaneenate et al. 2014; E. Pu and Pu 1999). An average yield of more than 40% was reported for hazelnut shell at a temperature of around 500^{o}C (E. Pu and Pu 1999), while in case of peanut shell

it was found approximately about 40% for the same range of temperature (Huff, Kumar, and Lee 2014). The economic availability and excellent conversion efficiency of bagasse fiber, hazelnut shell and peanut shell via pyrolysis, were the two main reasons that motivated the authors to explore their use in cement composites for the desired objectives. The entire carbonization process along with detailed synthesis of nano/micro inerts is discussed in chapter 3 section 3.1.7.

1.3 Objectives and Scopes of this Study

The primary objective of the current research was to explore new type of high performance cementitious building materials with enhanced mechanical strength as well as improved fracture toughness.

The major scopes covered in the research are:

1. Dispersion scheme of GNP and submicron carbonized particles in water and later in cement matrix is formulated. Also the fabrication technique of reinforced cementitious composites containing nano/micro carbonaceous inerts in six different proportions (i-e 0.025, 0.05, 0.08, 0.2, 0.5 and 1.0 wt. percentages of cement) is studied and discussed.

2. Synthesis and detailed characterization of the investigated carbonized particles produced from agricultural waste is reported and discussed.

3. Experimentally evaluated compressive strength, modulus of rupture, stiffness as well as fracture toughness of each batch is compared and discussed. Furthermore strengthening mechanism is evaluated in detail.

4. Effect of synthesized submicron reinforcing carbonized particles on the electromagnetic interference shielding effectiveness and porosity of cement composites is analysed.

Chapter 2. Nano/Micro Carbon Reinforcements in High Performance Cement Based Materials

2.0 General

This chapter covers a brief literature review concerning the previously investigated carbon based nano/micro sized reinforcements. The attained improvements or modification as well as the associated problems restricting their large scale usage has been summarized in the present chapter.

2.1 Reinforcements of High Performance Cementitious Composites

Since cement based materials are characterized by low tensile strength and low tensile strain to failure, therefore scientists and researchers have done a lot of work to evaluate different alternatives that may effectively reinforce the cement matrix. The purpose of adding reinforcing material is to enhance the resistance of cementitious matrices against cracking either by controlling their opening or by obstructing their smooth propagation. Reinforced cementitious composites possess pseudo post-cracking ductility induced as a result of crack bridging mechanism via reinforcement. Starting from the steel fibers at macro scale; the different types, aspect ratios and concentrations of reinforcements were investigated at macro scale, micro-scale and later on at nano scale levels after the advent of nanotechnology. The macro fibers are usually 10-60 mm long with 0.1-1.0 mm of least dimension, while micro fibers are 10-30 μm in diameter and less than 10mm long. Nano reinforcements possess at least one dimension in the nanometer (10^{-9} m) range.

The previously explored microscopic fibers included steel fibers, natural mineral fibers in which asbestos fibers are most renowned, glass fibers, polymeric fibers, textile fibers, natural vegetable fibers and carbon fibers (Ardanuy, Claramunt, and Toledo Filho 2015; Mai 1979; Peled et al. 2008; Promis et al. 2010; C. Wang et al. 2008). Where as in the nano scale, nano-Al2O3, nano-TiO2, nano-ZrO2, carbon nanotubes (CNTs), carbon nano-fibers (CNFs) and carbon black (CB) particles were analyzed (J. Chen and Poon 2009; Chuah et al. 2014; Chyad 1989; Gao, Sturm, and Mo 2009; G. Y. Li, Wang, and Zhao 2005; Ma et al. 2010; Sanchez and Sobolev 2010). All were found more or less effective to attain the requisite goal of improved mechanical strength and fracture toughness of

cementitious materials with certain limitations. The best material that gained an extreme popularity and still under investigation is carbon both in micro and nano forms due to its remarkable mechanical, electrical and thermal properties, quite low density and exceptional chemical and thermal stability (Qian et al. 2002; Rafiee et al. 2009). This chapter provides a systematic review on major progresses and advances in the fabrication, properties and mechanism as well as the structural applications of nano/micro scale carbon reinforcements in high performance cement based matrices. Also it covers a detailed discussion concerning the associated issues that restrict their wide spread structural applications.

2.2 Carbon Fiber Reinforced Cementitious Composites (CFRC)

Carbon fiber after being developed in 1960 by a Japanese researcher Dr. Akio Shindo, provided the first carbon based alternative to be used in conjunction with cement for improving the mechanical performance of the resultant cementitious composite. Carbon fibers are produced by pyrolyzing various types of organic fibers. The process of pyrolysis includes oxidative stabilization at lower temperature and carbonization at higher temperature in an inert atmosphere. This section reviews the effects of carbon fibers addition into the cementitious matrices.

2.2.1 Mechanical Properties of CFRC

Carbon fibers possess impressive characteristics in tension and flexure, low drying shrinkage, high specific heat, low thermal conductivity, high electrical conductivity, high corrosion resistance, and weak thermoelectric behavior (B. Chen, Wu, and Yao 2004; Wen and Chung 2000, 2001, 2007a). The research concerning their use as a reinforcement in cementitious matrices started in late 1970s and remained most popular till 1991. Recently researchers are more focused to explore the hybrid effects of multistage carbon reinforcements. Due to its excellent ability to enhance fracture properties, it was considered as the best replacement to conventional steel especially in corrosive environments.

The strength of concrete is much lower in tension that usually lies between 1/8 to 1/12 of its compressive strength in normal strength concretes but for high strength concretes it reduces further and ranges in between 1/17 to 1/20 of the strength in compression. Due to reasonable price, carbon fibers obtained from pitch material were considered as a reinforcing medium for cement based materials. The pitch based CFs exhibit tensile strength of 600-900 MPa which is 300-500 times more than plain concrete matrix and elastic modulus of 30-40 GPa. Wang et al. (C. Wang et al. 2008) reported an increase in

mechanical properties of CFRC with the content of added fibers up to 0.6 wt. percent of cement as plotted in Figure 2.1. An increment in elastic modulus and compressive strength by 26.8% and 20% respectively was attained where as a decrement of 12.9% was found in flexural stress at 0.6 wt. percent addition of CFs in high performance mortar composites (HPMC).

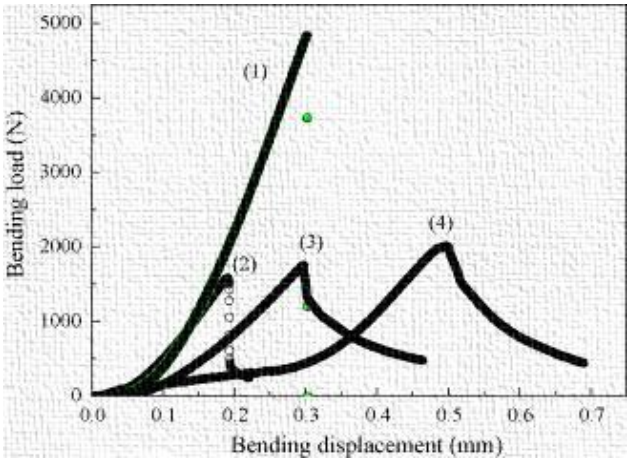

Figure 2.1 Relationship between the bending load and the bending displacement of CFRC specimens. (1) 0% CFs (2) 0.6% CFs (3) 0.4%. CFs and (4) 0.2%CFs (C. Wang et al. 2008)

Toutanji et al. (Toutanji, E-korchi, and Katz 1994) investigated the effect of CFs produced from poly-acrylonitrile (PAN) fibers, on the mechanical response of high performance cementitious composites (HPCC). It was found that there is a significant increase in the mechanical strength and fracture toughness even at the addition of very low volumes of CFs. The additions of CFs by 1%, 2% and 3% (by weight of cement) were found to enhance uniaxial tensile strength of CFRC by 32%, 48% and 56% whereas flexural strength by 72%, 95% and 138% respectively. Park et al. (Park and Lee 1993) concluded that there is an increase in tensile strength, flexural strength and fracture toughness of CFRC till the volume fraction of 3% beyond that the mechanical properties starts depreciating with the added content. Also the compressive strength was found to decrease even at the low volume additions of CFs. Due to superior intrinsic properties of PAN based CFs, they were observed to provide much better results in comparison to pitch based CFs as discussed by Park et al. (Park and Lee 1993).

The hybrid effect of carbon fibers with varying sizes on the reinforcement of HPCC was analyzed by Shu et al. (Shu et al. 2015). Both modulus of resilience and post crack toughness were reported to be significantly enhanced with the hybridization effect that controls the openings of cracks at multistage. The response observed in pre-peak and post-peak regions is displayed in Figure 5.2.

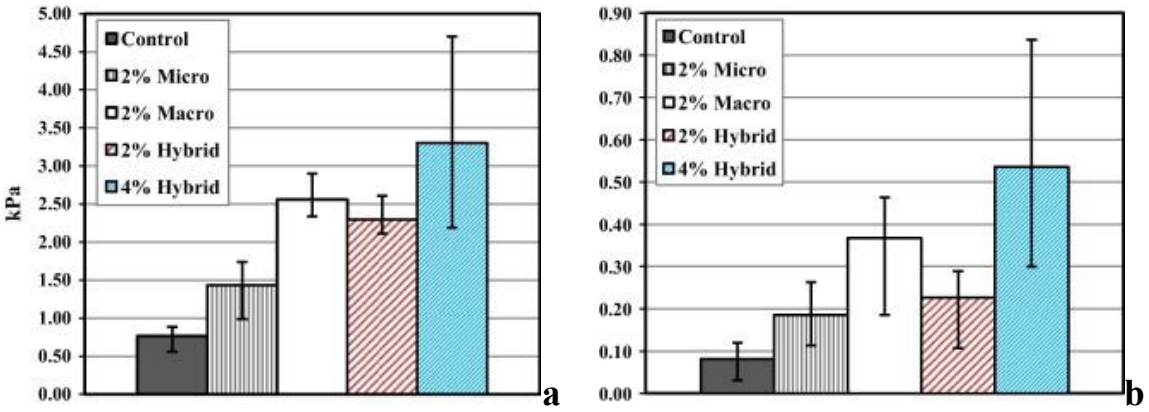

Figure 2.2 Modulus of Resilience (a) and Toughness indices (b) of CFRC from indirect tension test (Shu et al. 2015)

It is mostly believed that there are two mechanisms behind the improvement in the mechanical properties of CFRC i-e strengthening effect and the toughening effect (Shu et al. 2015; Toutanji, E-korchi, and Katz 1994). Due to exception mechanical properties, these CFs effectively resist the transmitted stresses at the cement/CF interface and thereby enhance the mechanical strength of the resulting reinforced composite. Also CFs prevent crack propagation by bridging the cracks as they are about to open and consequently delay the failure of concrete and improve its toughness.

2.2.2 Other Properties of CFRC

Due to their impressive electrical, electromagnetic and thermal properties, CFs have been investigated to induce electrical, electromagnetic, thermal, and sensing properties to cementitious matrices (Cao and Chung 2001; B. Chen, Wu, and Yao 2004; Chung 2001; Gao, Sturm, and Mo 2009). CFRC was the first cementitious material whose electrical properties were studied. Chung et al. (Wen and Chung 2000, 2001) discovered that induction of CFs in cementitious materials imparts conductivity and reduces the overall resistance of the CRFC composite. The extent of induced conductivity depends upon the percolation threshold of the added CFs which is related with the aspect ratio by the following equation as reported by Jing Li et al. (J. Li and Kim 2007) .

$$\mathrm{Pc} = \frac{27\pi \mathrm{D}^2 \mathrm{t}}{4(\mathrm{D} + \mathrm{IPD})} \qquad Eq.\,2.1$$

Where ‘Pc’ defines percolation threshold while ‘IPD’ stands for inter particle distance and ‘D’ and ‘t’ represents diameter and thickness of the material to be added.

Furthermore it was found that the change in electrical resistance of CFRC is responsive to the growth of a traction-free crack and thus can be used to monitor the crack growth and estimate the crack length (Wen and Chung 2000). Due to very high conductivity, the presence of CFs in an insulated cementitious matrix results in enhancement of microwaves absorption by the composites. Consequently improvements in dielectric constant and electromagnetic interference shielding effectiveness was also reported (Chung 2001).

2.2.3 Associated Problems with CFRC

Although the use CFs was proved to be an effective option to develop multifunctional cementitious composites but still there are major some issues that restrict their infield applications.

1. The workability of cementitious matrices reduces on addition of CFs and the extent of reduction is proportional to the added volume fraction as well as the aspect ratio of CFs (Park and Lee 1993).

2. The CFs need to be very well dispersed in order to have the desired improvements in CFRC. Due to entanglement problem CFs were found badly dispersed in most cases that resulted in inducing additional air voids and ultimately affecting the overall behavior of CFRC as showed in Figure 2.3a by scanning electron micrograph (Maggio 2013; Mindess and Young 1981; Park and Lee 1993). This is the reason that badly affects the statistics and consistency of enhancement achieved by different researchers in different times (Toutanji, E-korchi, and Katz 1994).

3. The interfacial bonding between CFs and the adjacent matrix is the major issue affecting the performance of CFRC. Due to poor connection small gaps at the interface are generated leading stress concentration and accelerated crack propagation. The weak CF/matrix bond cases pull out of CFs from cementitious matrices as indicated in Figure 2.3b and prevents satisfactory load transfer at the interface (G. Y. Li, Wang, and Zhao 2005; Maggio 2013; Shu et al. 2015).

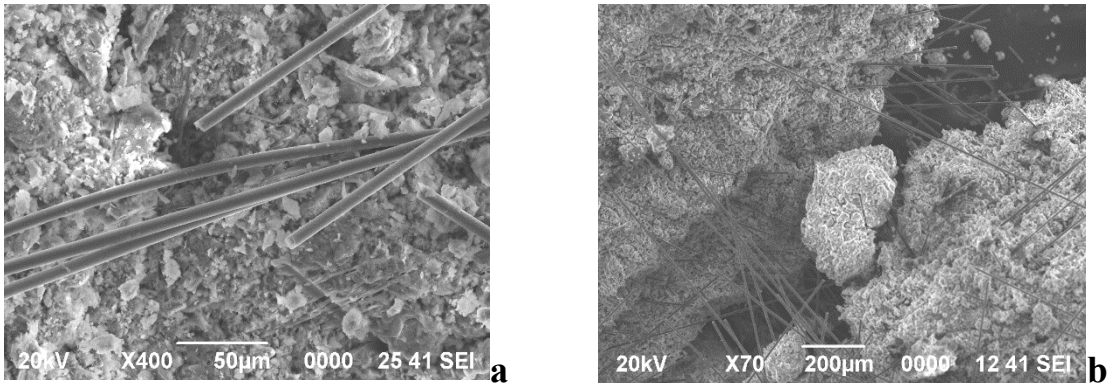

Figure 2.3 SEM fractal-graphs of CFRC showing CFs cluster (a) and pull out from matrix (b) (Maggio 2013)

2.3 Carbon Based High Performance Cementitious Nano-composites

The word nano-composite defines a multiphase solid material in which there is at least one phase with at least single dimension in nanometer range (Ajayan, Schadler, and Braun 2006). The characteristics exhibited by nano carbon particles (NCPs) of a specific material are quite novel and unique in comparison with its features of macro or micro sized forms due to significant alterations in surface electronics and crystal structure. The large specific surface area and strong interfacial interaction with the host medium were the main common properties of NCPs that broaden their spectrum of applications. The advent of nanotechnology opened new ways to bring advancements in cementitious matrices used for construction and a lot of ideas have been explored for producing high performance multifunctional cementitious nano-composites (Ajayan, Schadler, and Braun 2006; Chuah et al. 2014; B. Han et al. 2015; G. Y. Li, Wang, and Zhao 2005; Ma et al. 2010; Sanchez and Sobolev 2010).

The use of carbon based nanoparticles was found more beneficial for producing high performance multifunctional cementitious composites as compared with CFs. Due to very small size these NCPs were found effective in restricting the crack at very preliminary stage to open and successfully hindering its propagation (Konsta-Gdoutos, Metaxa, and Shah 2010a, 2010c). The nano-scale carbon reinforcement was reported as efficient filler with strong capability to reduce porosity and decrease stress concentration that ultimately results in enhancement of compressive strength and corrosion resistance of the NCPs reinforced cementitious composites (NRCC) (Nochaiya and Chaipanich 2011). Compared with CFRC, NRCC were found more conductive and the conductive networks possessed increased sensitivity during crack propagation which also describes its importance in structural health monitoring perspectives (Wansom et al. 2006).

2.3.1 Brief Introduction of NCPs used in Fabrication of NRCC

The study concerning the use of NCPs to produce NRCC was initiated in the 1990s. Since that time three types of NCPs have been explored for the fabrication of NRCC which include carbon nanotubes (CNTs), carbon nano-fibers (CNFs) and carbon black (CB). CNTs belong to one of the allotropic forms of carbon with a hollow cylindrical shaped nanostructure. The diameter of the cylinder lies in nanometer range while the length falls in microns. The number of rolled graphene layers categorize CNTs into two different types i-e single walled carbon nanotubes (SWCNTs) consisting a single rolled graphene sheet and multiwalled carbon nanotubes (MWCNTs) comprising multiple layers of rolled graphene sheets as shown in Figure 2.4. CNFs are also similar to CNTs with their diameters falling in between those of CNTs and CFs. Unlike CNTs and CNFs, CB particles are spherically shaped with their diameters lying in the range of nanometers. The typical representative properties of CNTs, CNFs and CB are listed in Table

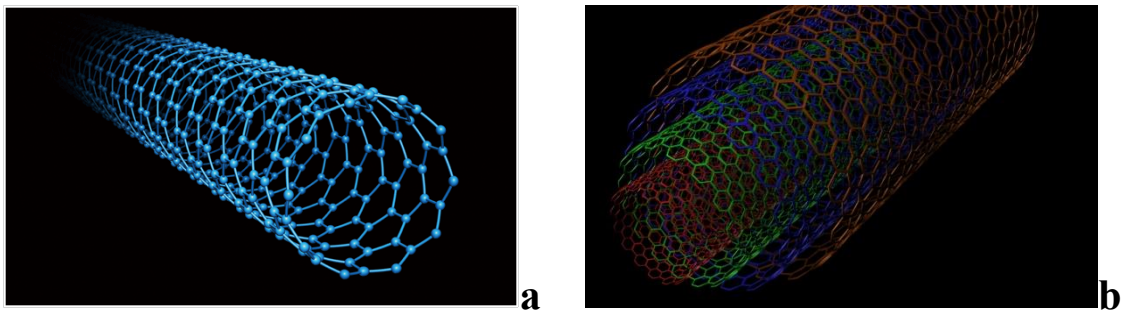

Figure 2.4 Structure of SWNTs (a) and MWNTs (b) (Giuseppe Ferro and Musso 2011)

Table 2.1 Properties of NCPs (B. Han et al. 2012, 2015; M. Li et al. 2012; Sixuan 2012)

Property	CNTs		CNFs	CB
	MWCNTs	SWCNTs		
Elastic modulus (TPa)	0.3-0.1	1.0	0.4-0.6	
Strength (GPa)	10-60	50-500	2.7-7.2	0.015-0.03
Electrical resistivity (μΩcm)	5-50		55	
Dimensions	2-30 nm 'dia'	2-30 nm	2-30 nm	30-120 dia
	0.1-50μm 'L'	0.1-50μm	0.1-50μm	
Surface area (m^2/g)	>400		~200	
Aspect ratio	~1000		100-500	

2.3.2 Dispersion of NCPs in Cementitious Nano-composites

Since the nanoparticles possess strong van der waals forces that cause agglomeration problem therefore it is very complex to have a quality dispersion inside the host material. Significant efforts have been made to resolve this issue as it can adversely affect the properties or may limit the nano enhancement/modification effect in case of poor dispersion. Generally there are two techniques usually adopted to have the effective dispersion of NCPs inside cementitious matrices. The first one is associated with mechanical separation while the second one involves chemical alterations. Mechanically, the NCPs are dispersed in the host matrix either with the help of ultrasonic or ball milling (Azhari and Banthia 2012; Bortz, Merino, and Martin-Gullon 2011; Caneba et al. 2010; Chafidz et al. 2014; Chaipanich et al. 2010; B. Chen, Wu, and Yao 2004; Chung 2012; Collins, Lambert, and Duan 2012a, 2012b; Giuseppe Ferro and Musso 2011; Habermehl-Cwirzen, Penttala, and Cwirzen 2008; B. Han et al. 2012; Kong et al. 2014; G. Y. Li, Wang, and Zhao 2007, 2005; M. Li, Lynch, and Li 2012; Metaxa et al. 2012; Nochaiya and Chaipanich 2011; Vaisman, Wagner, and Marom 2006; M.-F. Yu et al. 2000). Chemical modifications include surface treatment of NCPs using covalent or non-covalent approaches (Bahr and Tour 2002; B. Han et al. 2015; Ma et al. 2010). Both mechanical and chemical techniques have also been employed to overcome the issues concerning dispersion of NCPs (Alessandro 2012; Giuseppe Ferro and Musso 2011; Giuseppe Ferro et al. 2008; Hilding et al. 2003; Ma et al. 2010; Musso et al. 2009; Sobolkina et al. 2012; Yazdanbakhsh et al. 2010).

Recently researchers are using surfactants as well as mechanical dispersion via ultrasonic to attain effective dispersion of NCPs in cementitious materials. In some cases superplastcizer or water reducing admixture has been tried as a surfactant to disperse NCPs. Shah et al. achieved an effective dispersion of MWCNTs of varying lengths and concentrations in cementitious matrix materials by just applying poly-carboxylate based superplasticizers (Konsta-Gdoutos, Metaxa, and Shah 2010b, 2010c; Metaxa et al. 2012) . The superplasticizer contribute in proper dispersion by employing double dispersion effect on NCPs and cement grains as discussed by Han et al.(B. Han et al. 2012). Huang et al. also obtained proper dispersion of NCPs with the aid of superplasticizer as surfactant and ultrasonic probe (Sixuan 2012). Nasibulin et al. discovered new approach to resolve the issue concerning NCPs dispersion by growing CNTs/CNFs on the surface of cement, mineral admixture particles or sand (Nasibulin et al. 2013).

Even after much serious efforts since last decade, the dispersion of NCPs in cementitious composites is still the most crucial problem. It is essential to explore the best alternative for resolving this issue that should be much simple, repeatable and lower energy consuming.

2.3.3 Mechanical Properties of NRCC

The influence of NCPs on the mechanical response of cementitious composites depends upon number of factors; specifically the type of NCPs, dispersion level attained and the concentration inside the matrix to be reinforced. A huge work has been done on investigation of the effectiveness of CNTs, CNFs and CB to enhance the mechanical behavior of cementitious composites. These researches along with their outcomes are briefly summarized in Table 2.2 & 2.3. The addition of CB particles was found ineffective in enhancing the mechanical properties of cementitious matrices. Only a slight increase in the ultimate tensile strain was reported with negligible improvement in tensile and compressive strengths (M. Li et al. 2012; Wen and Chung 2007b).

Table 2.2 Modification in mechanical properties of cementitious composites by CNTs additions

Concentration of CNTs	Percent improvement in mechanical properties				Researcher
	Tensile strength	Compressive strength	Flexural strength	Fracture toughness	
0.3%	34.28	-	-	-	(Ludvig et al. 2009)
0.5%	19	-	-	-	(Hunashyal 2014)
0.5%	-	19	25	-	(G. Y. Li, Wang, and Zhao 2005)
0.02%	-	11.03	11.23	-	(Kerienė et al. 2013)
0.045-0.15%	-	50	10	-	(Habermehl-Cwirzen, Penttala, and Cwirzen 2008)
0.2%	-	29.5	34.45	-	(J Luo 2009)
0.5%	-	10-20	33	-	(Musso et al. 2009)
0.1%	-	22	-	-	(Bharj et al. 2014)
0.1%	-	-	-40	-	(Tyson et al. 2011)
0.5%	-	-	-	149.23	(Jianlin Luo, Duan, and Li 2009)

Table 2.3 Modification in mechanical properties of cementitious composites by CNFs additions

Concentration of CNFs	Percent improvement in mechanical properties				Researcher
	Tensile strength	Compressive strength	Flexural strength	Fracture toughness	
0.2%	22-26	-	-	-	(Gay and Sanchez 2010)
0.16%	-	42.7	-	-	(Gao, Sturm, and Mo 2009)
0.2%	-	-	82	270	(Tyson et al. 2011)
0.04%	-	-	46	-	(Peyvandi, Sbia, et al. 2013)
0.048%	-	-	45	-	(Konsta-Gdoutos, Metaxa, and Shah 2010c)

From the summarized literature it is revealed that the best performance enhancement of NRCC includes an increase of 34.28 % in tensile strength (Ludvig et al. 2009), a 50% increase of compressive strength (Habermehl-Cwirzen, Penttala, and Cwirzen 2008), an 82% increase in flexural strength and a 270% of maximum increase in fracture toughness (Tyson et al. 2011). Also the addition of NCPs resulted in significant improvement of Vickers's hardness, mid span deflection, resilience as well as the stiffness of cementitious composites. The typical stress-strain as well as load deflection in compression and flexure is displayed in Figure 2.5 as reported by (Abu Al-Rub, Ashour, and Tyson 2012; Chan and Andrawes 2010). The curves demonstrate some alterations in the mechanical constitutive relations as well on the addition of CNTs/CNFs.

The factors that contribute in enhancement of mechanical properties of NRCC include

a. Exceptional intrinsic properties of NCPs as described in (Table 1)
b. The nano size effect along with high specific surface area and large aspect ratio which promotes hydration of cement as well due to nucleation effect as observed by Marker et al.(Makar and Chan 2009).
c. Modification in the microstructure as well as the interfacial transition zone by effective refinement of pores even at the nano scale leading to more compacted and refined microstructure of NRCC.

d. Relatively strong interaction between NCPs with the adjacent host matrix especially observed in case of covalence modified CNTs/CNFs filled matrices (Peyvandi, Soroushian, et al. 2013).
e. Efficient bridging of cracks at their preliminary stages (Figure 2.6a) as well as the effects of crack pinning, crack deflection, fiber pullout and fiber breaking (Figure 2.6b).

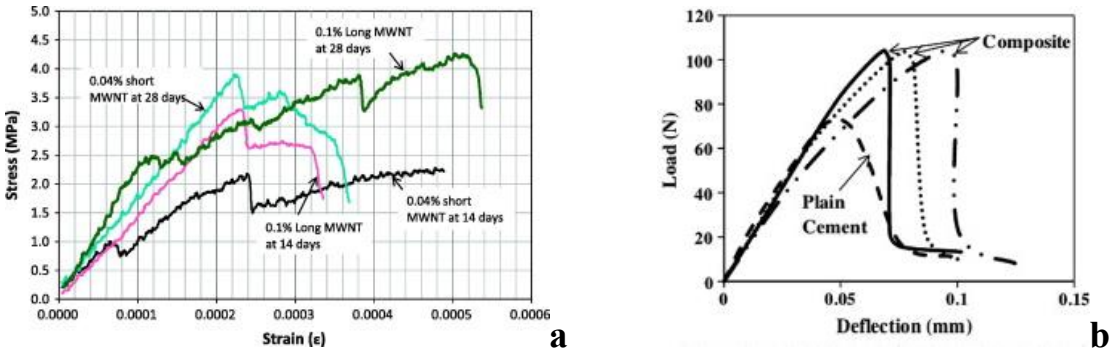

Figure 2.5 Mechanical properties of typical CNTs/CNFs filled cementitious composites in compression (a) (Abu Al-Rub, Ashour, and Tyson 2012) **and in flexure (b)** (Chan and Andrawes 2010)

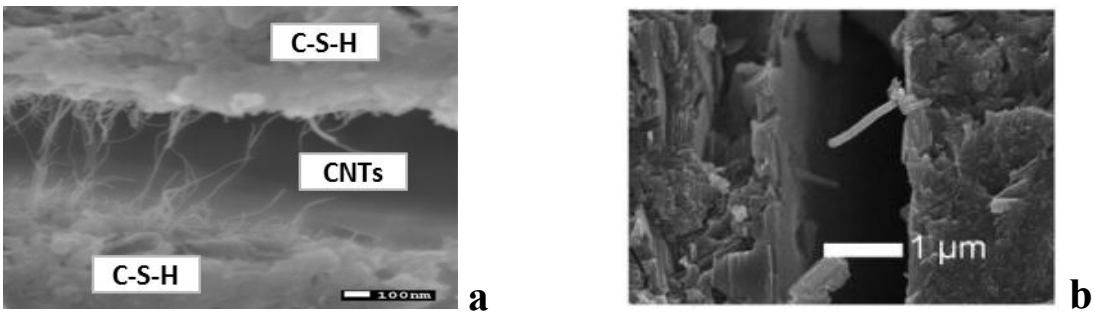

Figure 2.6 CNTs bridging action against cracking (Abu Al-Rub, Ashour, and Tyson 2012) **(b) and CNF pullout from matrix (a)** (Gopalakrishnan et al. 2011)

2.3.4 Other Properties of NRCC

The effect of NCPs on electrical conductivity, electromagnetic interference shielding effectiveness (EMI-SE), thermal behavior, dampness and other properties of high performance cementitious matrices was also investigated in detail. It was found that modification or improvement in any property of NRCC is dependent upon the type of nano carbon particles, their concentration inside the matrix, respective level of dispersion and the surface conditions as was the case with the mechanical aspects.

The addition of NCPs at their respective percolation values results a decrease of 1Ωcm in the electrical resistivity of cementitious composites and an increase in the electrical conductivity by almost 8 orders of magnitude measured against pristine cement composite as demonstrated in Figure 2.7a (Singh et al. 2013). The conductivity of NRCC is much more sensitive to any deformation or crack in comparison with CFRC due to their well dispersed large scale conductive networks established throughout the cementitious matrix which demonstrate its effectiveness as sensor. Sing et al. and Nam et al. analyzed the EMI-SE of cementitious composites filled with NCPs and reported a decrease by 27% in electromagnetic wave reflectivity at a frequency of 2.9 GHz on addition of 0.6 wt% of MWCNTs (Figure 2.7b) (Singh et al. 2013). Yakovlev et al. discovered that even a low content of CNTs reduces the thermal conductivity of foam concrete by 20% (from 0.07 W/m K to 0.056 W/m K) (Yakoveli et al. 2006). Also Veedu et al. concluded that the thermal performance of CNTs reinforced cementitious matrices is approximately 35% and 85% higher that the CFRC and plain cement composites respectively (Veedu 2011). An improvement in the workability of high performance cementitious matrices was also reported by addition of –COOH functionalized CNTs (Peyvandi, Soroushian, et al. 2013). Han et al. also found an enhancement in the transport properties (i.e. water sorptivity) of cementitious composites even at a very low content of CNTs addition demonstrating their effectiveness in the improvement of durability (B. Han et al. 2015).

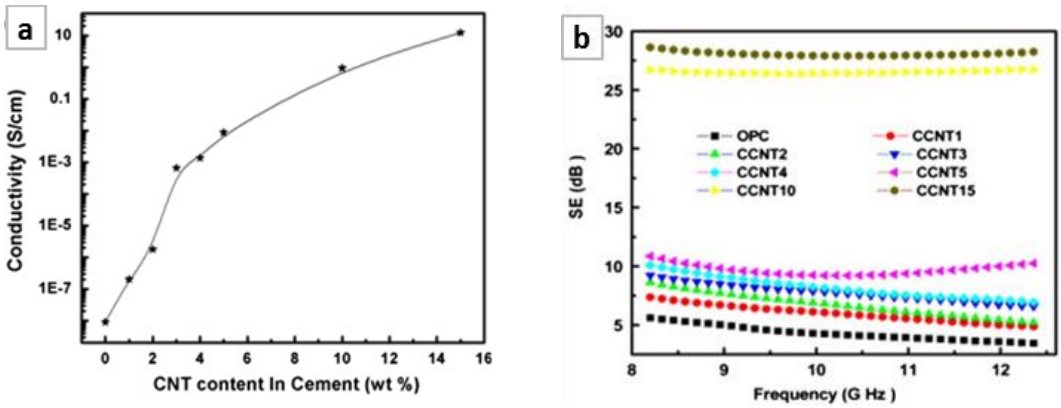

Figure 2.7 Variation in electrical conductivity (a) and EMI-SE (b) of cementitious composites with varying CNTs content (Singh et al. 2013)

2.3.5 Associated Problems with NRCC

Besides beneficial effects of NCPs there are still some serious associated issues that cause inconsistency in the attained results and affect the overall reliability. These problems are still an obstacle in the applications of NRCC on large scales.

1. The first issue is related with the dispersion of nano carbon particles. Due to strong Van der Waal's forces these NCPs are very complex to effectively disperse in the host matrix. In case of poor dispersion, the agglomerates of NCPs act as a defective site to accelerate or initiate the propagation of cracks as observed by Tyson et al. (Tyson et al. 2011). Use of surfactant is a viable option but some surfactants enhance the porosity of cement matrix due to foam formation and affect the desired improvement or modification in the mechanical properties of the resultant composites (Collins, Lambert, and Duan 2012a; Sobolkina et al. 2012).

2. The second major issue that restricts the efficiency of NCPs in cementitious matrix is related with the connection or bond of carbon nanoparticle with the adjacent matrix. Since CNTs exhibit tubular structure therefore reduced interfacial contact area is available as the outer face shields the inner face of the tube from being contacted with the adjacent matrix (Pan et al. 2011). Due to lacking in the interfacial contact, strong connection is not established which ultimately reduces the reinforcing efficiency of CNTs in the cementitious materials. Cwirzen et al. observed that MWCNTs added into the cement matrix along with a quality surfactant did not increase any of the mechanical strength and fracture toughness, even though well dispersion was attained (Habermehl-Cwirzen, Penttala, and Cwirzen 2008). This can be associated with poor bonding in between CNTs and cement matrix that causes CNTs to be pulled out from the cement matrix on the application of tensile stresses.

2.4 Significance of Present Research

To overcome the aforementioned issues concerning the dispersion and bonding of nano reinforcing materials with the host matrix, graphene nano sheets were explored for the first time as a reinforcing agent for high performance cementitious matrices. Graphene sheets are free form entanglement problems and therefore need comparatively lesser energy for proper dispersion. Due to very high specific surface area and large aspect ratio in comparison with CNTs they are much capable to develop strong interfacial bond with the host medium. In the commercialization of these nano carbon particles filled cementitious composites, one of the major concerns is the related expense. A little work has been done to explore the cost effective alternatives for the production of carbon nano particles to be used for modification or improvement in the properties of cement matrices. In recent wok by Prof. Ferro's research team it has been explored that carbon nano particles produced from coconut shells can be effectively used to improve the mechanical strength and fracture toughness of cementitious composites (G. Ferro et al. 2014, 2015). To continue with the productive research pertaining the cost effective production of carbon nano particles for high performance cementitious composites, bio-waste in the form of bagasse fibers, hazelnut shell and peanut shell was also investigated for the said purpose in the

current research. These particular types of agricultural wastes were selected keeping in view their economic availability as well as the excellent conversion efficiency via pyrolysis (Ferreira et al. 2015; Huff, Kumar, and Lee 2014; Nisamaneenate et al. 2014; E. Pu and Pu 1999). The present work encompasses complete characterization of the investigated materials, detailed study on their dispersion ability in water and the cement matrix, entire mechanical characterization of reinforced cementitious composites at varying proportions as well as their electromagnetic wave absorption properties in 0.2-10 GHz frequency range.

Chapter 3. Materials and Methods

3.0 General

This chapter has been divided into three phases. In the first phase, all the materials used in this research will be briefly discussed while the second phase will cover details related to number of mix proportions and the preparation scheme etc. In the last phase, the details of all the mechanical equipment used in the research work will be provided.

3.1 Materials

This section briefly discusses about the synthesis, physical, chemical, mechanical and morphological properties of the materials used in the present research work.

3.1.1 Cement

The cement used for the research work was ordinary Portland cement Type-1 (Buzzi Unicem 52.5R) confirming to the requirements of ASTM C150 (ASTM 2004). The chemical composition and physical properties of cement as per the product data sheet are presented in Table 1 & 2 (Buzzi-Unicem.SpA 2014).

Table 3.1 Chemical composition of cement

Oxides	CaO	SiO_2	Al_2O_3	Fe_3O_4	SO_3	MgO	K_2O
Content (% by mass of cement)	44	9.50	26.5	2.5	12	1.3	0.60

Table 3.2 Physical and mechanical properties of cement

Density (g/cm^3)	Color	Specific surface area (cm^2/g)	Compressive Strength (MPa)	
			3 d	28 d
2.80	Light grey	4800	50	65

3.1.2 Fine aggregates

Commercial medium grade fine aggregate purchased from "Societal Nouvelle du Littoral" satisfying European standard EN 196-1 was used for performing research on mortar specimens.

3.1.3 Water

Distilled water was used during the fabrication of cement paste and mortar specimens while curing of casted samples was done with portable water.

3.1.4 High-Range Water-Reducing Admixture (HRWRA)

Superplasticizers are chemical admixtures that are used to enhance the workability of cementitious systems at reduced water contents. It is considered to be an essential component from durability aspect of structures made in high performance concrete (HPC) or self-compacting concrete (SCC). It is possible to make HPC/SCC only with aid of superplasticizer or high range water reducing agent (HRWRA) which are able to effectively reduce water demand by 30 % in contrast to normal admixture that can reduce water content up to a maximum limit of 15%. The addition of superplasticizer prevents cement particles from agglomeration due to onset of hydration reaction and facilitates them to get dispersed into small pieces. Concrete pumping has also become possible with the advent of superplasticizer as it reduces the friction in between the pumped concrete and the pipe interface. Superplasticizers are also much effective in case of underwater concreting.

When the cement grains interact with water different surface charges develop at various phases of cement grains which motivate these grains to agglomerate in the form of clusters. Superplasticizer actually binds on the surface of cement grains and decrease surface potential which becomes negative for almost all phases of cement grains. Due to generation of similar electrostatic charges on their surface the cement grains remain well dispersed (Syed Ali Rizwan 2006).

There are three classes of chemical admixtures that are commercially used to improve the workability cement pastes, mortars and concretes. First class includes lingo-sulfonates (LS), the second class covers sulfonated naphthalene and melamine formaldehyde condensates (SNF/SMF) and the last class belongs to poly-carboxylate ethers (PCE). These classes are also named as first, second and third generation of plasticizers respectively. At normal dosage the first two generations of plasticizers are effective in

reducing water content by 5% and 12% respectively. At higher dosage these two classes have retarding effects. The third generation superplasticizer was developed in Japan and Germany in late seventies and eighties of the last century (Ramachandran 1996).

In current research work modified acrylic polymer based high range water reducer bearing commercial name "Mapei Dynamon SP1" was used. It is specially designed for precast industry by MAPEI and consists of water solution containing 30.5% acrylic polymers with no formaldehyde. The main features concerning physical and chemical characteristics of Dynamon SP1 are given in Table a below (Mapei n.d.):

Table 3.3 Features of Dynamon SP1 superplasticizer

Feature	Description
Consistency	Liquid
Colour	Amber
Density ISO-758 (g/cm^3)	1.09±0.02 at 20^oC
Dry content EN 480-8 (%)	30.5±1.5
Chlorides soluble in water EN 480-10 (%)	<0.1 (EN 934-2)
Alkali content (Na_2O equivalent) EN 480-12 (%)	<2.5

3.1.5 Dispersing Agents/Surfactants

Due to the non-suspensibility of nano particles in water, dispersant is needed to obtain stable liquid suspension, preventing precipitation or floating of nano particles. In previous literature various dispersants such as acetone, ethanol, nitrite acid, sulphate acid, gum arabic, alcohol and formic acid (G. Y. Li, Wang, and Zhao 2005) have been analyzed in preparing liquid suspensions containing carbon-based nano-particles such as carbon nanotube.

Wang et al. used gum arabic as a surfactant for the dispersion of multiwalled carbon nanotubes (MWCNT's) in cement paste and reported 57.5% enhancement of ultimate toughness index (B. Wang, Han, and Liu 2013). Pu et al. investigated the dispersion of graphene in aqueous solutions with four different types of surfactants, a cation type surfactant, tetradecyl-trimethyl-ammonium bromide; a non-ion type, poly-ox-ethylene (40) nonyl-phenylether; an anion type, sodium-dodecyl-sulfate; and a polymer type, poly-carboxylate (N.-W. Pu et al. 2012). He concluded that non-ionic surfactant poly-ox-ethylene (40) nonyl-phenylether is much efficient to properly disperse GNPs. Saez et.al. used gum Arabic as a dispersing agent for MWCNT's in cement paste and observed modest gains in compressive strength and Young's modulus (Sáez de Ibarra et al. 2006). Based on the previous research and availability in laboratory, the use of gum arabic and

sodium poly-naphthalene sulfonate from Schlumberger were investigated as dispersing agents for GNPs in cementitious matrices. The stability of GNP suspension made with such dispersants was visually monitored at various time intervals to assess the attained level of dispersion in water while dispersion inside cement matrix was determined via scanning electron microscopy. Finally on the basis of dispersion levels achieved in water, the best dispersant was selected for rest of the future analysis with high performance cementitious matrices.

The mechanism of dispersion is much similar to the mechanism of HRWRA. The dispersant/surfactant comprised of negatively charged organic molecules that bind primarily at the GNP particle-water interface. Initially GNP particles carry a mixture of positive and negative residual charges on their surface. In liquid suspension, the GNP particles tend to flocculate due to electrostatic attraction in between the oppositely charged adjacent GNP particles (Figure 3.1). Molecules of dispersant play their role in neutralization of surface charges carried by GNP particles and makes all GNP particles to carry similar charges. Due to electrostatic repulsion in between similar charged GNP particles they remain dispersed in the liquid suspension.

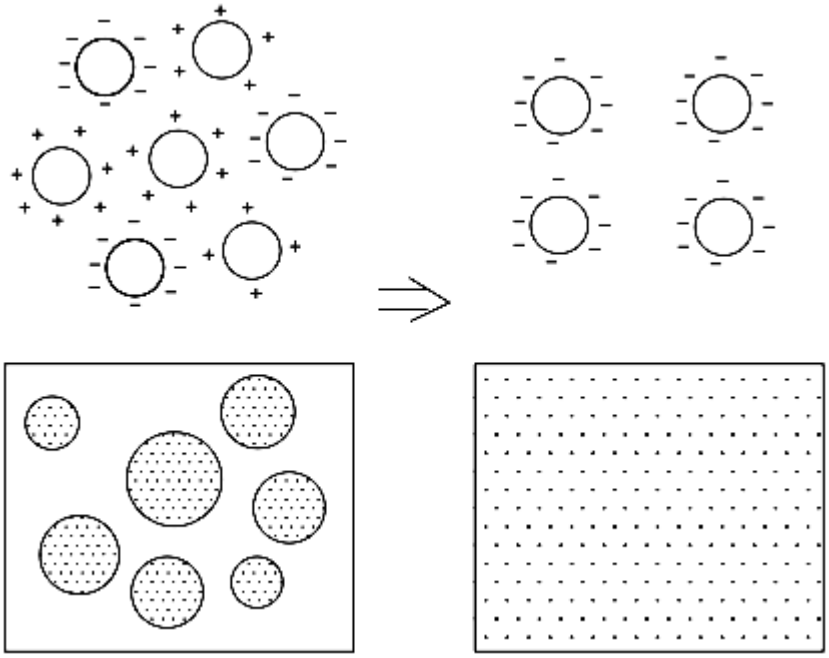

Figure 3.1 Dispersing action of a typical dispersant for GNP particles (Sixuan 2012)

3.1.6 Graphene Nano Platelets (GNPs)

GNPs are commercially available in two different grades of varying sizes at Cheap Tubes i-e Grade 3 which is known as an industrial grade and Grade 4 which is recognized as research grade, whose properties and cost is given in Table 3.4. GNPs Grade 4 (GNP _4) have been used in pristine form and after functionalization with COOH group.

Table 3.4 Properties of grade 3 and grade 4 GNPs

Property	Unit	Grade 3 GNPs	Grade 4 GNPs
Surface Area	m^2/g	600-750	>750
Thickness	Nm	8	<5
Layers		4-5 layers	<4
Particle dia	µm	≤ 2	
Cost	Per kg	450 $	2000$

3.1.7 Carbonaceous nano/micro inert particles (Synthesis/Properties)

Cellulose based carbon nano/micro particles were synthesized from agricultural bio-waste that include bagasse fibre, hazelnut and peanut shells. The entire synthesis scheme comprised on the following three stages:

3.1.7.1. Chemical Treatment of Bio-Waste

In the recent research on cellulose based carbon, it has been found that a chemical treatment of bio-waste with sodium hydroxide solution prior to carbonization reduces the content of hemicellulose and increases the final yield with an improved surface morphology (Cho et al. 2011; Y. H. Han et al. 2007). Kim et al. reported that pre-treatment with 10% alkali solution was quite useful in reducing the weight loss and increasing the ultimate product yield of kenaf fibres during carbonization (J. M. Kim et al. 2011). Cho et al explored the effect of chemical pre-treatment on jute fibres using 10% NaOH solution and observed significant modification in their surface morphology. The reduction in the hemicellulose content via alkali treatment was concluded by Han et al. and Mehar et al. in case of kenaf and jute fibres respectively (Afroz, Sadaq, and Mohammed 2013; Y. H. Han et al. 2007).

Keeping in view the aforementioned advantages of chemical pre-treatment, it was decided to treat the bio-waste with 1% NaOH solution prior to subjection on carbonization. The chemical pre-treatment was conducted by soaking each type of waste in 1wt% NaOH for the duration of 24 hrs. Finally the pre-treated bio-waste was neutralized (pH = 6.5) using

distilled water and dried at 90^{o}C for 24 h in an electric oven. A few prominent observations during chemical treatment are listed in Table 3.5 as follows:

Table 3.5 Treatment details for carbonized particles

Material	Treatment solution	Duration of treatment	Observations
Bagasse Fiber	1% NaOH solution (0.25M)	24 hrs	○ 9.11% mass loss observed ○ The solution became dark brown solution
Hazelnut Shell	1% NaOH solution (0.25M)	24 hrs	○ 2.1% mass loss was observed ○ The solution became dark brown
Peanut Shell	1% NaOH solution (0.25M)	24 hrs	○ 4.2% mass loss was observed ○ Color of solution changed to dark brown

3.1.7.2. Pyrolysis/Carbonization of Bio-Waste

Pyrolysis is a process that involves thermochemical decomposition of organic matter at elevated temperatures in the absence of oxygen. It is basically a combination of two greek words “pyro” defines fire and “lysis” defines separating. During pyrolysis simultaneous changes in chemical composition as well as physical nature of materials take place. These changes are irreversible and therefore permanent in nature. It is an endothermic process usually accompanied with the production of solid charcoal and flammable gases. The flammable gases produced are the combination of carbon di oxide CO_2, carbon mono oxide CO, methane CH_4, ethane CH_2 and water vapors.

The process of pyrolysis was carried out using a quartz reactor having internal diameter 8 cm, tube length of 40 cm and a heating zone of 20 cm, placed inside an electric furnace operated at an elevated temperature of 850^{o}C with a heating ramp of 1^{o}C/min. The holding time at the prescribed temperature was kept constant i-e 1hr for each and every type of bio-waste. The purging Ar (99.999% purity) gas was purged into the reactor at 0.2 bar throughout the carbonization process to maintain an inert atmosphere. The inert gas flow was maintained inside the reaction chamber till the time it attained back its normal room temperature condition to avoid any possible structural damage to the pyrolyzed material due to presence of oxygen.

The gases produced during the process of pyrolysis were passed through a scrubbing system to prevent nuisance. The detail of scrubbing solution is given in Table 3.6.

Table 3.6 Details of scrubbing solution used during pyrolysis

Scrubbing solution	Observations
Tap water	○ Water reduced the smoke and nuisance a little bit ○ Color of water was also turned brown ○ The water started giving vinegar type smell ○ The surface of water became oily due to the condensation of tar
20% (v/v) Acetic acid solution	○ Solution changed its color ○ It also reduced the nuisance, more effective than water ○ Solution turned to dark brown
1% NaOH solution (0.25M)	○ It substantially reduced the nuisance ○ Most effective than others

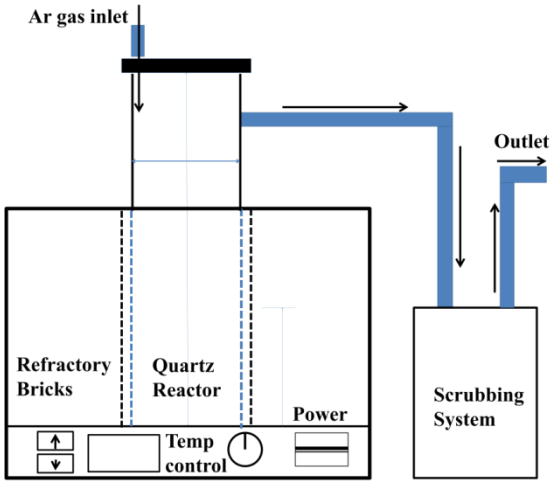

Figure 3.2 Setup for pyrolysis of bio-waste

3.1.7.3. Milling of Carbonized Bio-Waste to Nano size

The pyrolyzed bio-waste was ground into powdered form with particle size ranging from nano scale to sub-microns. After many trials the entire grinding process was divided into three main stages, ordered in such a way that every next stage results in more and more refinement of particle size. The first stage involves manual grinding while the next two stages involve grinding by mechanical means.

a. 1st Stage (Grinding into mm size)

Initially raw pyrolyzed bio-waste was ground into the coarse particles of approx. 1mm size using a manual milling technique. Mortar and pestle was used for performing the milling operation with its duration varying proportionally with the hardness of the material to be grinded. A few drops of ethanol were added during manual grinding to avoid dust particles from blowing off into the near surroundings.

b. 2nd Stage (Grinding from mm to microns)

The coarse particles of carbonized bio-waste were further ground to micron size by mechanical means i-e ball milling technique. The mm size powdered particles of pyrolyzed material were fed into plastic containers in solution form (1:5) along with 20 steel balls of 10 mm diameter. Ball milling operation was performed for 24 hrs. After that particle size D50 and D90 of powdered pyrolyzed waste was analyzed using laser granulometry.

c. 3rd Stage (Grinding from microns to sub-microns/nano scale)

For further refinement of particle size to nano scale or sub-microns level, attrition milling was selected as the last mechanical mode of grinding. The attrition milling is a device for mechanically reducing solids particle size by intense agitation of the slurry of material being milled and coarse milling media. It is usually adopted to produce particles of narrow size range with an average size of 100-250 nm (Sakthivel, Krishnan, and Pitchumani 2008). It is consisted of discs connected to a shaft that is driven by a motor. The rotations of discs produce high shearing stresses and vigorous movement of grinding material (small balls of alumina).

Powder to alumina balls ratio was kept 1:10. Ethanol was used as a grinding media. Attrition milling was performed for the duration of 1h. It was observed during grinding, that if the duration of attrition milling is exceeded more than an hour then the average particle size of powder tends to increase instead of decrease. The particles break down into smaller pieces initially during 1h milling but if the operation continued then they again start to re-agglomerate due to the development of the surface charges. The ground material was washed with H_2O to remove ethanol and dried in oven.


a
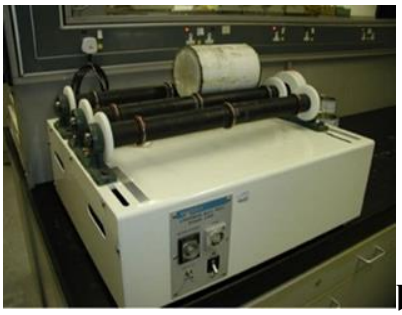
b

c

Figure 3.3 Milling of carbonized particles via mortar and pestle (a), ball milling (b) and attrition milling (c)

Particle size distribution curves of nano/micro carbonized particles generated on the basis of laser granulometry results are given in Appendix A. The distribution has been plotted after ball milling as well as the final distribution achieved at the end of attrition milling operation. Since the sensitivity of the measurements by laser apparatus was maximum up

to 1 micron therefore the steep slope of PSD curves is an indicator that the majority of the particles possess an average size of less than a single micron. To have an idea concerning the true particle size of carbonized particles scanning electron microscopy was done which will be discussed later on in chapter 4.

3.1.7.4 Physical Properties of Carbonized Nano/Micro Particles

Physical properties of the produced carbon nano/micro particles are very significant contributors towards the reinforcing action of these particles in cementitious matrices. The main physical characteristics of nano/micro carbonaceous particles are summarized in Table 3.7.

Table 3.7 Physical properties of carbonaceous particles

Nano/micro carbonized particles (NMCPs)	D 50 (nm)	D 90 (nm)	BET surface area (m^2/g)	Density (g/cm^3)
Carbonized bagasse fiber (CBF)	600	1250	19.2	2.26
Carbonized hazelnut shell (CHS)	750	1300	14.5	2.35
Carbonized peanut shell (CPS)	600	1200	19.4	2.20

3.2 Methods

This section covers the details about experimental procedures followed during the preparation and testing of cement composites as well as the mechanical equipment used to perform these experiments.

3.2.1 Mix Proportions

Total 32 batches of cement paste specimens and 06 batches of mortar specimens were prepared to analyze the effect of the type and the content of nano/micro carbon inerts on the mechanical properties. Among 32 batches of cement paste, 14 of them contain two different types of GNPs at varying percentages. For each batch of cement paste 4 prisms of 20mm *20mm *75mm sizes were prepared for flexural tests. While in case of mortar specimens each batch comprised on 3-prisms of 40mm *40mm *160mm in size.

For cement paste batches w/c ratio was fixed at 0.35 and the content of superplasticizer was kept as1.5 wt% of cement. The selected water cement ratio matches very well with the water demand of cementitious systems and not only gives adequate flow-ability to the fresh mix during preparation but also the attained strength is high enough to study the effect of nano particles on mechanical behavior of high performance cementitious

composites. Two types GNP particles with varying dimensions and three types of carbonized particles of varying origins were used in the research. The selected percentage additions of carbonaceous inerts were 0.025%, 0.05%, 0.08%, 0.2%, 0.5%, 1.0% by weight of cement in case of paste specimens. For mortar specimens only those optimum proportions were selected which have given best mechanical performance in the paste phase. The reason for the selected six proportions in paste phase was to gain a facilitation for comparison of results with the previous work done by Prof. Ferro group concerning effective application of carbon nanotubes and carbonized particles of coconut in cementitious composites (Alessandro 2012; G. Ferro et al. 2014, 2015). For mortar batches the water to cement ratio maintained at 0.35. The content of superplasticizer was increased from 1.5 wt% to 1.8 wt% of cement. Cement to sand ratio was kept as 1:1.5 as given in the literature as an ideal recipe for self compacting mortars (Basheerudeen and Sivakumar 2014).

3.2.2 Preparation Scheme

The mixing scheme of cementitious systems is very crucial for their performance in fresh as well in the hardened state. A consistent mixing regime was followed for the preparation of all the cement composite that is described below:

i. In the batch of GNP particles, GNPs were initially dispersed in water with the aid of dispersant (except for the control batches in which dispersing agent was not added) and probe sonication for 15 minutes using 750 watt Sonics Vibracell ultrasonic probe operated at amplitude of 30%. During probe sonication, the beaker containing GNP particles suspension was kept under water bath to lower the temperature of the system. Furthermore the beaker was covered from the top using paraffin to avoid evaporation of water. After dispersion, Dynamon SP1 was added as superplasticzer to attain the desired flow-ability.
ii. For the batches that contained carbonized particles produced from bio-waste, carbon suspension was prepared using mixing water and superplasticizer Dynamon SP1, sonicated in ultrasonic bath for 15 minutes before moving on towards their final mixing with cement.
iii. In the second stage, the prepared suspensions of GNPs or NMCPs were mixed with cement using a mechanical mixer.
iv. During casting, cement was placed inside plastic beaker and dry mixing was done for 1 minute at low mixing speed of 440 rpm.
v. GNP particles and carbonized inerts suspensions were added slowly into the cement with the mixing speed unchanged for duration of 1.5 minutes.

vi. Final finishing mixture was further mixed for duration of 2.5 minutes at a high mixing speed of 660 rpm.

The procedure adopted for the preparation of mortar specimens is more or less similar to the one adopted for the preparation of cement paste specimens. In case of mortar, mixing was carried out using a Hobart mixer of 5L capacity. Dry mixing of cement and sand was done for three minutes to attain a homogeneous mixture.

Paste specimens were casted using plexi-glass molds while for mortar specimens steel molds were used. The specimens were casted in three layers and tamping was done as guided by ASTM C109/C109 M-08 after placement of each layer to avoid consolidation issues. After preparation the paste specimens were kept in covered plastic box partially filled with water for initial 24 h while mortar specimens were covered with plastic sheets to prevent loss of moisture and to reduce drying shrinkage. After demoulding, specimens were immersed in water and final curing was done at room temperature ($20\pm2^{o}C$) for 28 days. Pure cement paste batch and plain mortar batch was casted as control batch for comparison.

3.2.3 Specimen Designation

The description against the notations by which specimens are designated in this research is given in Table 3.8. To further add information concerning the percentage addition of carbonized particles, the added content is placed after the notation using under-strike. Like GNP_3_0.025 represents a grade-3 GNP reinforced formulation with an added content of 0.025% by weight of cement.

Table 3.8 Specimen Designations

Notation	Description
GNP_3	Grade 3 graphene nano-platelets reinforced formulation
GNP_4	Grade 4 graphene nano-platelets reinforced formulation
CBF	Carbonized bagasse fiber reinforced formulation
CHS	Carbonized hazelnut shell reinforced formulation
CPS	Carbonized peanut shell reinforced formulation

3.2.4 Characterization Method of Measuring Flow

The workability of self-compacting paste or mortar (SCP/SCM) is generally monitored in terms of flow measurements. The flowing ability of high performance cementitious matrices is measured using Hagerman's mini slump cone of 60mm *70mm *100mm

dimensions. The flow measurement is taken just after 60s of mixing completion to retain consistency in the acquired results for each proportion. During the test, measurements of total spread with its associated time as well as T25 spread time are recorded for each proportion of HPMC. T25 spread time is defined as the time taken by paste or mortar to achieve a spread of 25 cm while T50 spread time is linked with a spread of 50 cm. The concept of T25 spread time was proposed by Rizwan et al (Rizwan and Bier 2012) based on the analogy of measuring T50 spread time in case of SCC using Abram's cone as in both cases the ratio of specified spread and the base diameter of respective measuring cone remains the same i-e 2.5. Therefore it is believed that inferences obtained from T50 spread time of SCC can be considered similar to those obtained from proposed T25 spread time of SCP and SCM. Based on the values of flow it is possible to analyze the effects of nano carbon particles addition on the fresh properties of cementitious matrices. The analysis of workability also supports in the discussion concerning the modification of properties of nano/micro carbon particles reinforced cementitious composites.

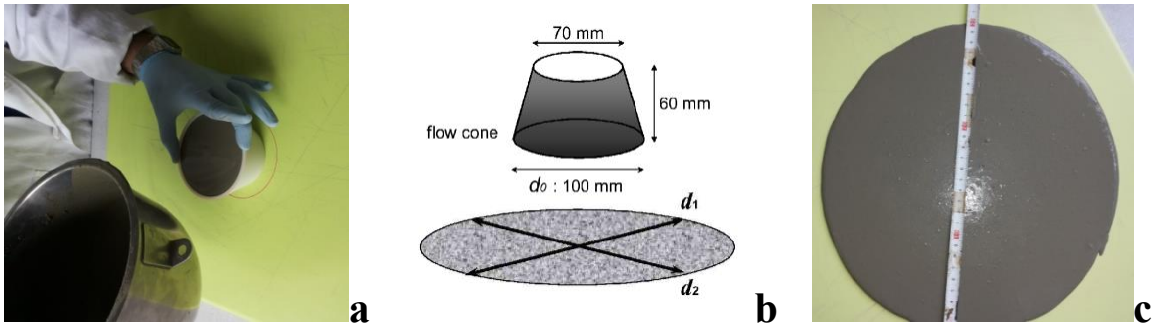

Figure 3.4 Flow measurements (a&c) and typical dimensions (b) of Hagerman's mini slump cone

3.2.5 Characterization Method of Mechanical Performance of Composites

The mechanical performance term covers the aspects of strength both in flexure and in the compression, as well as the ductility of the HPCC measured in the form of fractures toughness.

3.2.5.1 Characterization Method of Behavior in Flexure

Three point bending test with a clear span of 60mm was performed on 128 prism specimens of cement paste having dimensions of 20mm *20mm *75mm. The same test was repeated on 21 prisms of cement mortar with dimensions of 40mm *40mm *160mm at a clear span of 120mm. The tests were performed according to the standard set forth in ASTM C348. The specimen's surfaces were smoothened by a rotary polishing device with #180 WX FLEX paper. A standard 2mm wide and 12mm deep notch was carefully

machined in the center of each cement paste specimen while the notch size selected for mortar specimens was 2mm in width and 24mm deep due to their relatively large size. Remet type TR100S, s/n 3714 abrasive cutter with 2mm thick diamond cut-off wheel was used to groove notch in the center of each specimen. Finally notched specimens of cement paste and mortar were tested using Zwick-Line z010 single column flexural testing machine having maximum load capacity of 1kN as shown in Figure 3.5 while for the cement mortar sample 50 KN load cell was used. All tests were performed under CMOD (Crack Mouth Opening Displacement) control mode with an opening rate fixed at 0.003mm/min. Highly accurate and sensitive extensometer (clip on gauge) was employed for the measurement of crack opening and the data was digitally recorded.

3.2.5.2 Characterization Method of Behavior in Compression

The two broken halves of a prism specimen obtained from the three point bending test were tested in compression with accordance of ASTM C349 via Zwick-Line z010 machine carrying a maximum load cell of 100 KN. The rate of displacement was kept at 0.50 mm/min for loading and 0.80 mm/min for unloading the specimens. Total 190 cement paste specimens and 42 specimens of cement mortar were tested in compression. The results in compression represent the average value from six specimens.

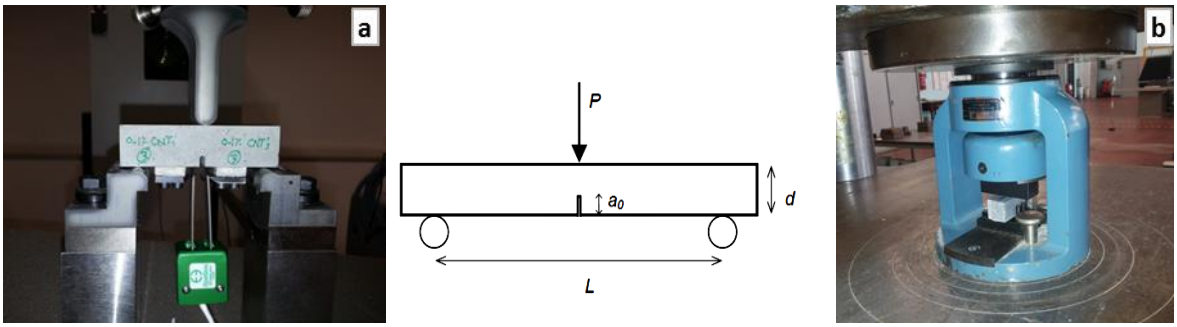

Figure 3.5 Experimental set up for CMOD controlled three point bending (a) and compressive strength test

3.2.6 Characterization Method for Microstructural Investigation of Composites

The porosity, microstructure and mineralogical phases of high performance cementitious formulations were investigated using mercury intrusion porosimetry (MIP) and scanning electron microscopy (SEM). To perform SEM and MIP analysis, very small pieces of approx. 1x1cm^2 in size were collected after compression test. These tiny broken chips were immersed in acetone for 24h to stop further hydration in the surface zone and then submerged in isopropanol to remove the traces of acetone left into the small pieces (Hewlett 1998). For SEM observations, the chip specimens were further treated for normal

preparations including vacuum drying and gold coating while for MIP the samples were oven dried at 105^{o}C for 24h duration before. Moreover, the contact angle of 140^{o} was selected while evaluating porosity through MIP analysis.

3.2.7 Characterization Method for Relative Water Absorption Measurement

The relative percentage water absorption was measured according to the standard set forth in ASTM C642. After initial moist air curing for the period of 24 h the specimens were demoulded, numbered and weighed. Thereafter these specimens were immersed in water for 28 days of submerged curing. Finally at the end of moist water curing, the specimens were taken out of water and weighed again in saturated surface dry (SSD) condition after removing the surface water from samples using a towel or a tissue paper. From difference in weights water absorption was calculated as given in Equation 3.1.

Initial weight at 24 hrs moist air curing = w_a
Final weight at 28 days moist water curing = w_b

$$\%\ absorption = \left(\frac{w_a - w_b}{w_a}\right) * 100 \qquad Eq.3.1$$

3.2.8 Characterization Method to Measure the Permittivity of Composites

Complex permittivity measurements of cement composite containing nano/micro carbonized filler is performed in the frequency range 0.20-10 GHz with a commercial dielectric sensor (Agilent 85070D) and a network analyzer (E8361A). The system was calibrated for water and air before starting measurements. Such measuring system was adopted keeping in view its feasibility to work on specimens with smaller dimensions and it also allows wide-band characterization as well. In all measurements it was tried to ensure perfect contact between sensor probe and specimen's surface. Measurements were taken at six different sites of each single specimen to ensure homogeneity and reduce error margin; the reported results in chapter 7 is the average of the six measurements. Also most of the details concerning the type of specimens investigated for this purpose, selected proportions and some numerical calculations as well as the comparison, all are compiled in chapter 7 of the dissertation.

Chapter 4. Characterization, Dispersion and Flow aspects of GNP and Submicron Carbonized Particles

4.0 General

This chapter includes detailed characterization of the investigated carbon particles comprising GNPs and synthesized NMCPs by thermo-gravimetry, scanning electron microscopy and Raman spectroscopy. Along with characterization, the major aspect of dispersing these reinforcing particles in the host cementitious matrix has been discussed in the second phase of the chapter. In the last phase, the effect of these reinforcing particles on flow-ability of high performance cementitious system has been analyzed.

4.1 Characterization of GNP and Submicron Carbonized Particles

4.1.1 Thermo-gravimetric Analysis (TGA) of Nano/Micro Carbon Particles (NMCPs)

Thermo-gravimetric analysis is a technique used to measure change in physical and chemical properties occurring inside a material either as a function of increasing temperature at the constant heating rate or as a function of time at constant temperature or constant mass loss. Physically it is effective to measure vaporization, sublimation, absorption, adsorption and desorption etc. while chemically it is much informative against chemisorption, desolvation, decomposition and solid-gas reactions. Usually it is used to identify those selected characteristics of materials that involve mass loss or gain due to decomposition, oxidation or loss of volatiles. Its major applications include

- Characterization of material based on its characteristic decomposition pattern
- Assessment of degradation mechanisms and reaction kinematics
- Determination of organic content
- Determination of inorganic content
- Especially useful to assess the thermal stability of polymeric materials, thermosets, elastomers, composites, plastic films, fibres, coatings and paints etc.

To understand the behavior of organic waste during pyrolysis, thermo gravimetric analysis (TGA) was performed. All the experiments were carried out at a flow rate of 35 ml/min and a heating rate of 10 °C/min in the temperature range from 25 °C to ~1000 °C. About 10 mg of each sample was spread in a uniform layer. All the experiments were repeated and the mean values of the resulting data were used to guarantee error margins to be limited within the range of 3%.

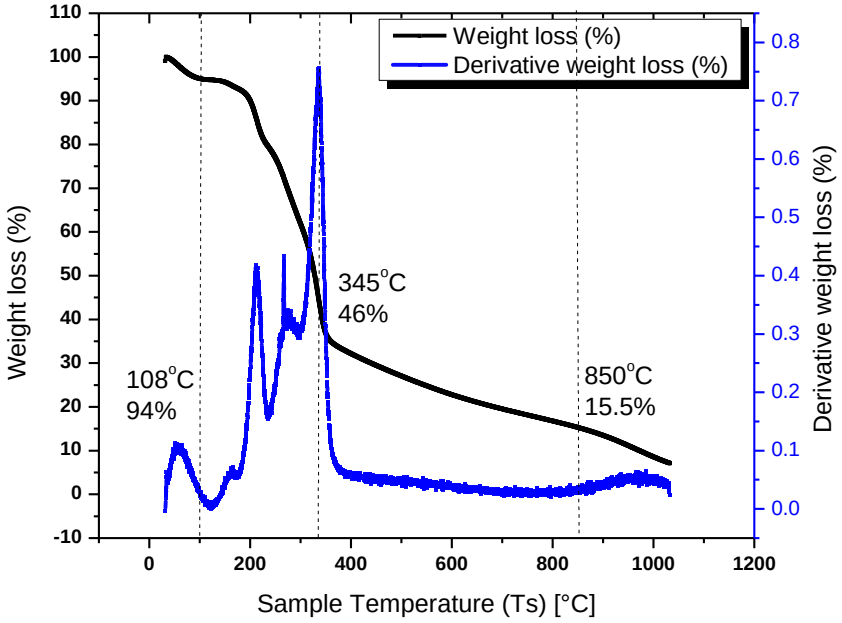

Figure 4.1 TGA and DTG of bagasse fiber in argon

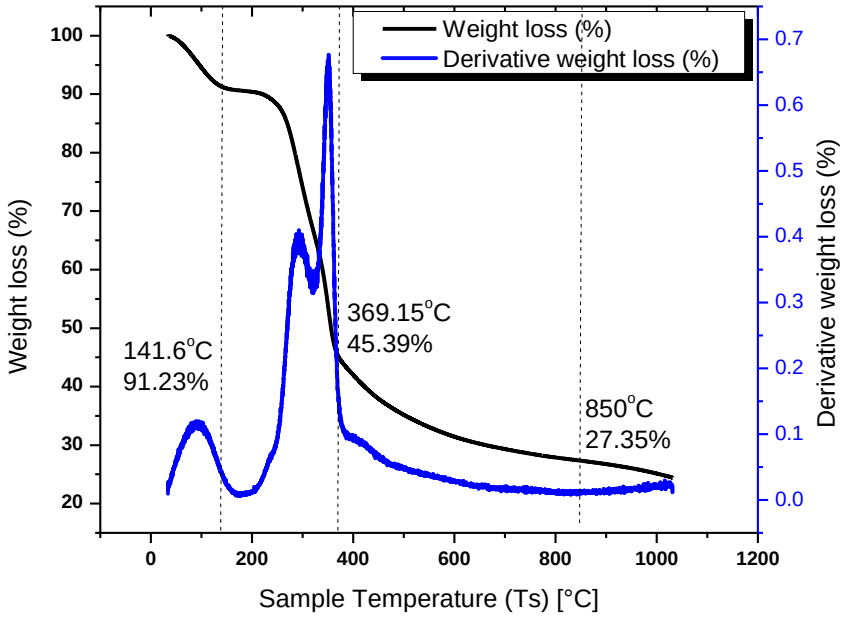

Figure 4.2 TGA and DTG of hazelnut shell in argon

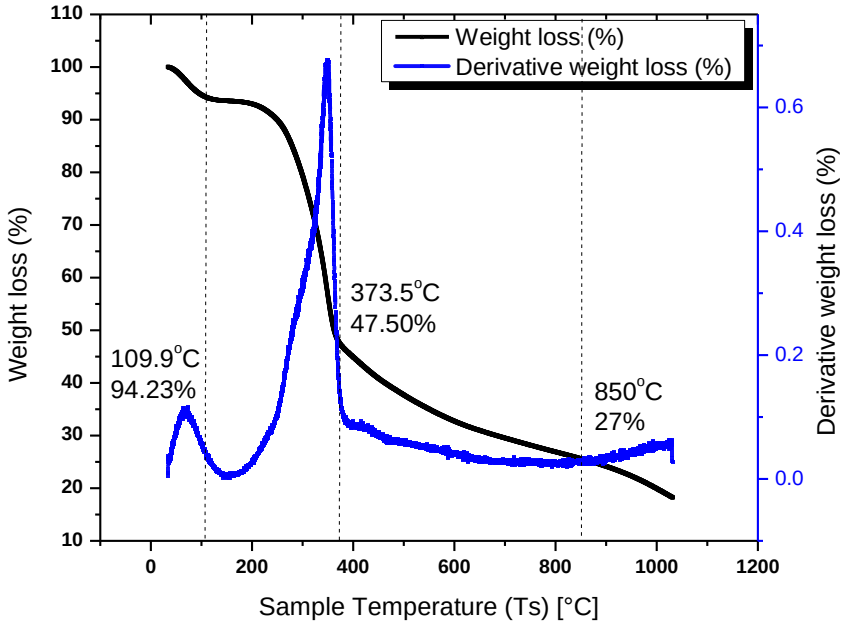

Figure 4.3 TGA and DTG of peanut shell in argon

From TGA it is observed that at the temperature of 600 ^{o}C, almost complete thermal degradation of biomass occurs. First mass loss was found in a temperature range of (50<T<150 ^{o}C) which is due to evaporation of moisture and some extractive compounds. The second major loss was observed in a temperature range of (200<T<360 ^{o}C) which is mainly associated with the thermal degradation of hemicellulose and cellulose. Lignin is more stable component and therefore it is much difficult to decompose. It presents a large range of thermal degradation from 150-900 ^{o}C or even higher than that varying with the type of biomass (Giudicianni, Cardone, and Ragucci 2013; Qian Liu et al. 2008; Yang et al. 2007). Therefore the final degradation step in a temperature range of (360<T<600 ^{o}C) is mainly associated with lignin degradation.

The final product yield differs with the type of biomass due to variation in the structure as well as in the percentages of cellulose, hemicellulose and lignin. The final yield is mainly based on the proportion of three basic constituents' i-e cellulose, hemicellulose and lignin present inside that particular biomass. In case of lignin the generated solid residue is much more than 40 wt% of its original weight as reported by Yang et al.(Yang et al. 2007). In the analyzed bio-waste of varying origins, the hazelnut shell produced maximum char content of approx. 28 wt%. In case of bagasse fibre and peanut shell the maximum product yield attained was almost 16% and 27% respectively.

The carbonized bio-waste was further thermally investigated in the temperature range of 25-1000^{o}C. The experiments were performed on powdered sample (~10 mg) in both treated and raw state with the constant airflow rate of 35 ml·min^{-1} during the entire experiment. The raw and chemically treated state of carbonized particles was differentiated with the addition of R or T before their designated names. The temperature ramp was fixed at 10^{o}C/min for all experiments. The experiments were repeated three times each to enhance the reliability and reduce the standard errors ±1 °C (within a confidence interval of 95%).

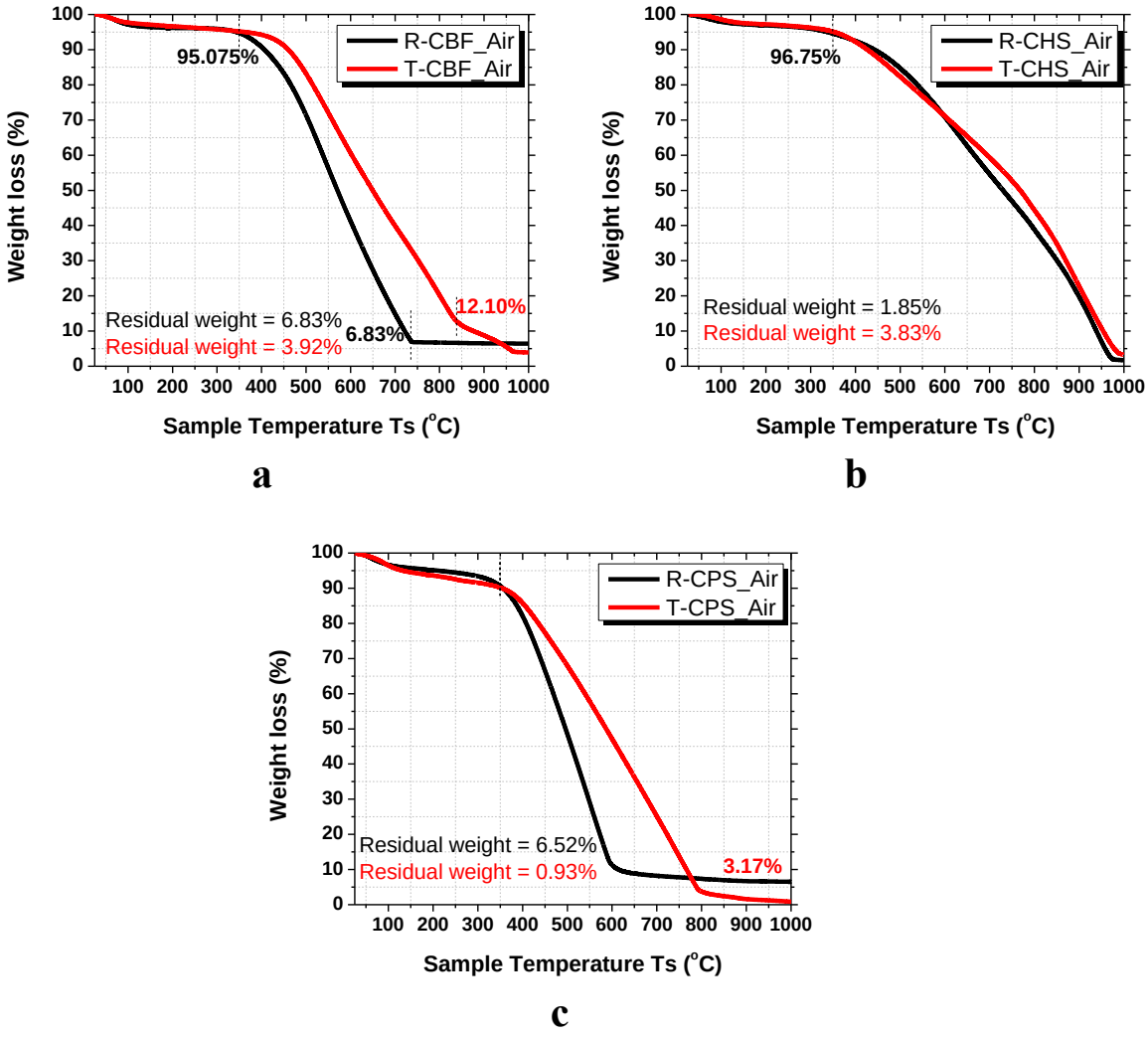

Figure 4.4 TGA of carbonized particles produced from bagasse fiber (a), hazelnut shell (b) and peanut shell (c)

In the TGA of carbonized bio-waste, two different exothermic reaction regions were observed (Figure 4.4 a, b & c). First region is due to the evaporation of moisture from the pores surface while second region is related to the combustion of fixed carbon (Kok and Özgür 2013). The residue obtained varies between 1.5-3% may be due to the unreacted inorganic compounds or silica present in biomass sample.

There is a slight variation observed in the initiation temperature and burnout temperature of chemically treated and untreated carbonized biomass especially in case of carbonized bagasse fibres and peanuts shell. It was observed that the chemical treated carbonized biomass sample degrades lesser at a given temperature than the untreated one but the ultimate mass loss is higher. Chemical treatment causes partial removal of hemicellulose

resulting in lesser degradation initially. The treatment also disintegrates lignin and cellulose resulting in more mass loss at the end. The treatment resulted in removal of some part of hemicellulose and some quantities of glucose molecules resulting in lesser smoke and smell production during large scale pyrolysis as was observed by Kok et al. (Kok and Özgür 2013). Due to chemical treatment thermal degradation range of carbonized bagasse fibre and peanuts shell was also observed to be expanded as displayed in Figure 4.4abc.

4.1.2. Surface Morphology by Scanning Electron Microscopy (SEM) and Composition by Energy Dispersive X-Ray (EDX) Spectroscopy

The field emission scanning electron microscopy was done using FE-SEM Zeiss Supra-40 Field Emission Scanning Electron Microscope on powdered samples of GNP and NMCPs. The purpose was to identify the microstructure, morphology, particle size and surface texture of the investigated powder particles. In addition to the FESEM micrographs, qualitative chemical composition by EDX analysis was also obtained for each sample.

SEM micrograph of GNP_3 particles is shown in Figure 4.5 at 10k and 100k magnifications. Physical appearance of GNP_3 particles present considerable degree of intercalation showing great needs for dispersion and ultra-sonication. Almost all the particles are less than 2μm in diameter. From SEM micrographs displayed in Figure 4.6, GNP_4 particles are observed as thinner plates of less than 5nm thickness and possess large aspect ratio revealing their excellent reinforcing efficiency. Another striking observation is the wrinkled surface texture of GNP_4 particles. The wrinkled surface can provide efficient mechanical interlocking between graphene sheet and the cement matrix, thereby may contribute to enhance the interfacial load transfer between the graphene sheet and the cement matrix resulting in better bond strength.

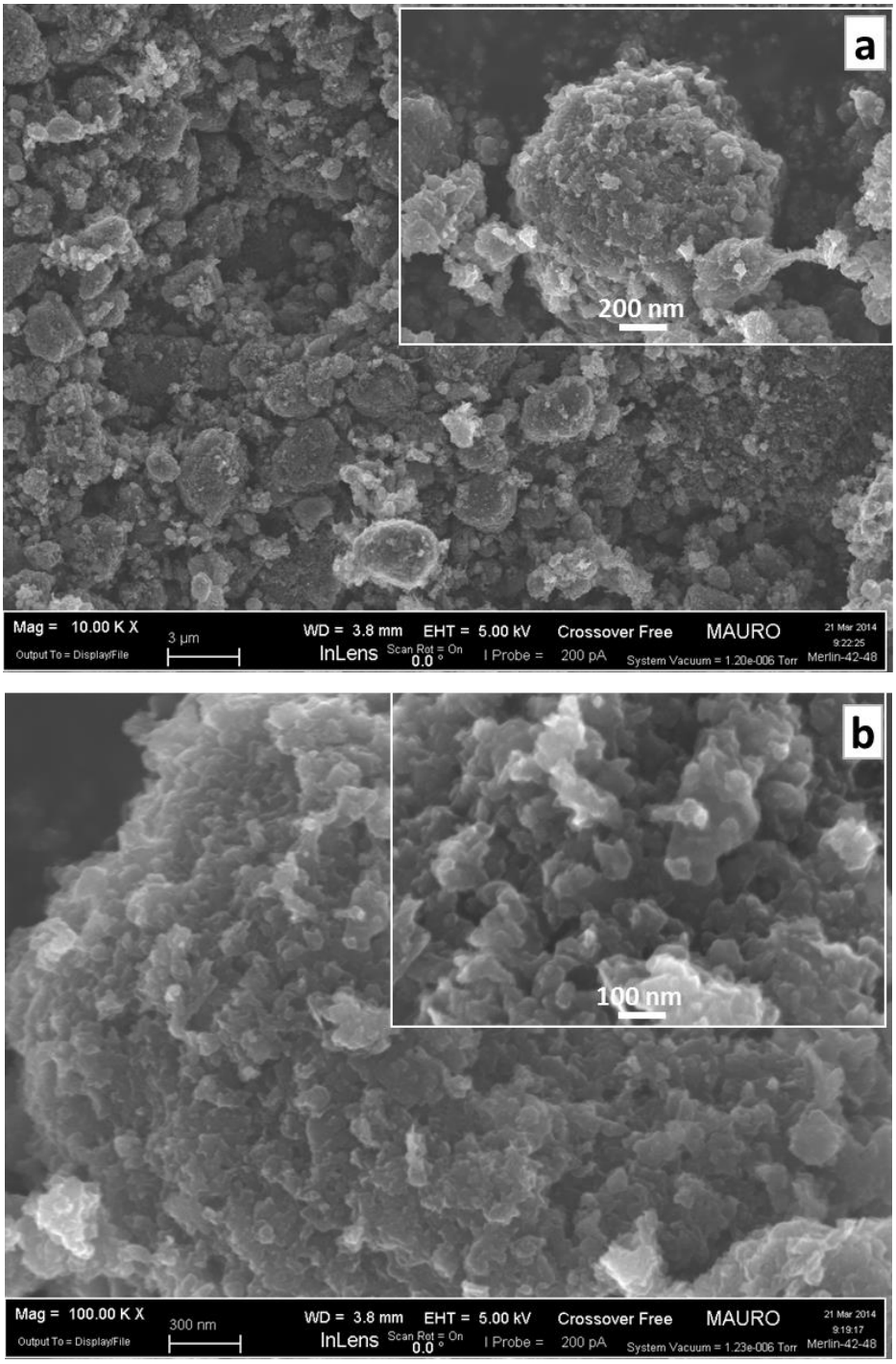

Figure 4.5 FESEM micrograph of grade-3 GNP particles at 10k (a) and 100k (b) magnifications

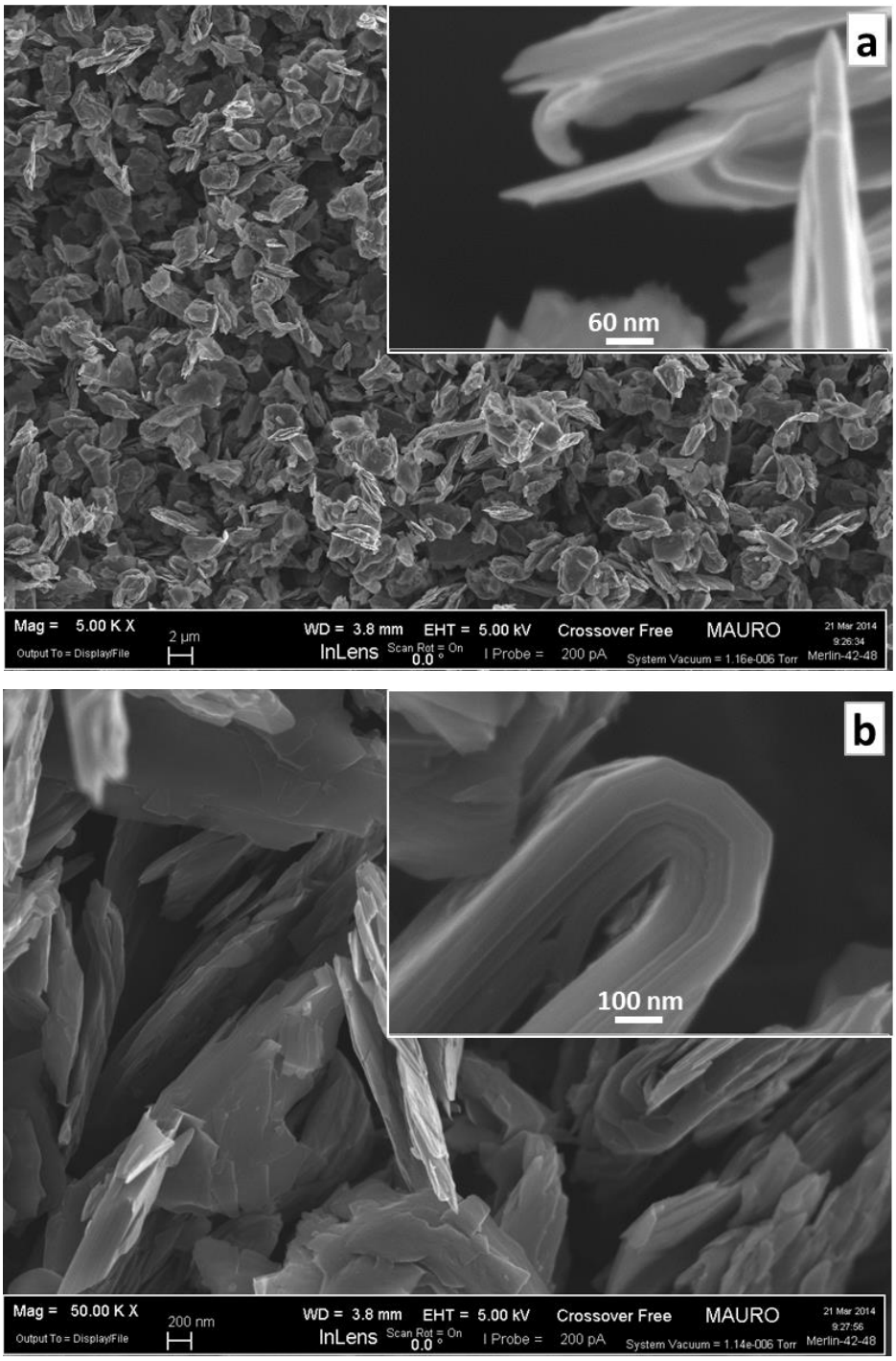

Figure 4.6 FESEM micrograph of grade-4 GNP particles at 10K (a) and 100k (b) magnifications

SEM micrographs shown in Figure 4.7 demonstrate that carbonized particles of bagasse fibers are in the form of plates/flakes with shape varying from angular to flat and elongated. These plates exhibit glossy and smooth texture with average plate size restricted to less than 800 nm and thickness varying from less than 100 nm up to 300 nm.

Such plates seem to be free from entanglement problem as associated with nanotubes and nanofibers, therefore it would be relatively easy to disperse them in the cement matrix.

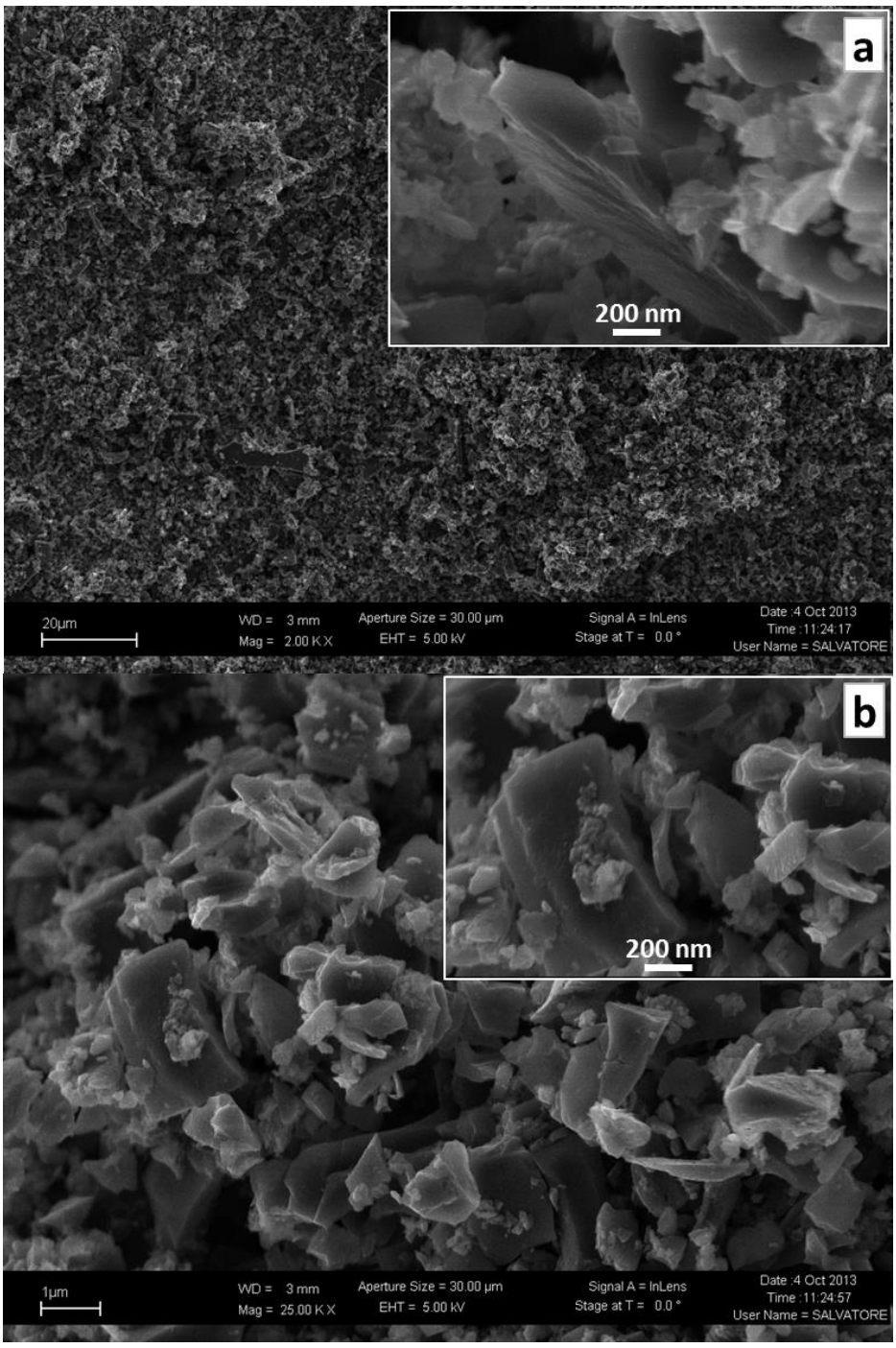

Figure 4.7 FESEM micrograph of CBF particles at 2K (a) and 25K (b) magnifications

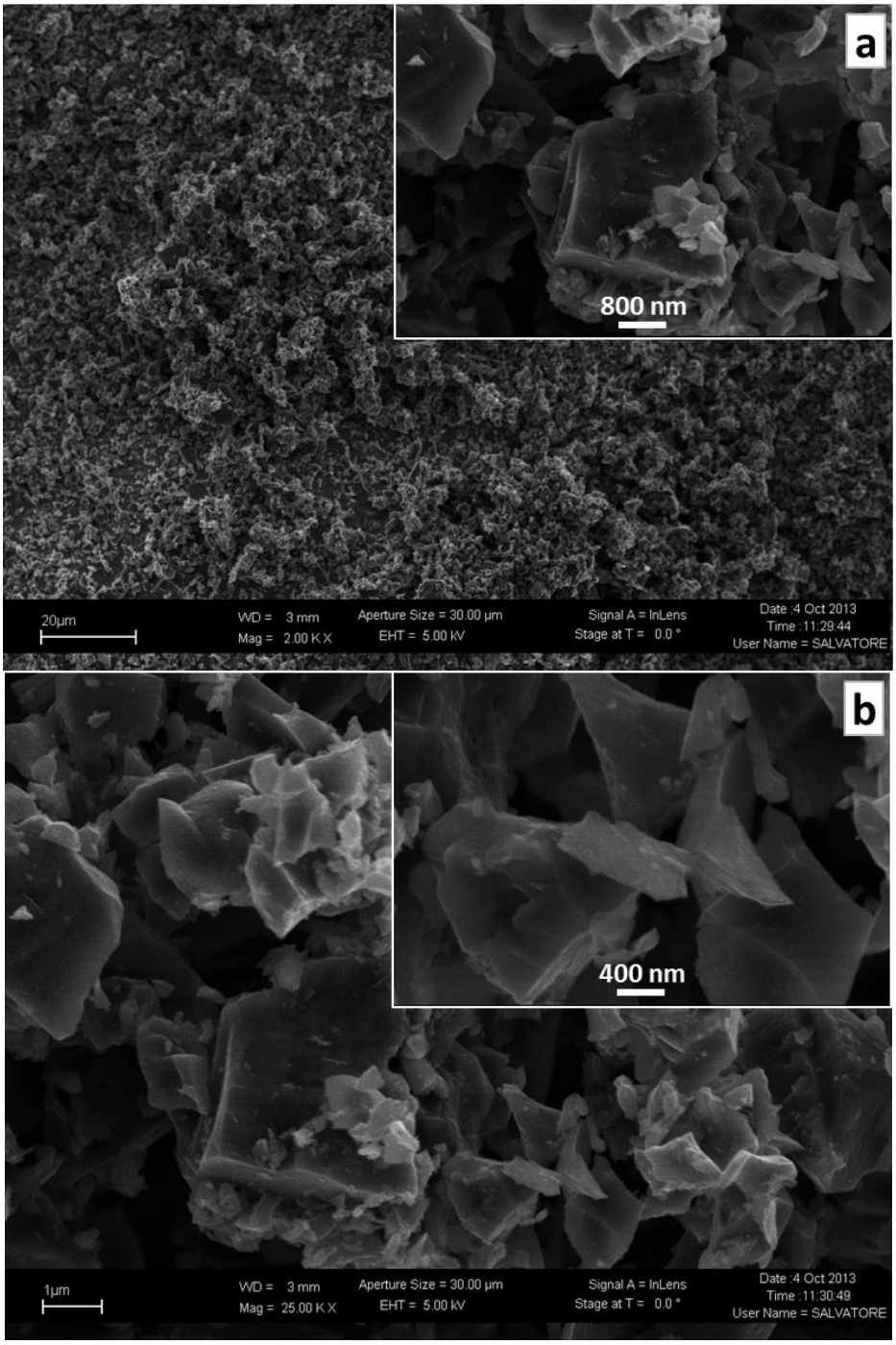

Figure 4.8 FESEM micrograph of CHS particles at 2K (a) and 25K (b) magnifications

In Figures 4.8 and 4.9, the displayed SEM micrographs of carbonized peanut and hazelnut shell particles reveal that they exhibit heterogeneous morphologies. Physically, these particles appear like fractured pieces with distinct and sharp edges. Particles are distributed in a wide range of size varying from finer particles of nearly 100nm to the

coarser ones with 1.5 microns size. As they contain much variety in shape and size so it can be said that they will be quite effective in filling voids of different dimensions ranging from gel pores to capillary pores in cement matrix and thereby possess the strong ability to improve the mechanical performance and microstructure of cementitious matrices.

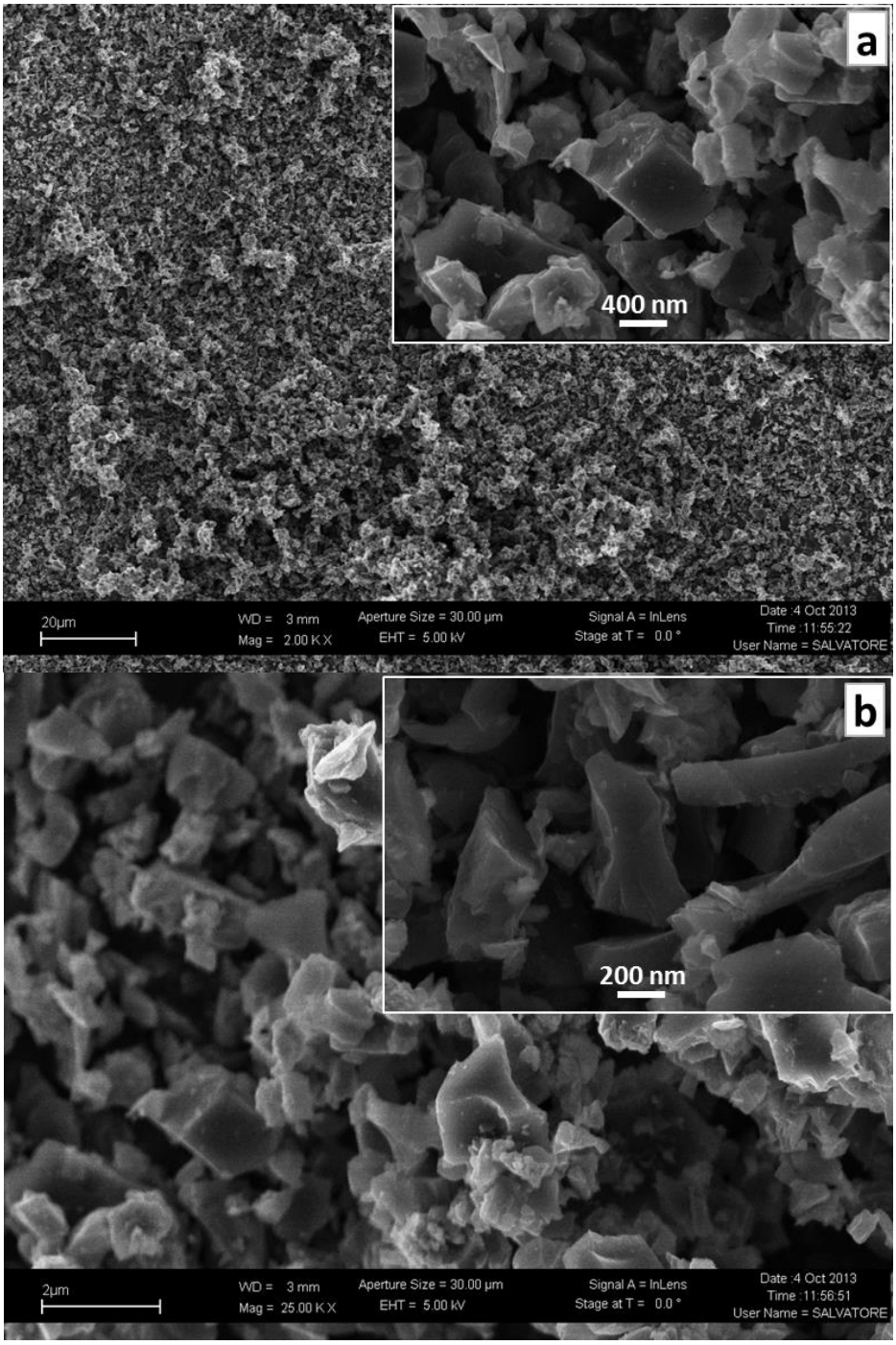

Figure 4.9 FESEM micrograph of CPS particles at 2K (a) and 25K (b) magnifications

In comparison with graphene sheets, these carbonized particles are very well distributed in nano to submicron size indicating their high potential as an efficient filler as well as strong ability to hinder the cracks at multiple stages. Unlike graphene sheets, the carbonized particles obtained from selected bio-waste possess relatively rough and abrasive texture that will contribute positively in developing strong bond with the host matrix. The irregular shapes of carbonized particles seem to affect the fresh properties of high performance mix to be measured in terms of flow. FESEM micrographs of graphene sheets and carbonized particles at different magnifications provide us with clear understanding related to their particles shape, size and surface texture. This would be helpful in effectively analyzing the experimental results related to mechanical properties, micro-porosity and electromagnetic interference shielding effectiveness discussed later in chapters 5, 6 and 7.

Table 4.1 summarizes a brief comparison in between elemental analysis of carbonized particles through EDX spectroscopy. It was found that carbonized particles possess more than 80% of carbon content by weight. The elemental analysis in both raw and chemically treated state was performed and results revealed that chemical pretreatment is also effective in attaining the better content of yielded carbon as observed by Kim et al. while working with kenaf fibers (J. M. Kim et al. 2011). A few traces of Mg, Al, Si, K, Ca, Cl and Na were also found. However, it should be noted here that the analysis appeared to be of just qualitative nature and definite quantitative results should not be expected. Detailed EDX plots are given in Appendix B.

Table 4.1 EDX analysis of carbonized particles

Elements (wt%)	CBF		CHS		CPS	
	R-CBF	T-CBF	R-CHS	T-CHS	R-CPS	T-CPS
C	81.87	90.08	93.77	94.47	87.68	80.37
Mg	0.47	0.44	0.43	--	0.53	0.56
Al	13.60	1.03	3.01	3.60	5.09	9.28
Si	2.55	2.52	0.23	--	1.14	1.26
K	1.51	--	1.36	0.79	3.90	0.69
Ca			1.20	1.29	0.54	6.23
Cl	--	1.27	--	--	--	--
Na	--	1.51	--	1.85	--	1.61

4.1.3 Raman Analysis

To characterize the structural order of carbonized bio-waste, Raman spectroscopy was carried out by means of Renishaw micro-Raman analyzer with green laser of 514 nm wavelength. Laser beam was focused using 100X objective lens on specimen's surface in 2 μm spot size. The Raman spectrum was restricted in the wavenumber range of 500-3500 cm^{-1} and displayed in Figure 4.10.

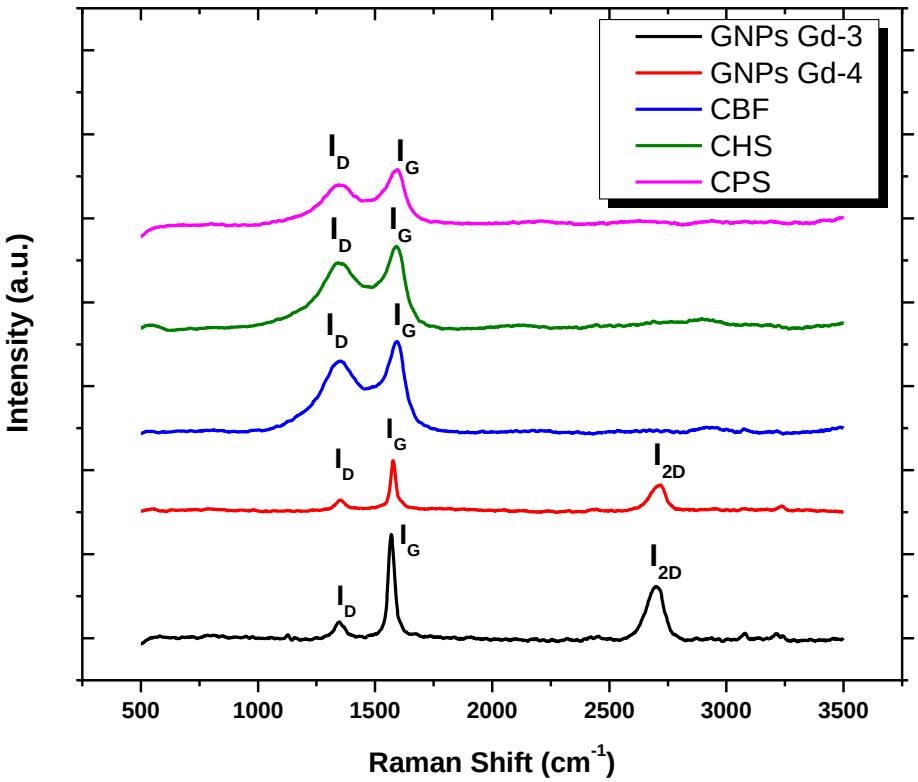

Figure 4.10 Raman spectra of GNP and NMCPs

Table 4.2 Displacement and intensity ratios of GNP and NMCPs through the Raman spectroscopy

Specimen ID	D band (cm^{-1})	G band (cm^{-1})	I_D/I_G
GNP-Gd_3	1345.2	1569	0.833
GNP-Gd_4	1345	1576	0.934
CBF	1346	1592	0.973
CHS	1342	1594	0.980
CPS	1346	1593	0.983

The most relevant wave number range related with Raman spectrum is 1000-1700 cm^{-1}. It is prominent due to the presence of D (defect grade I_D) and G (graphitization grade I_G) bands; which are displayed at approximately 1346 cm^{-1} and 1592 cm^{-1} wavenumbers for CBF, at 1342 cm^{-1} and 1594 cm^{-1} wavenumbers in the case of CHS and at 1346 cm^{-1} and 1593 cm^{-1} wavenumbers in the case of CPS respectively as shown in Table 2. The ratio of the two bands is a good indicator related to the quality of carbonaceous filler; there are quite high structural defects if these bands approach to similar intensity and vice versa. The minimum ratio of D to G band was observed in case of GNP grade 3 particles followed by GNP grade 4 particles. The lower ratio of I_D to I_G band means that their structure contains lesser intensity of atomic scale defects.

4.2 Study on Dispersion of GNPs and NMCPs

The major challenge faced during the preparation of cementitious nano-composites is related to the dispersion of nano particles inside cement matrix. Due to presence of strong van der Waals forces in between nano particles, it is an extremely complicated task to prevent their agglomeration (Grobert 2007). Poor dispersion leads to the formation of defects in the matrix and badly affects the overall performance of nano-reinforcements (Musso et al. 2009). To overcome issues concerning the dispersion and poor performance of nano-reinforcing particles a detailed study was done in this section to analyze the effect of different types of surfactants and the ultra-sonication technique.

4.2.1 Dispersion in Water

The distribution of graphene sheets in the cement matrix is largely affected by their dispersion state in water as observed with graphene oxide (Pan et al. 2011). Preliminary investigations were done on nano particles suspensions in water to select the most effective dispersant from the candidates. The stability of nano suspension was analyzed on the basis of its visually observed homogeneity versus time.

On the basis of previous research and taking safety as well as availability in to considerations; MAPEI dynamon SP1, Sodium poly-napthalene sulphonate and gum arabic were selected as the candidates of GNP dispersant in this study. Among these dispersant candidates, gum arabic is a natural polysaccharide extracted from the acacia tree. It is used primarily in the food industry as a stabilizer. It is also a key ingredient in traditional lithography and is used in printing, paint production, glue, cosmetics and various industrial applications, including viscosity control in inks and in textile industries. Gum arabic used in this study is purchased from Sigma-Aldrich in the form of white

powder. It is extremely soluble in water and the solution can be used to prepare GNP suspensions.

Table 4.3 Dispersing scheme of GNPs and NMCPs suspensions

ID	Water (g)	NMCPs wt (g)	NMCPs type	Dispersant type	Dispersant content	Sonic-ation	Result
A	50	1.43	GNP-gd3	--	--	15 minutes bath	unstable suspension
B	50	1.43	GNP-gd3	Dynamon SP1	2.14	15 minutes bath	unstable suspension
C	50	1.43	GNP-gd4	Dynamon SP1	2.14	15 minutes bath	unstable suspension
D	50	1.43	CPS	Dynamon SP1	2.14	15 minutes bath	stable suspension
E	50	1.43	CHS	Dynamon SP1	2.14	15 minutes bath	stable suspension
F	50	1.43	CBF	Dynamon SP1	2.14	15 minutes bath	stable suspension
G	50	1.43		Dynamon SP1	2.14	15 minutes bath	stable suspension
H	50	1.43	GNP-gd3	Dynamon SP1	2.14	15 minutes probe	stable suspension
I	50	1.43	GNP-gd3	SPS	0.72	15 minutes probe	stable suspension
J	50	1.43	GNP-gd3	Gum Arabic	--	15 minutes probe	stable suspension

Figure 4.11 Stability test for GNPs and NMCPs suspensions; (a) 5 minutes and (b) 2h after mixing

As displayed via Figure 4.11, the stability of GNPs or NMCPs suspension could be easily judged by looking at the distribution of the black color in a test tube, since the black color was displayed by these carbon particles, while the dispersant solutions without carbon particles are colorless (formulation G). All types of nano/micro carbonized particles

produced from bio-waste formed stable suspension with water using superplasticizer dynamon sp1 and 15 minutes of bath sonication (formulation D to F). While some sort of sedimentation was observed in the case of GNP particles which can be related to their high specific surface area resulting in strong Van der Waal interactions as observed in formulations B and C.

To cater for the issue concerning the dispersion of GNP particles other types of dispersants including gum arabic and SPS were explored with probe sonication for 15 minutes. It can be seen that GNP suspension in gum arabic (formulation J) showed the best stability because the black color remained going through the liquid even after 2 h. GNP suspension in dynamon SP1 and SPS solution (formulation H and I) also showed good stability; only little segregation phenomenon was observed on the surface of the liquid after 2 h. Considering that during cement casting, the GNP suspension only needed to be kept stable for about 10 minutes before being added to the cement mixture which is far less than 2 h, dynamon SP1 was selected. For gum arabic, its weak acidity makes it reactive in alkaline cementitious environment that may result in generation of excess water during the mixing process. Besides this it also needs enough stirring effort and time to make the gum arabic powder dissolved in the water. Based on the knowledge of the author, this is the first time that dynamon SP1 is used as a dispersant for carbon-based nano-particles in cement matrix. Due to double dispersion effect of dynamon sp1 it acts like a dispersant for GNPs/NMCPs as well as a superplasticizer for the cement grains. In this way the use of dispersant is also avoided that may impair the properties of cementitious matrix including hydration and mechanical properties. In some cases added dispersant was found to make the cementitious matrix highly porous due to foam formations resulting in decreased mechanical performance of resulting cementitious composites (Collins, Lambert, and Duan 2012b; Sobolkina et al. 2012).

4.2.2 Dispersion in Cement Matrix

The dispersion of GNPs or NMCPs in water does not ensure 100% their proper distribution inside the cement matrix as well. To evaluate the dispersion of GNP and NMCPs in high performance cementitious matrices FE-SEM analysis was performed on the fractured cement specimen chips of 1x1 cm extracted from each formulation after the compression test.

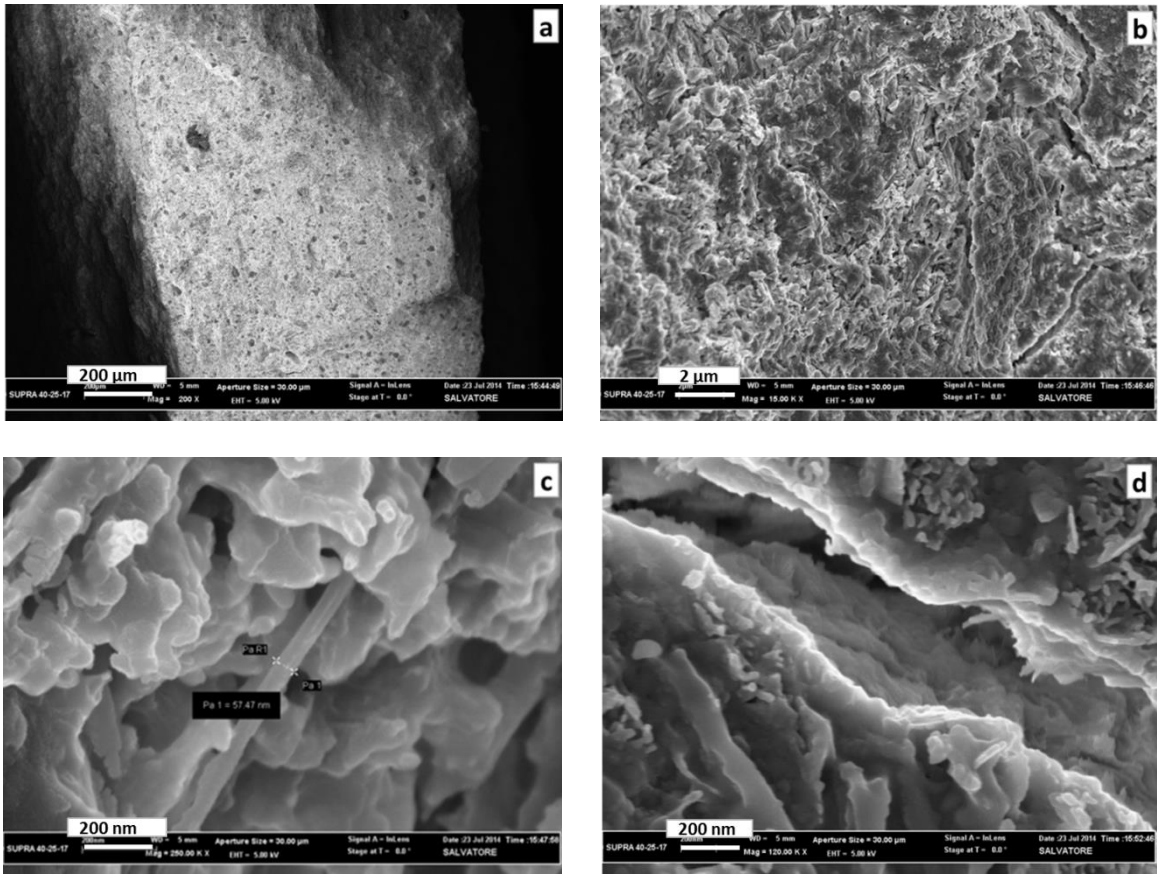

Figure 4.12 FESEM micrograph of GNP_3 (a,b) and GNP_4 (c,d) particles embedded in cement matrix

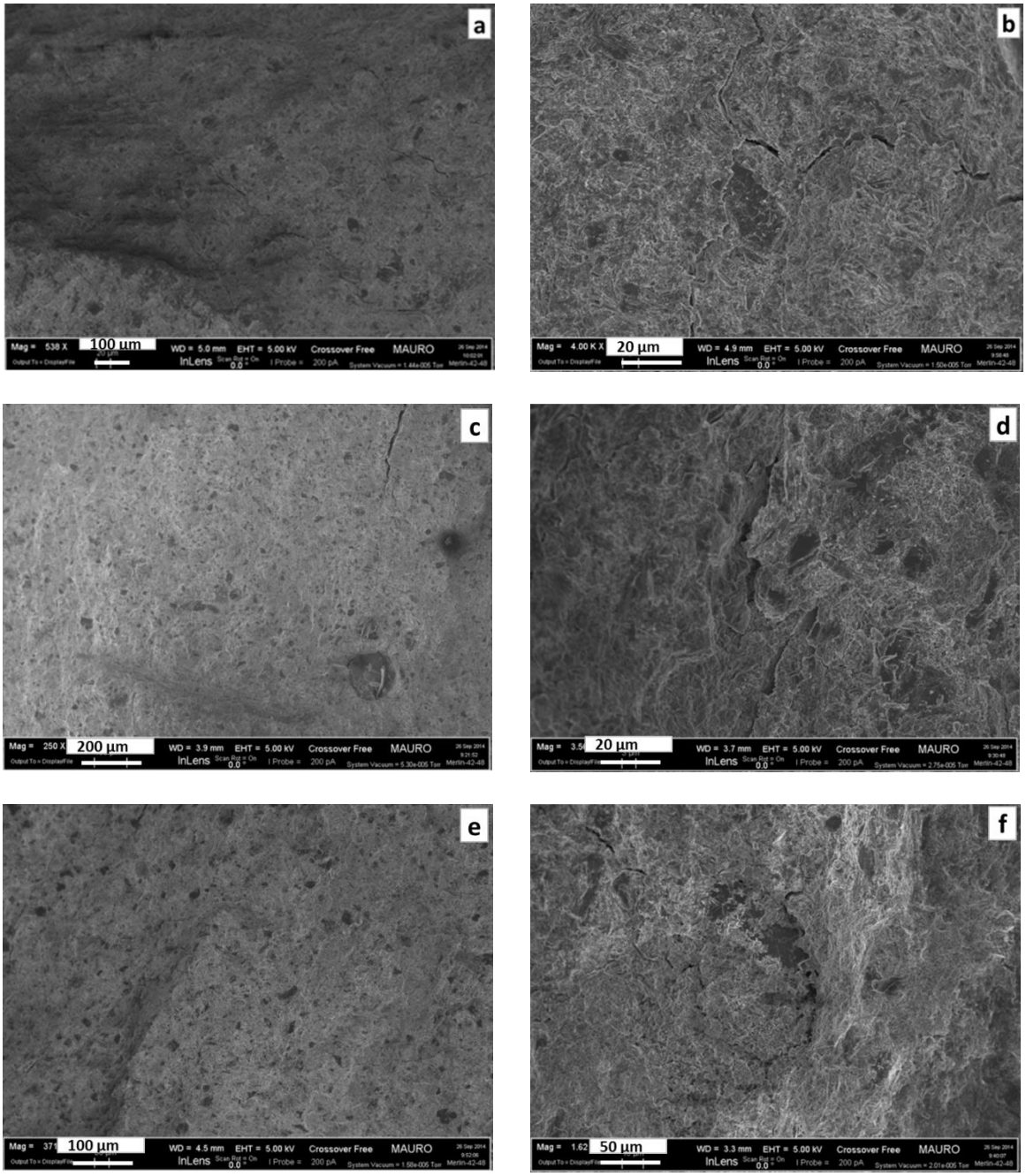

Figure 4.13 FESEM micrograph of CBF (a,b), CHS (c,d) and CPS (e,f) particles embedded in cement matrix

SEM micrographs displayed better dispersion of graphene sheets and nano/micro carbonized particles inside the cementitious matrix. In the entire microstructure of reinforced cementitious matrix, there was not even a single observation displaying any signs of large agglomerations or clustering of the embedded fillers. Some nano/micro dispersed cracking patterns are visible with no indication concerning the filler's pull out

from the matrix across the crack due to effective dispersion. Better dispersion results in creation of more and more interfaces which ultimately enhance the mechanical performance and crack resistance property of cementitious matrix.

4.3 Effect of GNP/NMCPs on Flow-ability of HPCC

A high flow-ability and moderate viscosity is necessary for the ease of compaction and placement of cement-based materials, while ensuring adequate cohesion stability, to ensure the homogeneous distribution of engineering properties in concrete. A low workability is generally associated with poor compaction capacity which may lead to non-homogeneity due to entrapped large air voids that are retained in the composite. Cwirzen et al. found that the addition of CNTs decreases the strength of cement paste because of higher non-homogeneity as a result of improper compaction at low workability (Habermehl-Cwirzen, Penttala, and Cwirzen 2008). A similar phenomenon was also observed in steel fiber/cement composites.

The effect on workability of cementitious matrix by the addition of carbon particles is measured and compared in Figure 4.14. It was observed that the addition of GNPs and NMCPs by 0.2 wt% of cement leads to a slight reduction in the workability. The content of 0.2 percent addition was selected after its exploration as the most optimum content for enhancement in the mechanical performance of cement composites with details included in chapter 5. The results demonstrate that there is a decrease in the values of total spread while an increase in the values of T25 time evidencing the respective enhancement in the yield stress as well as viscosity of the concerned mix. Maximum reduction in flowing ability was recorded in the cement matrix with GNP_4 reinforcements which may be related with its large specific surface area compared to other investigated reinforcing materials. However, the workability of GNPs and NMCPs embedded cement matrices is still comparable to that of plain cement paste due to a low weight fraction of the additives.

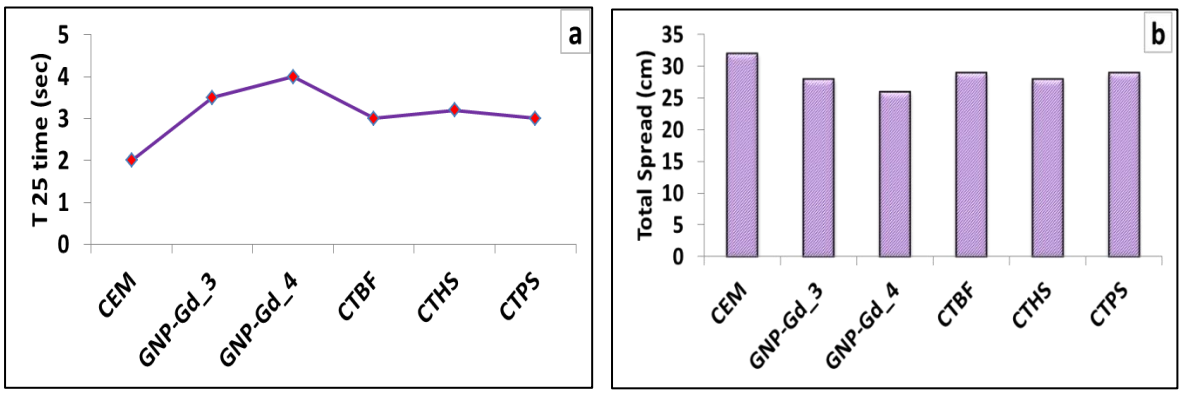

Figure 4.14 Variation in T 25 time (a) and total spread (b) of GNP and NMCPs embedded cementitious matrices

Chapter 5. Mechanical Properties of GNP/NMCPs Reinforced Self Compacting Cement Paste and Mortar

5.0 General

This chapter provides a detailed investigation on mechanical performance of self-compacting cementitious paste and mortar system containing GNP or other types of synthesized nano/micro carbonized particles as reinforcements.

5.1 Flexural Response of HPCC

In the first phase cement paste specimens were analyzed in flexure via three point bending using crack mouth opening displacement control mode and in the second phase their uniaxial compressive resistance was analyzed. Since cement paste plays the key role in modifying the behavior of high performance concrete as well as act like a vital item of concrete constituents therefore it was selected for preliminary investigations. Based on the results of this phase we may predict the behavior of the investigated GNP and NMCPs on next two phases of high performance mortar and concrete. The optimum contents of investigated carbon reinforcements explored during the analysis of paste phase were further investigated in the mortar phase to strengthen the conclusions of the present research as well as to widespread the scope of the work. Post crack response in three point bending of cement paste prisms was analyzed in terms of fracture toughness and residual strength factors according to the standard set forth in ASTM C 1018 (ASTM C 1018-02 1998). Modulus of rupture was also evaluated in accordance with ASTM C 378 (ASTM C 348-08 n.d.). The averaged values from experimental results regarding the mechanical properties of HPCC have been tabulated in Appendix C.

5.1.1 Load-CMOD Curves

Experimentally evaluated load-CMOD curves of various formulations with and without reinforcements in the form of nano/micro carbon particles are displayed in Figures 5.1 to 5.5. The comparison load-CMOD curves comprise on the typical specimen's curve randomly selected from each formulation to have the idea concerning modification in the

cracking behaviour of cementitious matrices on addition of reinforcing nano/micro carbon particles.

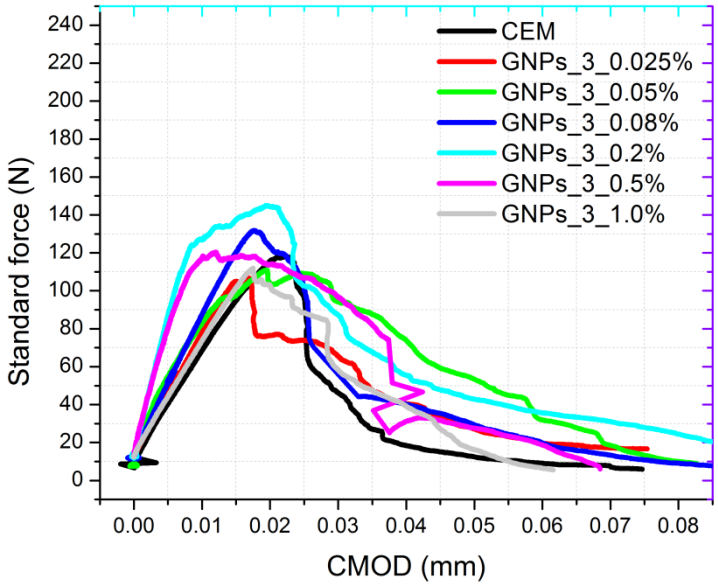

Figure 5.1 Comparison of load-CMOD curves of plain and GNP_3 reinforced cementitious paste composites

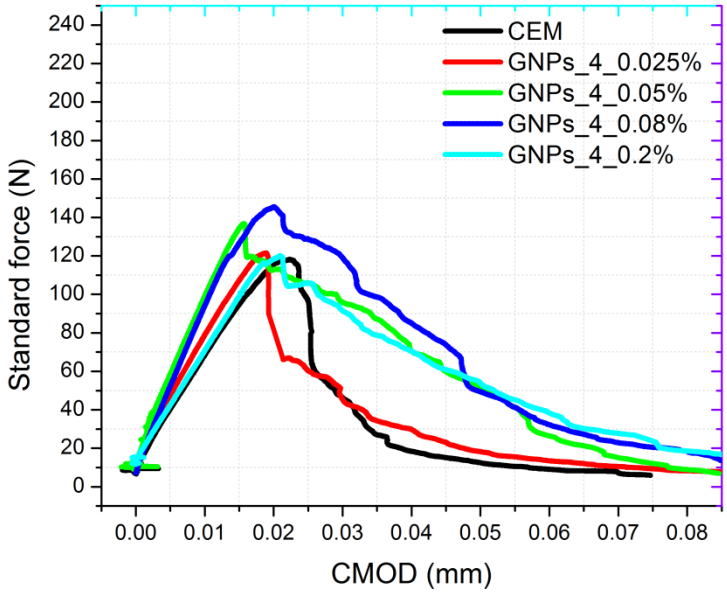

Figure 5.2 Comparison of load-CMOD curves of plain and GNP_4 reinforced cementitious paste composites

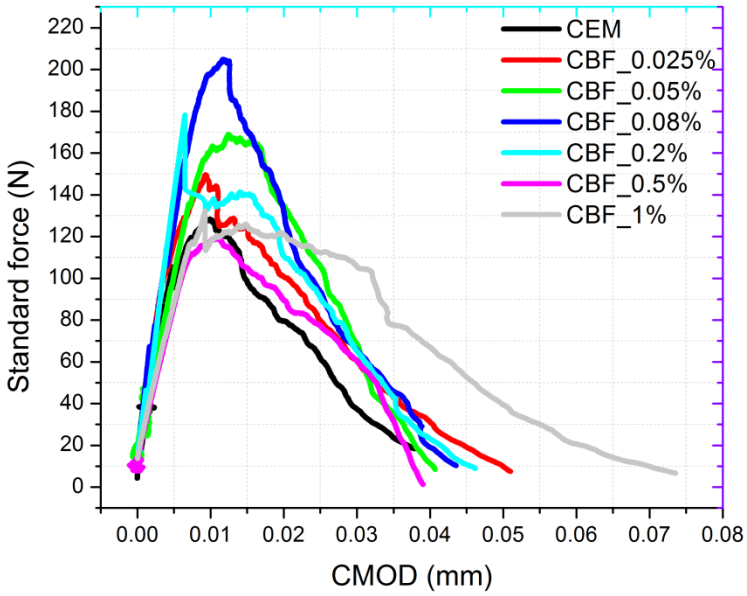

Figure 5.3 Comparison of load-CMOD curves of plain and CBF reinforced cementitious paste composites

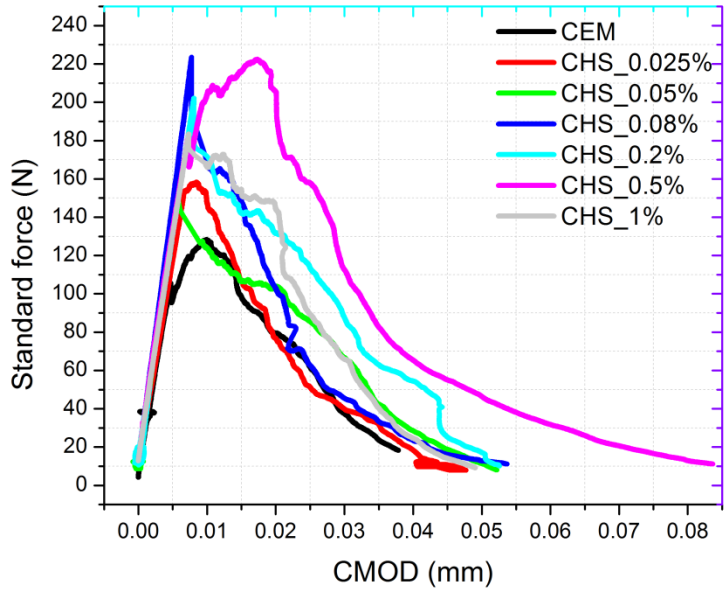

Figure 5.4 Comparison of load-CMOD curves of plain and CHS reinforced cementitious paste composites

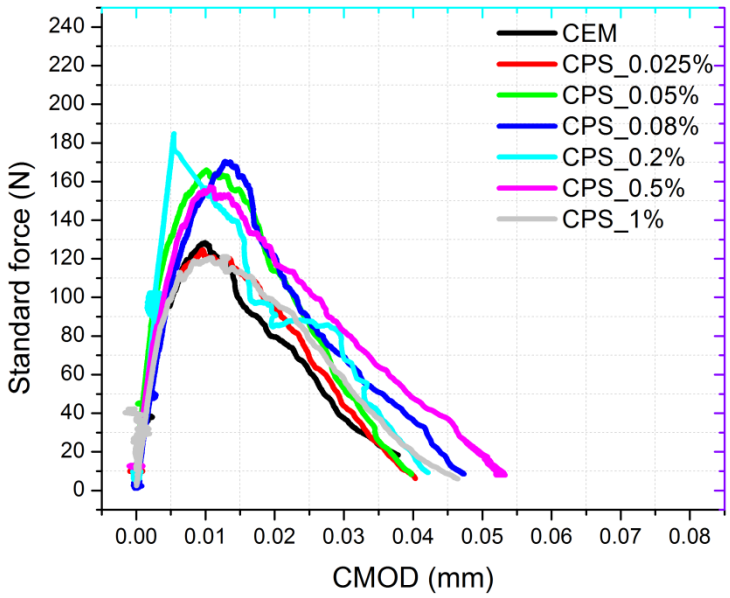

Figure 5.5 Comparison of load-CMOD curves of plain and CPS reinforced cementitious paste composites

From load-CMOD curves it is observed that all the investigated types of added carbon particles are effectively enhancing the mechanical performance of cementitious matrices. Both the flexural strength as well as fracture toughness have been observed to increase due to nano/micro modifications as revealed form the curves. Most of the formulations offering maximum resistance in flexure contain GNP or NMCPs in the content of 0.08 to 0.2 wt% of cement. The GNP reinforced specimens load-CMOD curves (Figure 5.1 & 5.2) show relatively better post crack behavior in comparison with the corresponding NMCPs reinforced ones. Maximum crack width of 0.1mm is observed in case of GNP_4 reinforced cementitious matrix while it is ranging in between 0.06-0.08 mm for NMCPs embedded matrices and for the pristine cement it is recorded as only 0.04mm. The peak value of flexural strength is attained on addition of CHS particles at an optimum content of 0.08 wt%. The variations in the mechanical behavior of various formulations may be associated with the shape, size, surface texture as well as the origin of the added nano/micro sized carbon particles.

If we relate the ascending part of the curve with the stiffness of the concerned matrix then it can be said that there is a little influence of the added carbon reinforcements on the stiffness of the matrix. But there are significant modifications observed in the descending part which have been evaluated with detail in terms of toughness indices T.I (I_5, I_{10} and I_{20}) and residual strength factors ($R_{5,10}$ and $R_{10,20}$) in the coming sections.

5.1.2 Modulus of Rupture

Modulus of rupture is defined as maximum surface stress at the failure of specimen in three point bending test. It is given by the following relation:

$$\sigma = \frac{3*F_{max}s}{2wh^2} \qquad \textit{Eq. 5.1}$$

where "F_{max}" is the maximum applied force on the prism at the instant of failure, "s" is the effective span, "w" is the prism width and "h" is considered as the height of the specimen under the point of the application of the load. Based on experimental load-CMOD curves, values of MOR for formulations containing different types of fillers were evaluated.

For the formulations reinforced with GNP particles, maximum increase in MOR by 29.89% is achieved with 0.08 wt% addition of GNP_4 particles. The trend of increase is more or less similar in the matrices reinforced with GNP particles of varying grades as shown in Figure 5.6ab. The addition of GNP particles is effectively increasing the values of MOR in proportion to the added content till the percentage addition of 0.2% in case of grade 3 while 0.08 % in case of grade 4 GNP particles. So these values of additions can be regarded as their optimum contents to attain maximum improvement in the MOR of high performance cementitious matrix. It is also observed that the performance of GNP_4 particles is relatively better in comparison with GNP_3 particles which may be associated to its high quality, wrinkled texture and significant large specific surface area.

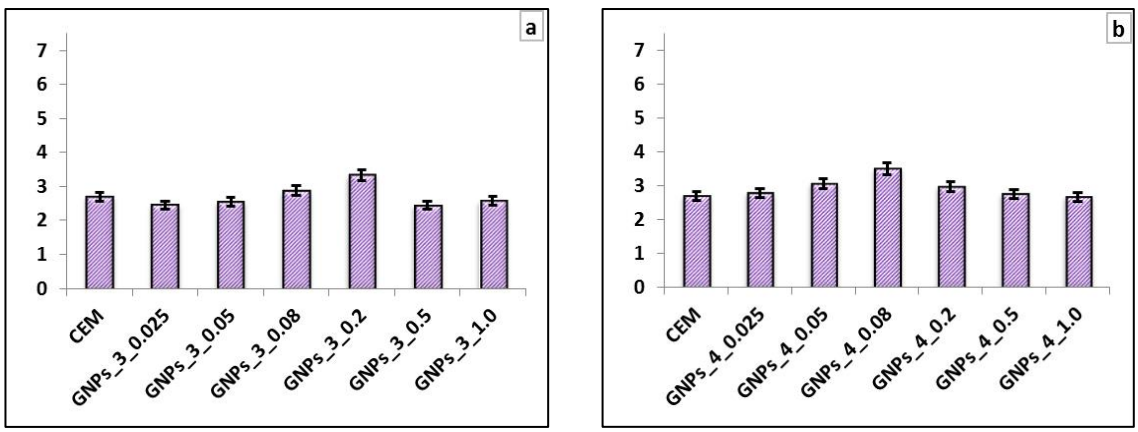

Figure 5.6 Variation in MOR on varying contents of GNP_3 (a) and GNP_4 (b) particles in cementitious composites

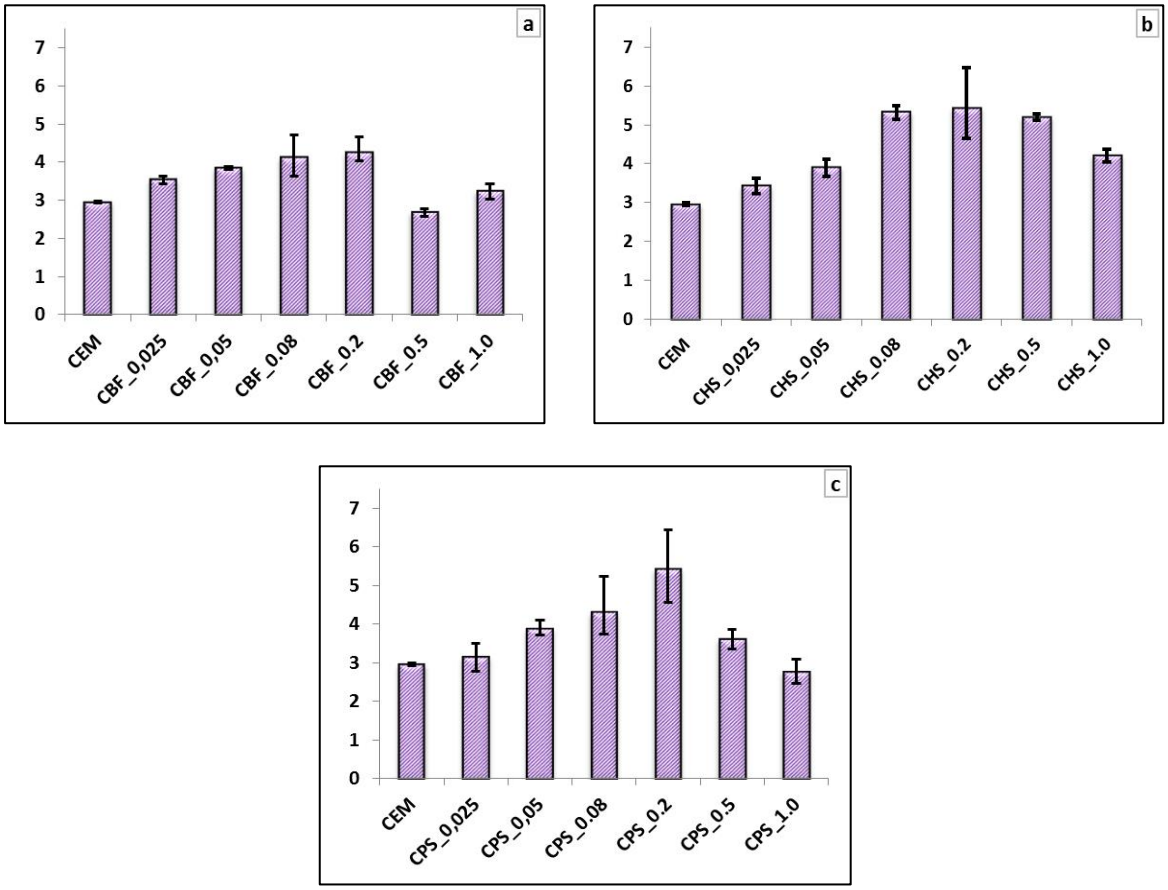

Figure 5.7 Variation in MOR on varying contents of CBF (a), CHS (b) and CPS (c) particles in cementitious composites

For the cement formulations reinforced with nano/micro carbon particles produced from bio-waste the maximum increase by 83.9% and 88.4% is attained on addition of CHS and CPS by 0.2 wt% respectively as given in Figure 5.7bc. For the bagasse fibers similar trend of increment is observed with an optimum addition of 0.2 wt%. The maximum improvement obtained on CHS and CPS additions may be associated to their finer particle size, angular shape and high graphitization grade (Figure 4.10) relative to CBF particles. These results conclude the efficient performance of the synthesized carbon particles in effectively filling the voids and strengthening of the resulting matrix.

The comparison of modified MOR values on the addition GNP or NMCPs at varying proportions is briefly summarized in Figure 5.8. The entire cluster of points is on an increasing mode till they reach their respective optimum value which is observed as 0.08 wt% in case of GNP_4 reinforcements while 0.2 wt% in the other remaining types of investigated carbon reinforcements. The best results of MOR have been recorded on the addition of CHS and CPS particles by 0.2 wt% of cement. On further increase in the content beyond 0.2 wt% the values of MOR start depreciating due to enhanced proportion

carbonized particles in the matrix. It is mostly believed that the optimum content of addition for CNTs is 0.08wt% as observed by Metaxa et al. which is similar to the one observed for GNP particles in the current research (Konsta-Gdoutos, Metaxa, and Shah 2010a; Metaxa et al. 2012).

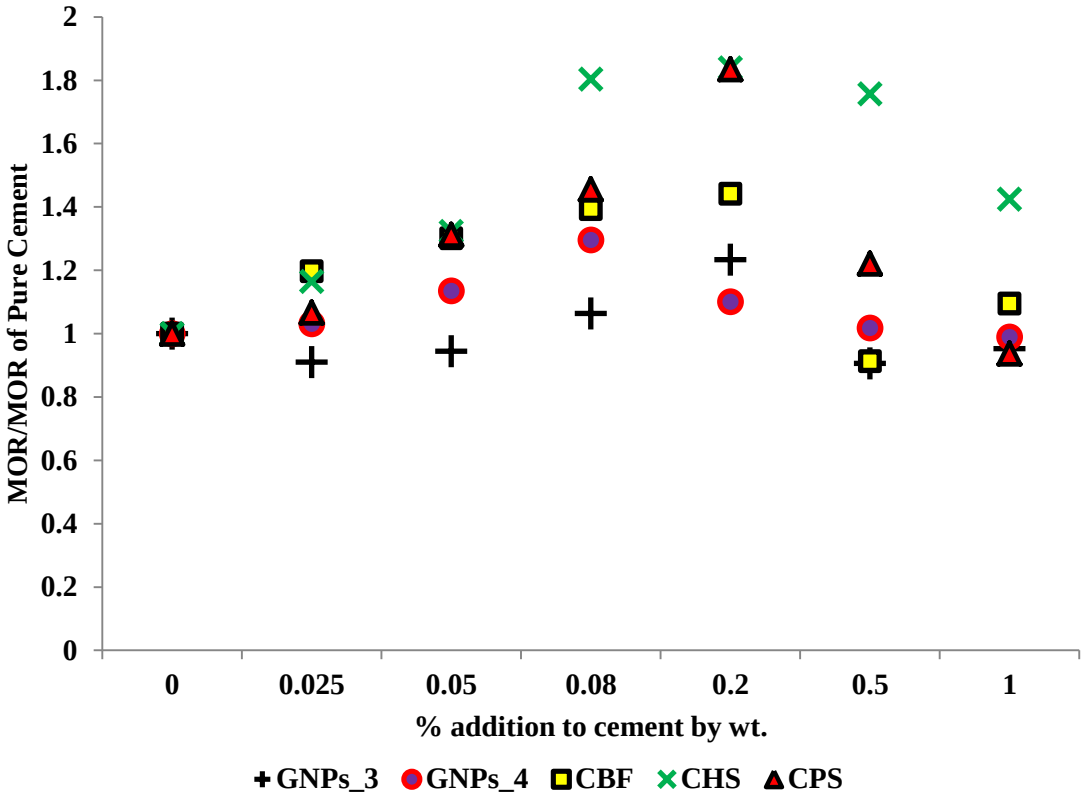

Figure 5.8 Relative increase in MOR of nano/micro reinforced cement composites with reference to the plain cement

5.1.3 Fracture Toughness

The post crack behaviour of cement matrix was investigated in terms of total fracture toughness, toughness indices T.I (I_5, I_{10} and I_{20}) and the residual strength factors $R_{5,10}$ and $R_{10,20}$.

5.1.3.1 First Crack Toughness and Ultimate Toughness

Fracture energy is a material intrinsic property that is defined as the work of fracture for unit crack width and unit crack extension. Fracture toughness is divided into two classes: first crack toughness and ultimate toughness. First crack toughness corresponds to area under load-CMOD curve till the onset of first crack in vicinity of 6mm deep notch. Ultimate toughness corresponds to area under load-CMOD curve till the point of complete

failure as discussed in Rilem Recommendations and ASTM C 1018 (ASTM C 1018-02 1998). First crack load is usually curve's peak load beyond which it attains a descending pattern. We may say that first crack toughness is linked to the energy absorbed by prism till the onset of first crack while ultimate crack toughness is associated with total energy absorbed during initiation and propagation of crack. Based on experimental load-CMOD curves, first crack toughness and total fracture toughness /fracture energy of prescribed formulations were estimated (Figure 5.9 & 5.10).

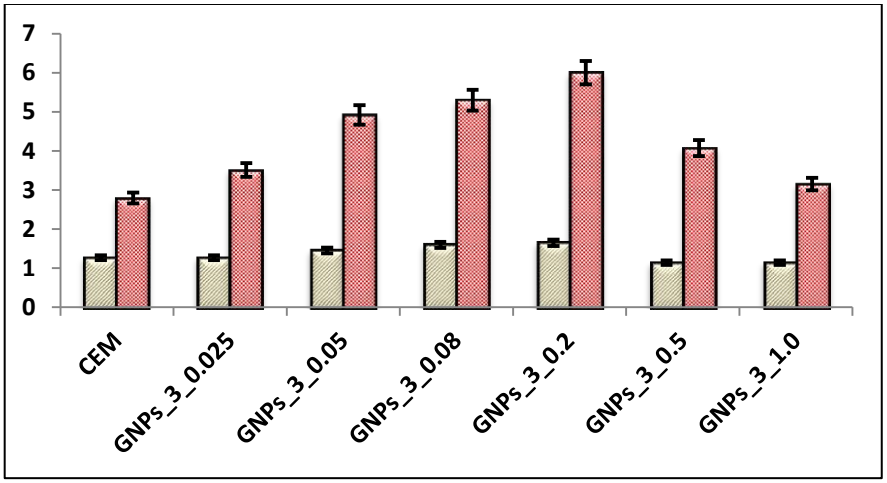

a

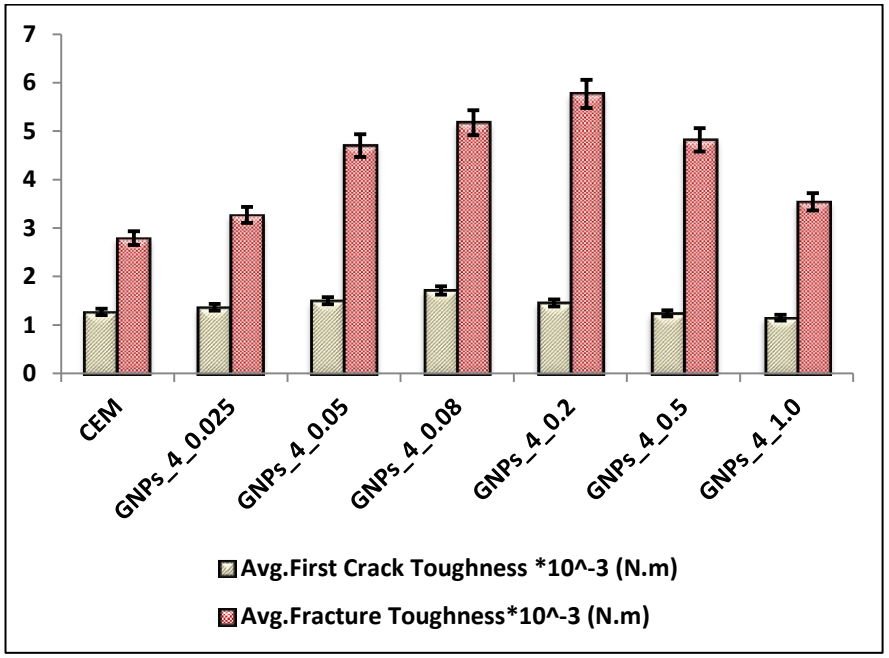

b

Figure 5.9 Variation in fracture toughness of HPCC with the addition of GNP_3 (a) and GNP_4 (b) particles

It is observed that the influence of GNP particles on fracture toughness of HPCC is more or less in the similar trend as was observed for the MOR. The only difference is the optimum value which has been shifted towards little increased content i-e from 0.08% to 0.2 % by weight of cement as given in Figure 5.9. The performance of GNP_3 particles in toughening the cementitious matrix is slightly more significant relative to the reinforcing particles of GNP_4. The best formulations from toughening perspectives possess 114.8% & 106.5% enhanced fracture toughness in comparison to the pristine cement specimens and can be produced with addition of 0.2 wt% GNP_3 and GNP_4 particles. Like MOR the increment in the values of first crack and ultimate fracture toughness reduces at higher contents of 0.5 wt% and 1.0 wt%.

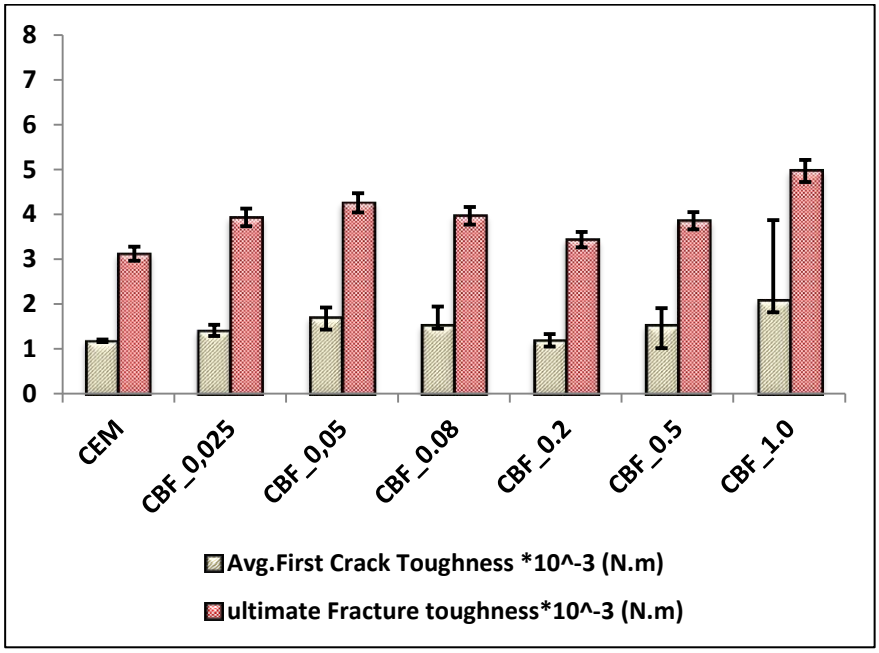

a

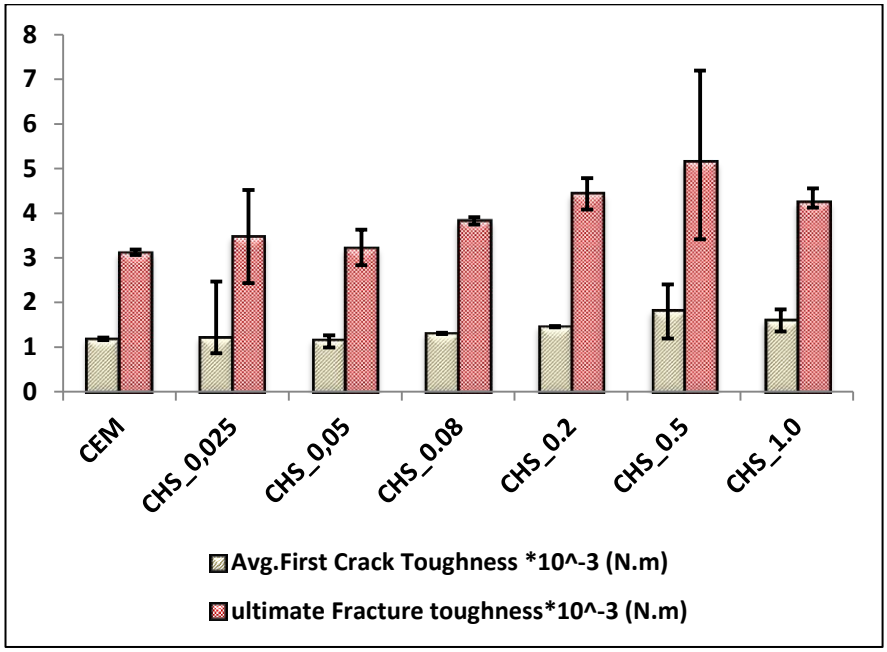

b

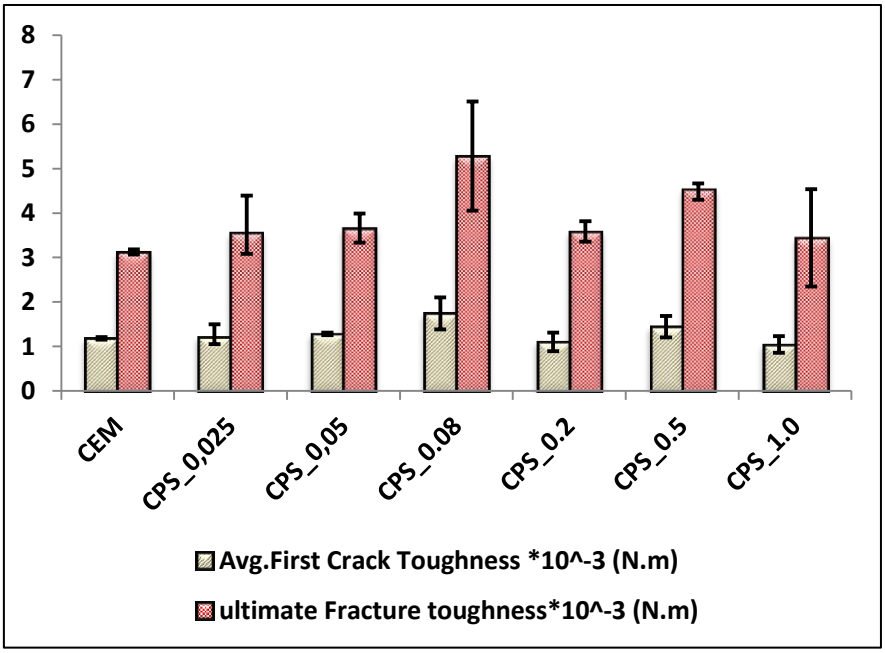

c

Figure 5.10 Variation in fracture toughness of HPCC with the addition of CBF (a) CHS (b) and CPS (c) particles

From Figure 5.10abc it has been explored that the addition of NMCPs is an effective solution to modify the cracking behavior or the post crack response of high performance cementitious matrix. Both first crack that is usually related with the onset of macro crack

as well as total toughness compiling the onset as well as propagation perspectives related to cracks; were found to be enhanced with the inclusion of such heterogeneities in the form of carbonized bio-waste particles of nano/micro sizes. The modification trend is not the same for the three types of carbonized particles as observed during the analysis of MOR. The trend is varying with some types showing the best toughening values at small proportions as recorded in case of CBF particles while in some cases the best results were obtained at the higher contents of additions. It can be said that the percentage increase in toughness depends upon the number of reinforcing particles encountered by the crack from its onset till the complete fracture. The maximum increase in total fracture toughness by 68.9% was observed in case of 0.08 wt% CPS additions while 64.7% and 36.3% increments were attained with CHS and CPS reinforcing particles added by 0.5 and 0.05 weight percentages respectively.

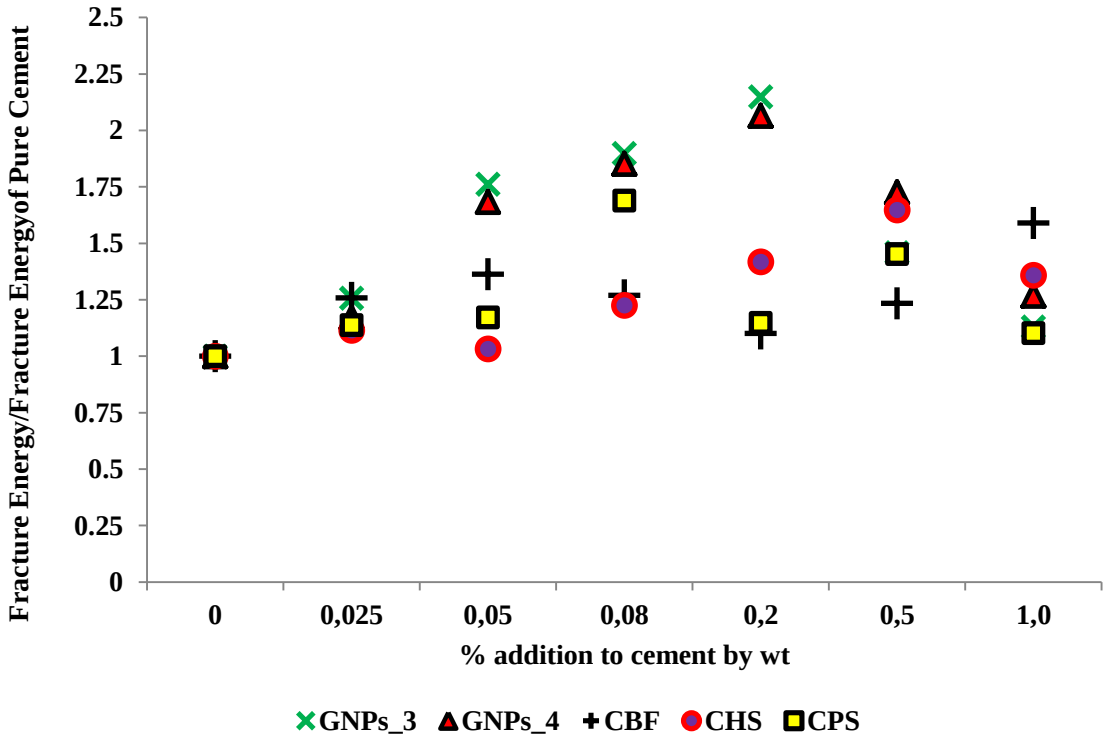

Figure 5.11 Relative increase in fracture toughness of nano/micro reinforced cement composites with reference to the plain cement

From the comparison curve shown in Figure 5.11 it is concluded that GNP particles are relatively more effective in enhancing the overall toughness by offering strong resistance against the propagation of cracks. The peak values have been observed at the content of additions approximately similar to the ones reported for maximum MOR i-e 0.08 wt% and 0.2 wt%. The better performance of GNP particles in enhancing fracture toughness can be

linked to their aspect ratio in the range of 50-900 (Table 1.1) that is large enough to efficiently restrict the propagation of a crack along a straight path.

5.1.3.2 Toughness Indices and Residual Strength Factors

ACI Committee 544 defines the toughness index as the ratio of the amount of energy required to deflect a fiber reinforced prism by a prescribed amount to the energy required to bring it to the point of first crack. Three toughness indices $\boldsymbol{I_5}$, $\boldsymbol{I_{10}}$ and $\boldsymbol{I_{20}}$ have been calculated dictating the post crack toughness pattern of reinforced prisms. ASTM C 1018 (ASTM C 1018-02 1998) standard' defines $\boldsymbol{I_5}$, $\boldsymbol{I_{10}}$ and $\boldsymbol{I_{20}}$ as the ratios of area under the load-CMOD curve up to the deflections of 3, 5.5 and 10.8 times the first-crack deflection to the area up to first-crack respectively.

$$\boldsymbol{T.I(I_5) = \frac{Area\ under\ the\ Load-Deflection\ curve\ up\ to\ 3times\ the\ 1^{st}\ crack\ Deflection}{Area\ under\ the\ Load-Deflection\ curve\ up\ to\ 1^{st}\ crack\ Deflection}} \qquad Eq.\ 5.2$$

$$\boldsymbol{T.I(I_{10}) = \frac{Area\ under\ the\ Load-Deflection\ curve\ up\ to\ 5.5times\ the\ 1^{st}\ crack\ Deflection}{Area\ under\ the\ Load-Deflection\ curve\ up\ to\ 1^{st}\ crack\ Deflection}} \qquad Eq.\ 5.3$$

$$\boldsymbol{T.I(I_{20}) = \frac{Area\ under\ the\ Load-Deflection\ curve\ up\ to\ 10.5times\ the\ 1^{st}\ crack\ Deflection}{Area\ under\ the\ Load-Deflection\ curve\ up\ to\ 1^{st}\ crack\ Deflection}} \qquad Eq.\ 5.4$$

Residual strength factors, which are derived directly from toughness indices, characterize the level of strength retained after first crack simply by expressing the average post-crack load over a specific deflection interval as a percentage of first crack load. Mathematically they are defined as follow:

$$\boldsymbol{R_{(5,10)} = 20 * (I_{10} - I_5)} \qquad Eq.\ 5.5$$

$$\boldsymbol{R_{(10,20)} = 10 * (I_{20} - I_{10})} \qquad Eq.\ 5.6$$

Based on above experimental load-CMOD curves, average values of toughness indices are plotted in Figure 5.12 and 5.13 and evaluated residual strength factors are reported in Table 5.1.

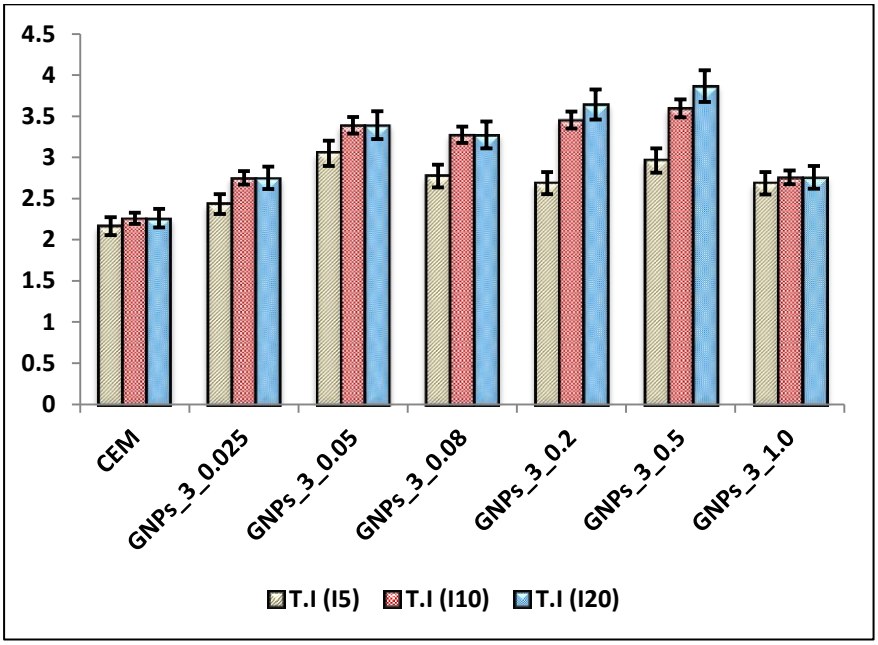

a

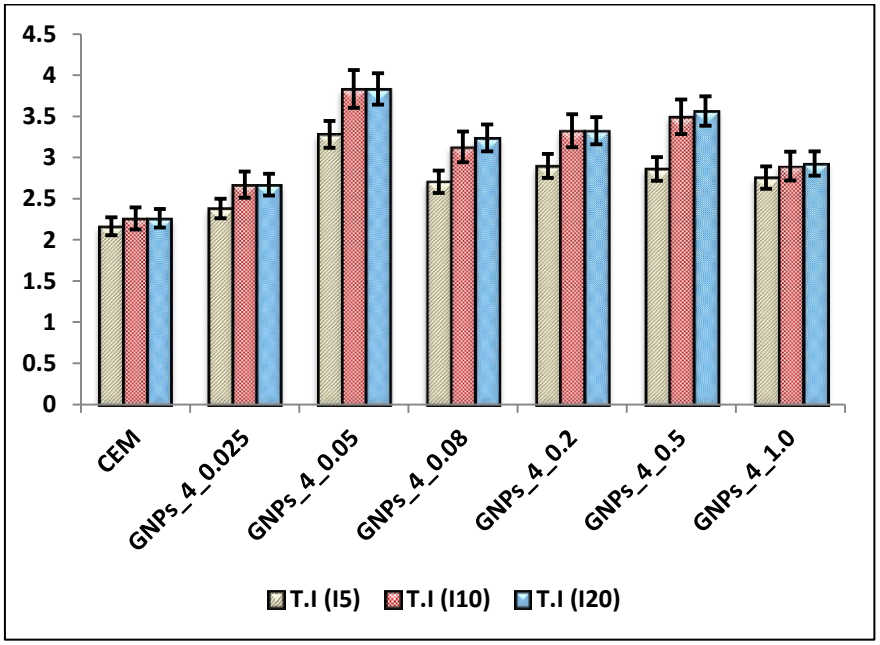

b

Figure 5.12 Evaluated toughness indices for GNP_3 (a) and GNP_4 (b) reinforced cementitious matrices

An appreciable improvement in the values of toughness indices as well as residual strength factors has been observed on incorporation of GNP particles as a reinforcing medium. It is clear in Figure 5.12 that the values of toughness indices in case of pristine cement are approximately same for T.I (I_5), T.I (I_{10}) and T.I (I_{20}), showing least resistance against the propagating crack or brittle post-cracking behavior. The addition of GNP particles had

contributed effectively to obstruct or block the smooth propagating mechanism of the cracks. The hindrance offered by the nano sized GNP particles of large aspect ratio results in the need of more energy input to continue with the failure along that plane by overcoming the encountered obstruction. The reinforcing effect of GNP particles can be easily observed by relative increase in the values of toughness indices in the order $I_{20} > I_{10} > I_5$ and in comparison to the same values obtained for the pristine cement matrix.

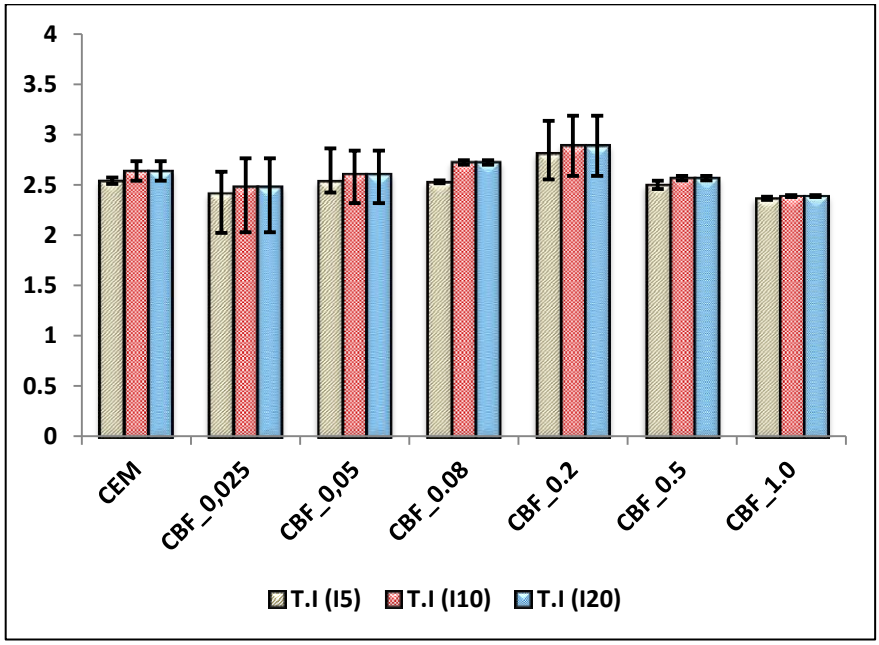

a

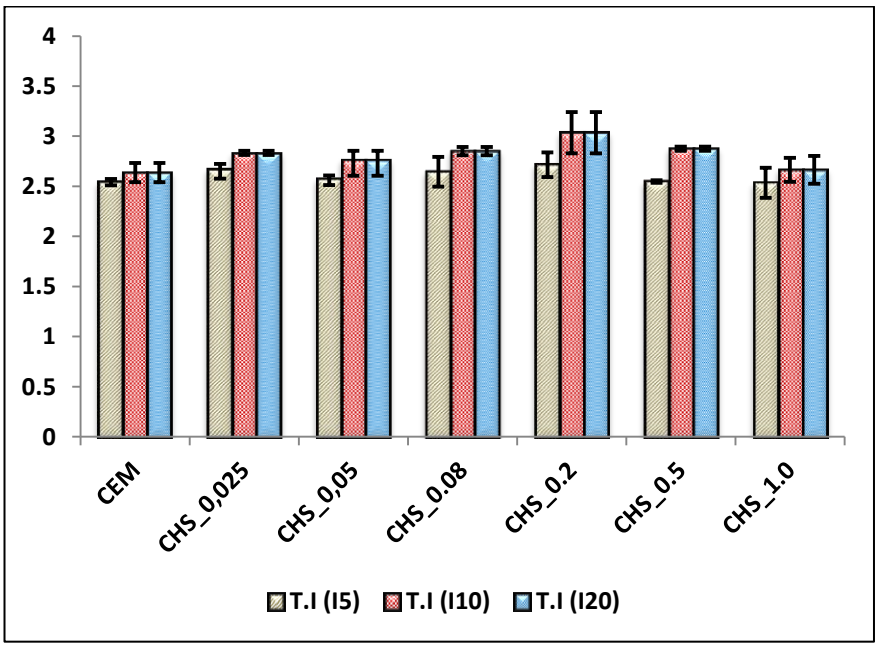

b

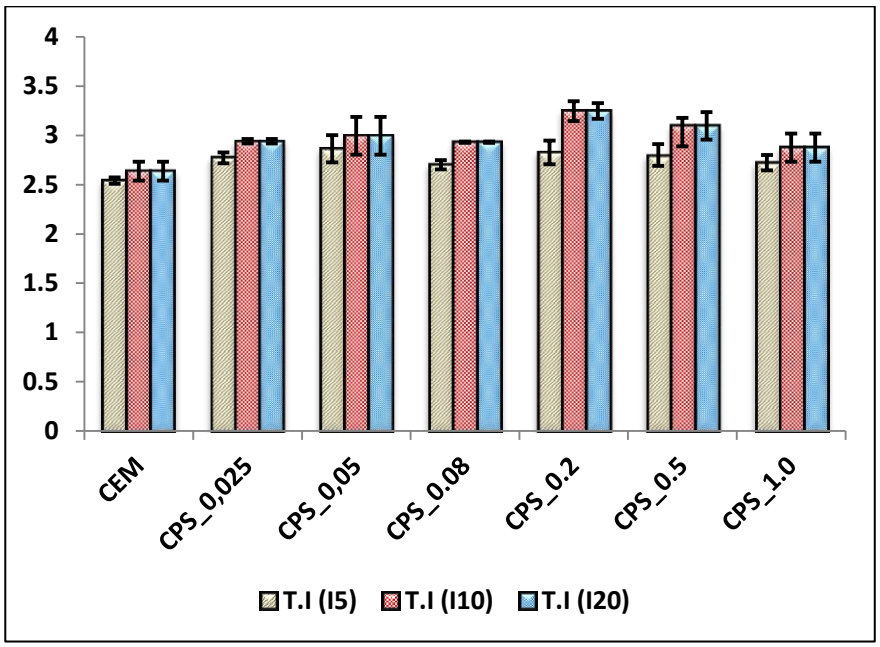

c

Figure 5.13 Evaluated toughness indices for CBF (a) CHS (b) and CPS (c) embedded cementitious matrices

On the addition of carbonized particles there is a significant modification in the post crack behavior of high performance cementitious composites as revealed from the calculated values of fracture toughness plotted in Figure 5.13. Due to angular and flaky shape these carbon particles are effective in introducing heterogenic intrusion in the path of the crack and thereby improve the resistance of cementitious matrix against brittle and smooth fractures. The observed enhancement in toughness of HPCC on addition of NMCPs from bio-waste is comparatively lower to the one observed for GNP particles reinforced cementitious matrices which can be related to their relatively small aspect ratio in comparison with GNPs.

Table 5.1 Residual strength factors of plain and nano/micro reinforced high performance cementitious composites

Specime ID	Residual Strength factors (RSF)	
	$R_{(5,10)}$	$R_{(10,20)}$
CEM	1.94	0.00
GNP_3_0.025	6.38	0.00
GNP_3_0.05	6.81	0.00
GNP_3_0.08	7.81	0.00
GNP_3_0.2	15.30	1.90
GNP_3_0.5	12.69	2.70
GNP_3_1.0	1.42	0.00
GNP_4_0.025	5.78	0.00
GNP_4_0.05	11.05	0.00
GNP_4_0.08	8.48	1.09
GNP_4_0.2	8.57	0.00
GNP_4_0.5	12.69	2.70
GNP_4_1.0	1.42	0.00
CBF_0.025	1.29	0.00
CBF_0.05	1.39	0.00
CBF_0.08	1.68	0.00
CBF_0.2	1.55	0.00
CBF_0.5	1.32	0.00
CBF_1.0	0.47	0.00
CHS_0.025	3.28	0.00
CHS_0.05	3.78	0.00
CHS_0.08	4.14	0.00
CHS_0.2	6.40	0.00
CHS_0.5	6.54	0.00
CHS_1.0	2.59	0.00
CPS_0.025	2.91	0.00
CPS_0.05	3.75	0.00
CPS_0.08	4.60	0.00
CPS_0.2	8.38	0.00
CPS_0.5	6.15	0.00
CPS_1.0	3.05	0.00

5.2 Compressive Response of High Performance Cement Paste Composites

The compressive strength is the measure of material's ability to sustain or withstand compressive loads while the ultimate compressive strength is the value of uniaxial compressive stress reached at the instant of complete failure. Figure 5.14 & 5.15 shows the average compressive strength values of different formulations with and without nano/micro reinforcements. Bar represents the mean value, and the top and bottom error bar represents the third and first quartile, respectively.

The observed variation in the values of compressive strength on addition of GNP particles is exhibiting the similar type of trend as observed in case of MOR with maximum improvements achieved at 0.2 wt% and 0.08 wt% additions of GNP_3 and GNP_4 particles respectively. The maximum attained enhancement is 111.4% in case of GNP_4 particles while for the GNP_3 particles it is recorded as 89.1%. We can conclude from the bar charts displayed in Figure 5.14 that the GNP particles are quite effective in filling the voids of HPCC and thereby enhance their resistance in compression. Due to finer particle size and relatively large surface area as well as the aspect ratio, the performance of GNP_4 particles is observed to be comparatively better than the corresponding proportions of GNP_3 particles. The optimum content of addition seems to range in between 0.08 wt% and 0.2 wt% of cement.

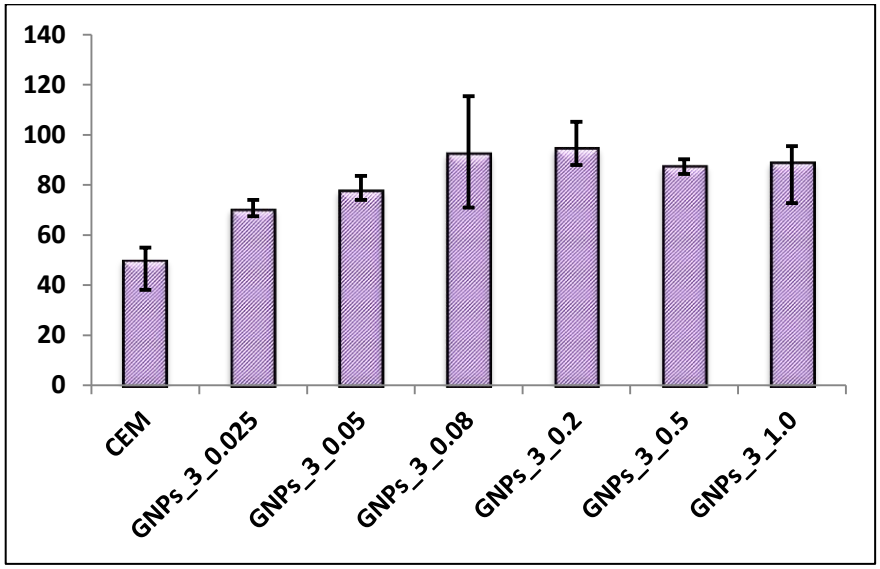

a

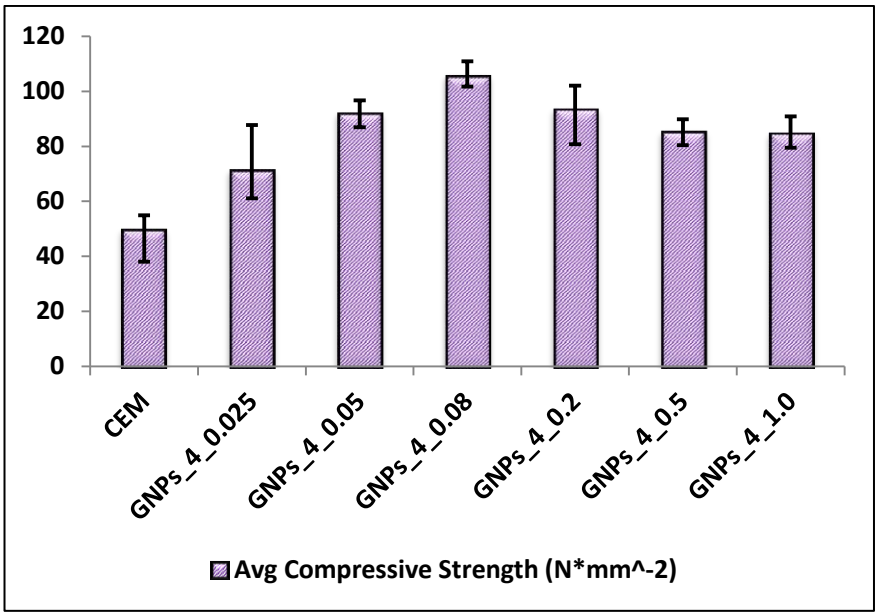

b

Figure 5.14 Maximum resistance in compression of HPCC with increasing contents of GNP_3 (a) and GNP_4 (b) particles

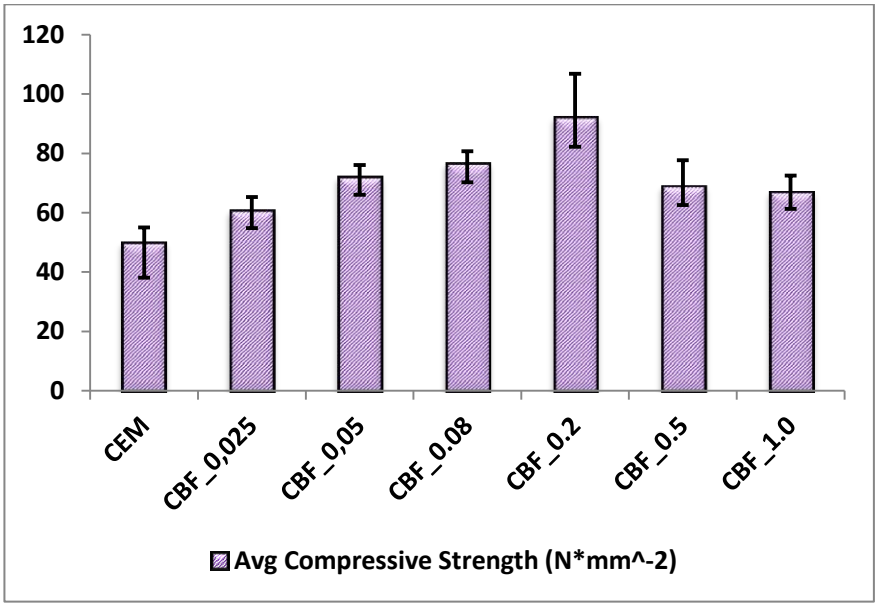
120
100
80
60
40
20
0
CEM
CBF_0,025
CBF_0,05
CBF_0.08
CBF_0.2
CBF_0.5
CBF_1.0
Avg Compressive Strength (N*mm^-2)

a

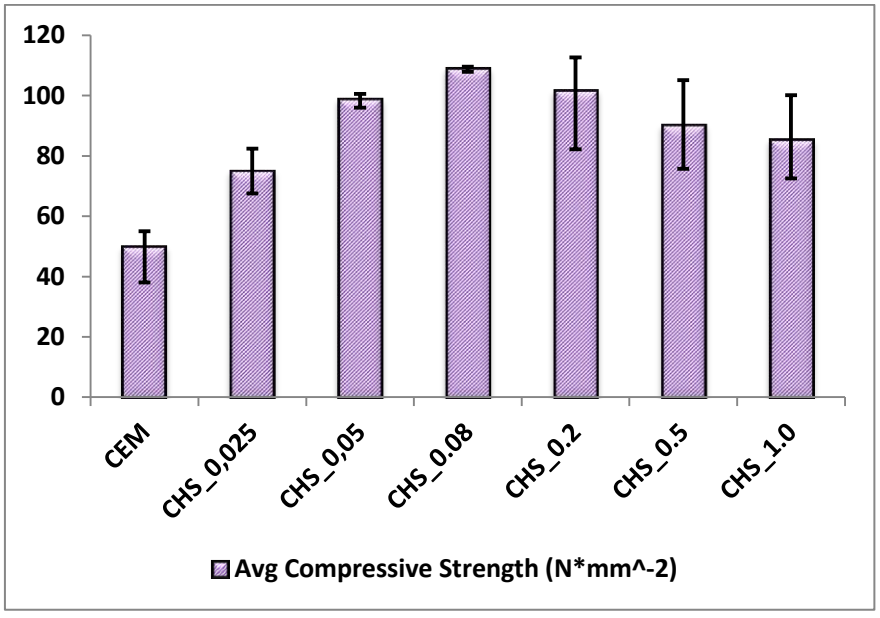
120
100
80
60
40
20
0
CEM
CHS_0,025
CHS_0,05
CHS_0.08
CHS_0.2
CHS_0.5
CHS_1.0
Avg Compressive Strength (N*mm^-2)

b

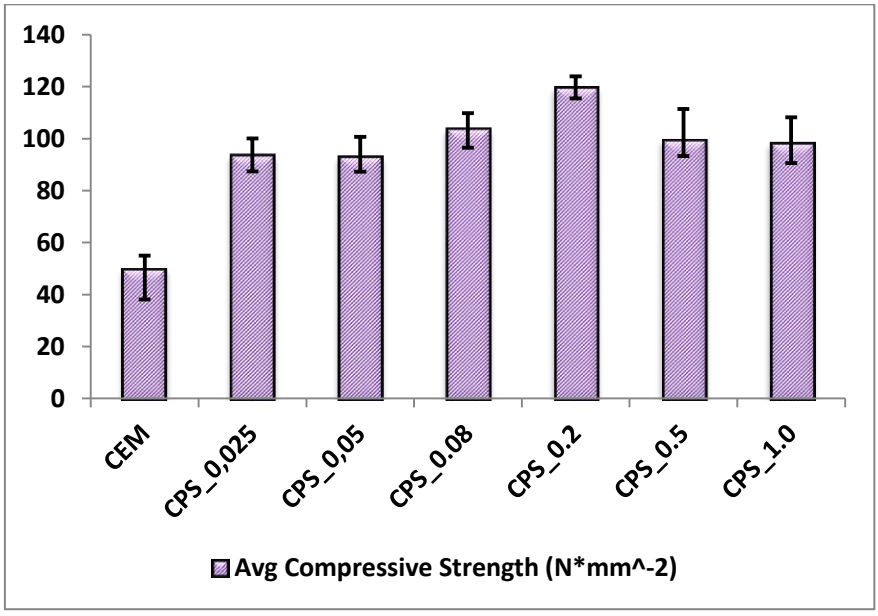

c

Figure 5.15 Maximum resistance in compression of HPCC with increasing contents of CBF (a), CHS (b) and CPS (c) particles

There is a remarkable improvement observed on addition of NMCPs in the compressive resistance of HPCC. The best results were obtained with CPS additions by 0.2wt% that resulted in a significant increase of 139% in the compressive strength of cementitious composites. An increase of 118% and 84% was achieved on the addition of CHS by 0.08 wt % and CBF by 0.2 wt% respectively. The efficient compressive behavior of CPS in comparison with CHS and CBF may be associated with its relatively high specific surface area, low specific gravity, high graphitization grade, lower particle size as well as the presence of surface defects. Since the particle size of NMCPs ranges in between nano to micro size therefore they possess the strong ability to effectively act as a filler for the voids of varying dimensions and consequently the resistance in compression of cement matrix is enhanced.

Previously in the investigations on other carbon based reinforcements, it was found that the maximum increase of 70% can be obtained in the compressive strength of HPCC on addition of 0.05 wt% CNTs (Yakoveli et al. 2006). Also Tyson et al. observed the exceptional increase by 82% in the compressive strength of cementitious composites reinforced with 0.15 wt% of CNFs (Tyson et al. 2011). The present research has explored an extraordinary increase by more than 100% on addition of GNPs as well as cost effective synthesized carbon nano/micro particles. The optimum contents recorded for the investigated carbon materials range in between 0.08-0.2 wt% which is the optimum value not only for the single mechanical characteristic because at the optimum contents most of

the mechanical properties including strength in flexure, strength in compression and fracture toughness were approximately recorded at their best.

5.3 Flexural Response of HPMC

To further expand the scope of present research, the second phase of high performance mortar composites (HPMC) was investigated for the mechanical performance on addition of GNP and NMCPs reinforcements. In this phase mortar specimens were prepared at the optimum level additions of reinforcing materials explored during the analysis of cement paste phase. The averaged values from experimental results regarding the mechanical properties of HPMC have been tabulated in Appendix D.

5.3.1 Load-CMOD Curves

Based on the load-CMOD results of the paste phase, the second phase of tests were performed on high performance cement mortar reinforced with GNP and NMCPs embedded at their optimum content.

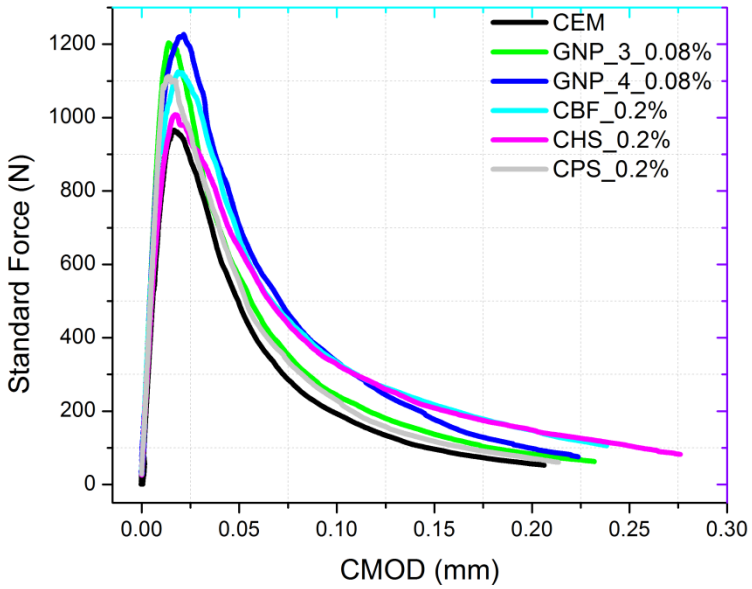

Figure 5.16 Comparison of load-CMOD curves of plain and nano/micro reinforced cementitious mortar composites

It is observed that the formulations reinforced with GNP particles have given best performance in this phase relative to other NMCPs reinforced matrices. Similar to the paste phase, the ascending portion of the curve in mortar phase exhibits more or less the

same slope for all the formulation with and without nano/micro reinforcements evidencing the similarity in their respective values of stiffness. The post-peak portion seem to suffer with a lot of modifications which were evaluated by the comparison of fracture toughness and toughness indices in section 5.3.3.

5.3.2 Modulus of Rupture and Uncracked Stiffness

The evaluated values of MOR based on Eq. 5.1 are plotted in Figure 5.17a along with the uncracked stiffness evaluated using slope of the load-CMOD curve as given in Figure 5.17b.

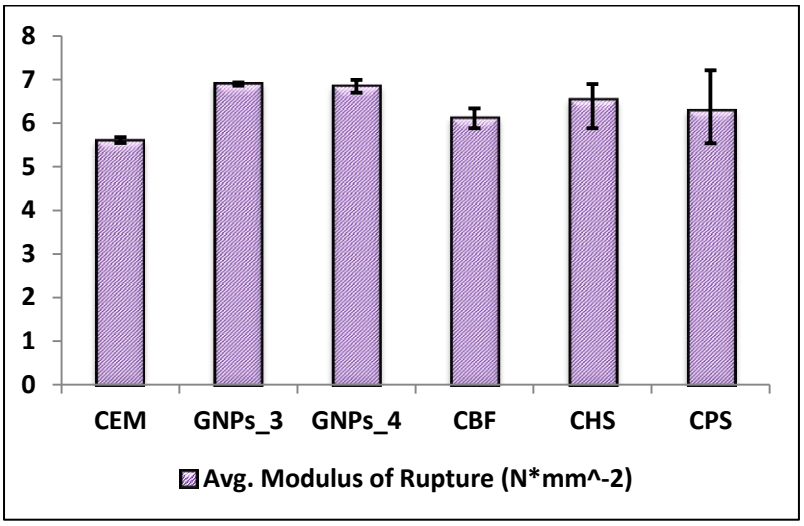

a

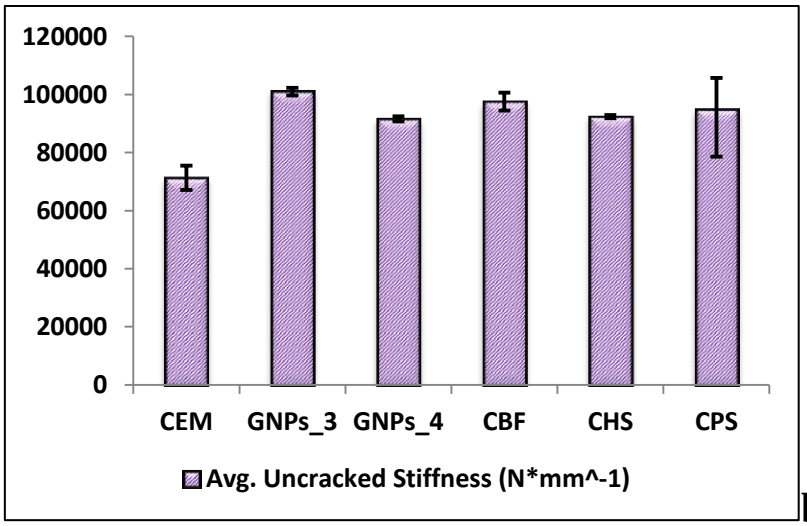

b

Figure 5.17 Average MOR (a) and uncracked stiffness (b) of plain and nano-reinforced cement mortar formulations

5.3.3 Fracture Toughness

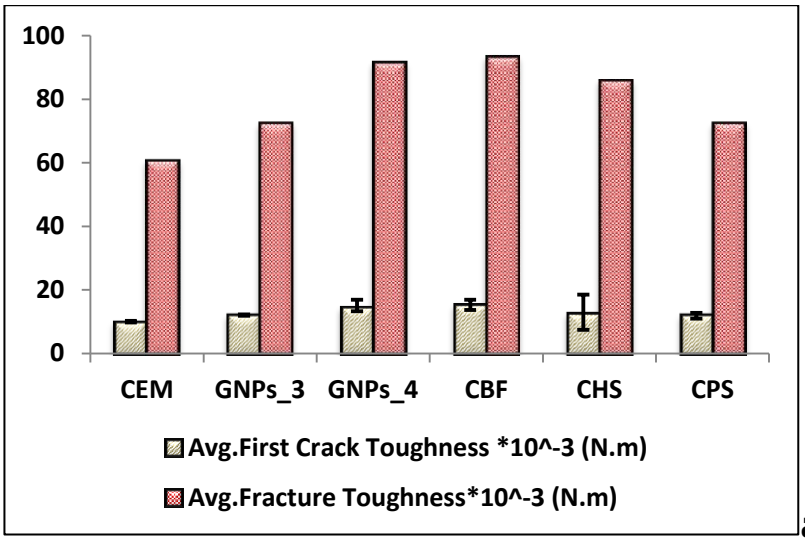

a

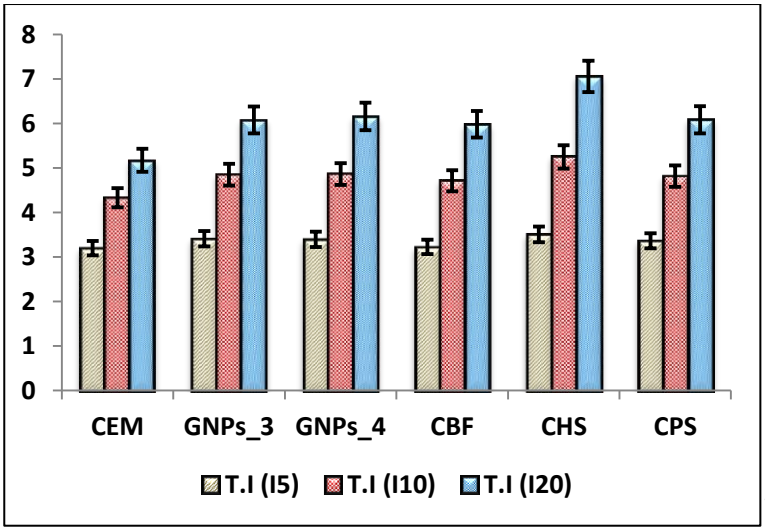

b

Figure 5.18 Average fracture toughness (a) and TI (b) of plain and nano-reinforced cement mortar formulations

The results displayed in Figure 5.18 clearly demonstrate that in the mortar phase even with the addition of aggregates, the investigated carbon reinforcements continued to evidence their performance in enhancement or modification of mechanical behavior of HPMC. In this phase best results have been reported with the addition of 0.08 wt% of GNP_4 particles.

5.3.4 Weight Efficiency Factor

To compare the efficiency of investigated carbon reinforcements, an efficiency factor of weight fraction is introduced. This factor is defined as the ratio of the fractional increases in flexural strength to the weight fraction of the additives.

$$WEF = \frac{\%\ increase\ in\ MOR}{\%\ added\ content} \qquad Eq.5.7$$

The WEF evaluated on the basis of plain and reinforced HPMC results is plotted in Figure 5.19 with a brief summary given in Table 5.2.

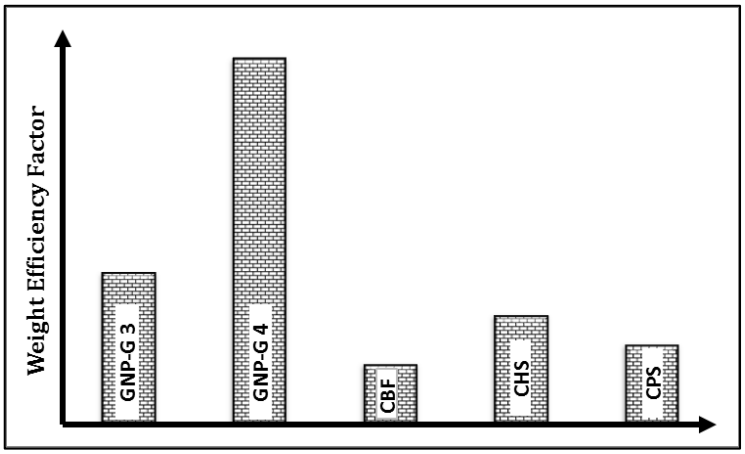

Figure 5.19 Weight efficiency factor for GNP and NMCP reinforcements

It has been observed that GNP_4 reinforcements possess WEF of 278 that is far greater than the values calculated for the other types of carbon reinforcements. CHS and CPS also attain the values of 83% and 61% respectively.

Table 5.2 WEF for nano/micro reinforced HPMC

Sample name	% increase in avg. MOR	Additive to cement ratio (%)	weight efficiency factor
GNPs_G3	23.12	0.20	115.58
GNPs_G4	22.25	0.08	278.17
CBF	9.29	0.20	46.45
CHS	16.71	0.20	83.53
CPS	12.25	0.20	61.26

Chapter 6. Microstructural Investigation and Enhancement/ Modification Mechanism of GNPs and NMCPs Reinforced Cementitious Matrices

6.0 General

This chapter covers the detailed investigation concerning the effect of graphene and nano/micro carbonized particles on the microstructure, porosity and developed phases during hydration process of cement paste composites. The critical paths followed by the cracks in case of nano/micro inclusions are also discussed in detail. The mechanism involved in the modification of mechanical behavior by the addition of nano/micro particles to cementitious composites has also been discussed in the recent chapter.

6.1 Microstructural Investigations

Microstructural investigations include porosity and pore size distribution measured by mercury intrusion porosimetry technique and electron-microscopic imagery of HPCC samples via FESEM analysis.

6.1.1 Mercury Intrusion Porosimetry (MIP) of HPCC formulations

The porosity and pore size distribution were measured using MIP. The results are reported in Table 6.1. MIP was performed on selected specimens of HPCC formulations with the addition of reinforcing carbon particles at their optimum contents. The results clearly indicate decrease in porosity and average pore radius on induction of carbon filler. A significant reduction in porosity and average pore radius was observed by the addition of carbon particles as compared to the reference pristine cement formulation. This is one of the reasons contributing to the better mechanical performance of these nano/micro reinforced HPCC formulations. Among the formulations reinforced with NMCPs, CTPS/cement formulation showed significantly reduced porosity and average pore radius at the age of 28 days. This explains why this particular formulation showed better mechanical performance among all other HPCC formulations embedded with synthesized nano/micro carbon inerts.

Table 6.1 Pore sizes and total porosity of plain and nano/micro reinforced HPCC formulations

Sample ID	Avg. Pore radius (nm)	Max. pore radius (nm)	Total porosity (%)	Porosity (%) (diameter ≤ 100nm	Porosity (%) (diameter ≥ 100nm)
CEM	10.1	56741.5	17.4	69.4	30.6
0.2_GNPs_3	6.4	54651.2	12.54	82.54	17.8
0.2_GNPs_4	5.2	52564.1	11.48	84.51	15.4
0.2_CBF	7.2	56169.5	14.58	74.56	21.85
0.2_CHS	6.6	55742.4	14.42	77.52	18.74
0.2_CPS	6.5	54852.4	13.54	78.65	18.24

6.1.2 Scanning Electron Microscopy of plain and reinforced cement formulations

It is observed in the FESEM micrographs of high performance cementitious matrices (Figure 6.1 and 6.2) that the induction of nano/micro carbonaceous inerts remarkably interrupted the straight and smooth trajectory of crack as attained in case of pristine cement matrix. The plain cement paste (Figure 6.1a) showed major cracks usually pass through dense hydration products in a relative straight direction. The cement composites with nano/micro heterogenic particles showed a number of fine cracks with occasional branch and considerable discontinuity. The entire phases of crack arresting phenomena were successfully observed through microscopic visuals.

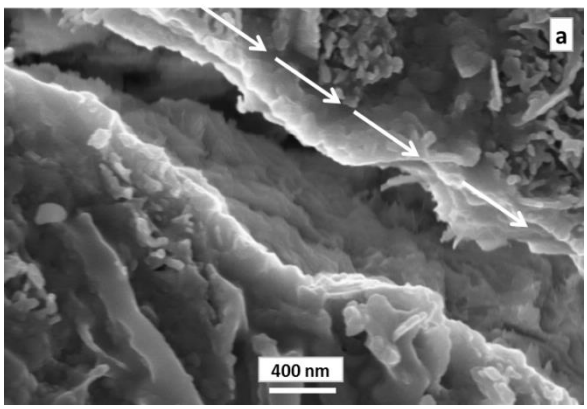

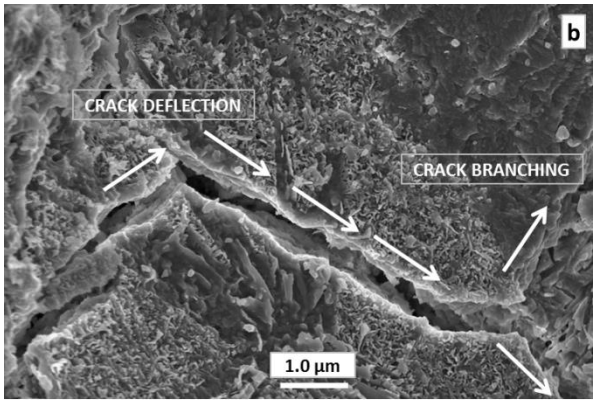

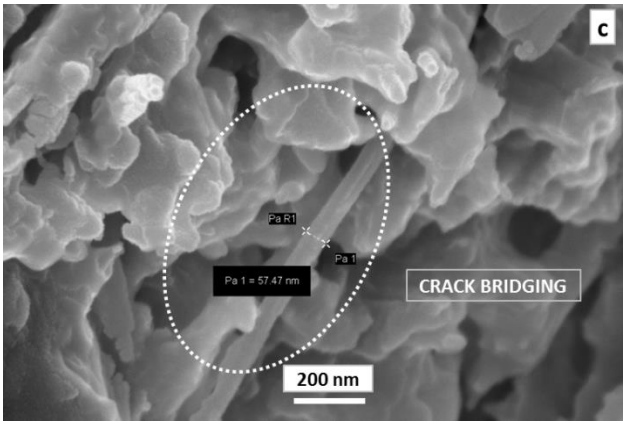

Figure 6.1 Micro-cracking pattern in plain (a), GNP_3 (b) and GNP_4 (c) reinforced cementitious composites

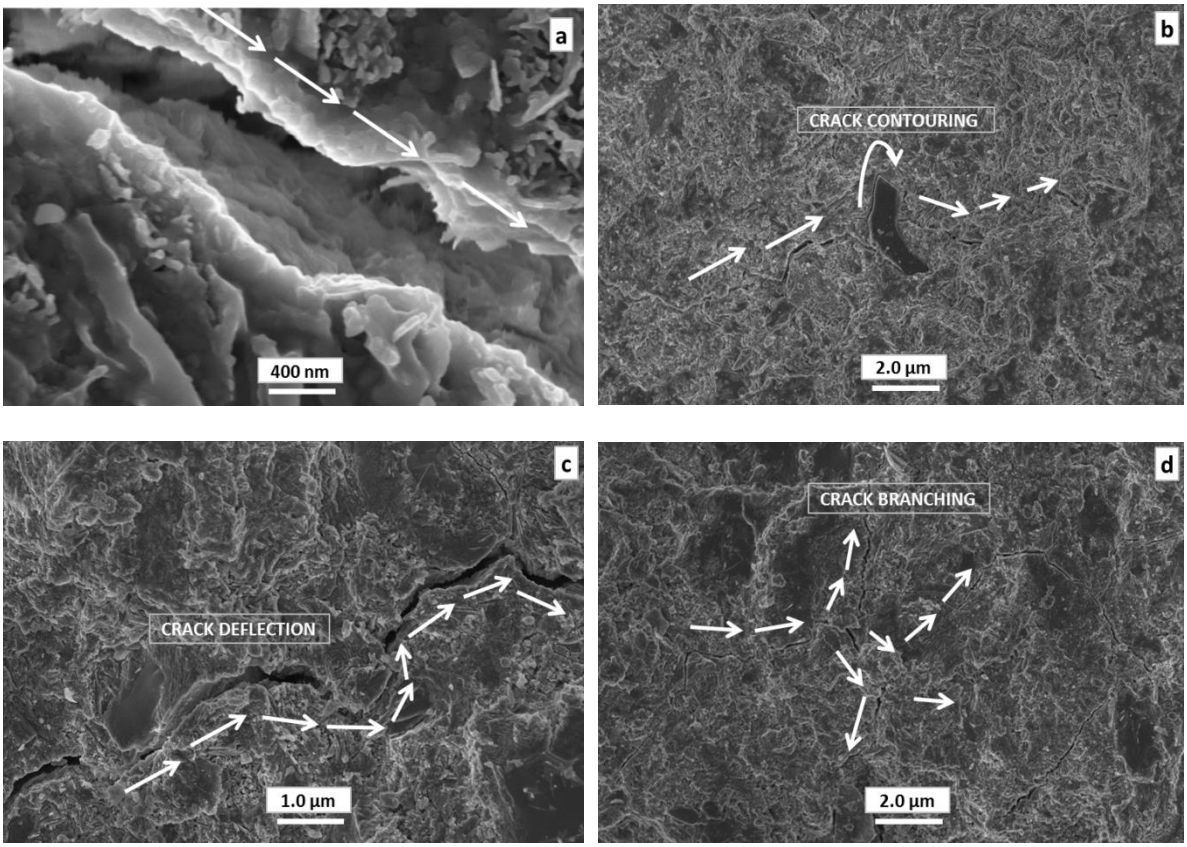

Figure 6.2 Micro-cracking pattern in plain (a), CBF (b), CHS (c) and CPS (d) reinforced cementitious composites

The micrograph of HPCC formulation reinforced with GNP_4 particles presents quite clear picture of the bridging action by GNP_4 plate across the crack as recorded in Figure 6.1b. Due to large aspect ratio GNP particles effectively contributed in restricting the propagation of cracks by crack bridging phenomena. In case of CBF and CHS particles

reinforced cement formulations the major signs of crack pinning/crack defections have been observed which are demonstrated by Figures 6.2bc. Due to the angular shape of CBF and CHS particles, the crack gets diverted from its original trajectory in case of encounter. Such crack deflection or crack contouring results in the requirement of an extra energy input to further propagate the crack along a different path and consequently enhanced fracture toughness of the reinforced HPCC is attained. The phenomena of crack branching which is related with the division of the propagating micro crack into multiple finer cracks was observed in formulations containing GNP_3 and CPS particles as reinforcing agents (Figure 6.1b and Figure 6.2d). In particular, as compared with other fillers, graphene sheets exhibit unique two-dimensional structure which can effectively deflect, or force cracks to tilt and twist around the sheet. The process helps to absorb the energy that is responsible for propagating the crack and thereby enhances the toughness of the composite. On the basis of FESEM observation, It is concluded that carbon particles contouring by the crack, crack pinning, crack bridging, crack diversion and crack branching are the mechanisms, which can explain the increase of toughness in the composite samples.

Note that at a low weight fraction of graphene sheet, it was rather challenging to identify the graphene sheet by SEM analysis due to its planar geometry and the cement coating on the GNP sheet. A detailed examination of micrographs also confirms that no signs of a large agglomeration or clustering of the fillers were observed. Fillers pullout commonly observed in CNTs reinforced cementitious composites was not observed in these nano/micro reinforced cement composites.

6.2 Strengthening Mechanisms for Cementitious Composites Reinforced with Carbonaceous Nano/Micro Inerts

Being the type of nano-particle GNPs and NMCPs also possess the features likes “small size effect” and “surface effect” which are much influential for the modification in the mechanical properties of cementitious composites. Besides the two features related with the size and surface area of carbonized particles there are some other contributing factors that significantly affect the mechanical performance of resultant cementitious matrices which include filler effect, crack-arresting effect and improvement in the interfacial transition zone (ITZ). The strengthening mechanisms for GNP and NMCPs reinforced high performance cementitious composites are summarized and discussed in this section.

6.2.1 Small Size Effect

In some conditions it is observed that on reducing the particle to the extent of nanoscale there are some qualitative variations in the particle properties occurring along with the quantitative change in the form of particle size. It basically refers the phenomena that particles reduced to nano scale possess entirely different properties compared with those exhibited in their macro sizes (Sanchez and Sobolev 2010). The reason is the periodic destruction of crystals boundary conditions which takes place on reducing the particle size comparable to some specific physical characteristics such as the wavelength of light, the de Brogile wavelength, the coherence length or the penetration depth of the superconducting state, etc resulting in reduction of atoms near the particle surface. Since the carbon particles investigated in the present research have particle ranging in nanometers so they possess a quite large interface along where the atoms are ordered in the confusing form. When the matrix containing these reinforcing particles is subjected to the external load or deflection, these confusingly arranged surface atoms have the ability to easily migrate resulting in an improvement in the values of absorbed energy causing increase in the resistance of concerned matrix against deformation. Therefore when the GNPs and NMCPs were added into the intrinsically brittle cementitious materials, a remarkable increase in the mechanical properties was attained.

6.2.2 Surface Effect

This is also one among the major contributing factors resulting in the enhancement or modification of mechanical strength by the addition of GNPs or NMCPs. Since the proportion of atoms present along the surface boundary of particles is inversely related with its average size therefore nanoparticles possess much higher percentage of surface atoms providing a large surface area and high surface energy that leads to much stronger absorption ability and chemical reactivity compared with normal materials (Sixuan 2012). There large surface area provides much enhanced interface to develop strong bondage with the host matrix. Moreover these particles act as a nuclei and provide high surface area around which the network structure of calcium silicate hydrate gel is deposited resulting in modifying the homogeneity of hardened cement paste. It was observed by Markar et al. that CNTs act as a nucleation sites for the deposition of tri-calcium silicate hydration products (Makar and Chan 2009). All these effects result in the refinement of microstructure of the composite and thereby modify its mechanical performance.

6.2.3 Filler Effect

It is a well-known fact that concrete consists of porous and non-homogeneous structure in which the porosity has a strong relation with its mechanical behavior as well as with the durability. The pores having diameter greater than 20 nm are generally considered harmful for the mechanical properties of cement matrix. The main strengthening component formed as a result of cement hydration i-e silica gel is also identified as a type of nanomaterial with millions of gel pores inside (Ramachandran 1996). Therefore it indicates that nano particles addition can effectively enhance the mechanical performance of cementitious materials by physically interacting with silica gel at the nano-scale. The small size, large surface area and high surface energy make GNP and NMCP to be among the one kind of efficient fillers. Although they do not interact chemically as with the case of silica fume particles but their physical filler action contributes to make them an effective alternative for reduction in porosity of the matrix.

As observed through the results of MIP analysis given in Table 6.1 that the addition of GNPs/NMCPs fines pore size distribution and substantially decrease the values of total porosity of composites by filling the gaps or pores in between the hydration products such as CSH gel and ettringite. As a consequent, the composites become much more compacted with enhanced resistance against compression and flexure.

6.2.4 Improvement in Interfacial Transition Zone (ITZ)

The concrete is composed of three major components that include the cement paste, the aggregates and the ITZ. ITZ is believed to be the most crucial component of concrete as it establishes a connection in between the two heterogenic phases. The ITZ is quite less resistive against cracking in comparison with the other two components and therefore considered as the weak zone of concrete. One of the reasons behind the weak performance of this zone is enhanced porosity that results due to the inability of the cement particles to pack efficiently around the aggregates, a well-known phenomenon called the ‘wall effect’. Another phenomena associated with the weakness of ITZ is bleeding, during which water migrates upward and accumulates around the aggregate which is the only hindrance encountered during its travelling. As a result the moisture content in the ITZ is increased leading to enhanced porosity and reduced strength of this particular constituent in comparison with the others. On addition of GNPs and NMCPs into the cementitious matrix, their large surface area and high surface energy make them absorb a large amount of water, by which bleeding phenomena in cement mortar is reduced and the possibility of forming water films is significantly decreased. Thus strengthening of the bond between aggregate and cement paste is achieved along with the improved resistance of ITZ against cracking. Even though the thickness of ITZ only ranges between 20-40μm but it covers

almost 20-40% of the total volume of cementitious matrix and modification of this weak link can result in remarkable improvements of strength, stiffness as well as fracture toughness of cementitious composites (Mindess and Young 1981).

6.2.5 Crack-Arrest and Particle-Interlocking

The cracking phenomena initiates from the nano scale and with the increase in applied force, it approaches to micro and then macro scales till the complete rupture of the material. Similarly, in case of concrete cracking originates internally developing in to a network of micro cracks and at last fracture of concrete is identified with a multiple or major cracks cut through it. To enhance strength as well as the fracture toughness it is essential to obstruct the initiation and then the propagation of cracks in an effective way. The investigated carbon reinforcements have performed exceptionally well in restricting the onset and then the propagation of nano/micro cracks that resulted in significant enhancement of mechanical strength as well as fracture toughness of the reinforced composites. Due to large aspect ratio of GNP particles and angular shape of NMCPs, the investigated carbon reinforcements were found quite resistive against the successive propagation of cracks.

From SEM observations (Figure 6.1 & 6.2) it is much clear that whenever there is an encounter in between the propagating crack tip and the carbon particle, there is huge disturbance occurred in its normal straight trajectory of that particular crack. The reinforcing particles are found successful in interrupting the normal crack propagation either by diverting it onto a completely new deflected trajectory as observed in Figure 6.1b and 6.2c or convincing it to contour in the surroundings along the weaker region (Figure 6.2b). In some cases, on interaction with the reinforcing carbon particle, the crack has been divided in to several finer cracks with deflected paths which is termed as crack branching as observed in Figure 6.2d on encounter with CPS particle. Due to relatively high aspect ratio GNP_4 particles are also observed much efficient in bridging the two faces of the propagating crack depicted in Figure 6.1c. The interlock between the crack and the introduced heterogenic carbon reinforcement results in the blockage of crack propagation requiring extra energy to overcome the obstacle. With an addition energy input the phenomena of crack deviation, branching or multiplication take place leading to ultimate increase in the total area of fracture surface which becomes several times the area of the cross-section of the element. The complex and tortured fractured face is also a sort of evidence to the fact that these heterogenic inclusions interrupt the smooth propagation of crack either by crack deflection, crack pinning or branching it into number of fine cracks as shown in Figure 6.1 & 6.2. Hence all these mechanisms contribute in one way or

the other to modify the fracture properties of reinforced HPCC and delay the fracture process by increasing crack length.

a

b

c

Figure 6.3 Typical fracture planes of plain (a), GNP_3 (b) and CBF (c) reinforced cementitious composites after 3-point bending test

Chapter 7. Electromagnetic Interference Shielding Effectiveness of Submicron Carbonized Particles Reinforced Self Compacting Paste

7.0 General

In this chapter the electromagnetic interference shielding effectiveness of cement composites has been numerically evaluated on the basis experimentally determined real and imaginary permittivity values using a Matlab program. The role of cost effective synthesized nano/micro carbon particles addition in improvement of electromagnetic wave absorption properties of cementitious composites is studied. The research discussed in this chapter has been recently published in the journal of *Construction and Building Materials*.

7.1 Introduction

Besides many advantages, modern developments in electronics especially in wireless and communication systems are contaminating our surroundings with electromagnetic waves (EMWs) pollution. Presence of EMWs in the environment at such an alarming level uplifts the risks of electromagnetic interference (EMI), which may affect the normal functionalization of many electronic and communication devices. Excessive exposure to such radiations is hazardous to human health, as they can enhance the probability of tumors growth in human body (Andrews and Savitz 1999; Beall et al. 1996; Bender et al. 2007; Thomas et al. 1987). Such issues have motivated many researchers and scientists to explore new ways and methods to provide shielding against the severe exposure of EMWs (Ameli, Jung, and Park 2013; Cao and Chung 2003; B. Dai et al. 2013; Das, Bhattacharya, and Kalra 2012; Eswaraiah and Ramaprabhu 2011; Fan et al. 2006; Fang et al. 2007; Giorcelli et al. 2013; Kuzhir et al. 2013; Zhao et al. 2006). Military stealth technology or LO technology (Low observable technology) also demands new ideas concerning effective electromagnetic shielding.

Cement is the basic building material exhibiting vital role in construction industry. Cement matrix possess poor shielding against EMWs. Some researchers and scientists have done serious efforts to enhance shielding effectiveness of cement composites by making conductive intrusions (Bantsis et al. 2012; Baoyi et al. 2011; Y. Dai et al. 2010; Guan et al. 2006; Qinglei Liu et al. 2012; Pretorius and Maharaj 2013; Singh et al. 2013; Zhang

and Sun 2010). Wang et al. (B. Wang et al. 2013) investigated EMWs absorbing properties of cement nano-composites with varying contents of CNTs and reported maximum absorption at 0.6 wt.% CNTs inclusion in the frequency ranges of 2–8 GHz and 8–18 GHz. Nam et al. (Nam, Kim, and Lee 2012) analyzed the influence of CNTs dispersion on the electromagnetic interference shielding effectiveness (EMI-SE) of CNTs/cement composites and attained maximum enhancement at 0.94 GHz, 1.56 GHz, 2.46 GHz and 10 GHz frequencies using 0.6 wt.% CNTs and 20 wt.% silica fume. Kong et al. (Kong et al. 2014) used 3D carbon nanotubes/graphene (CNTs/G) hybrids to achieve adequate dispersion and concluded that these hybrids meet the requirement of impedance matching, lower EM reflection and improve the EMWs absorption capability of cement matrix.

Although CNTs and graphene possess ideal properties in terms of high specific surface area, low density, high aspect ratio and very high conductivity (Alkhateb et al. 2013; Al-Saleh, Saadeh, and Sundararaj 2013; Chung 2001; Y.-H. Li and Lue 2007; Savi et al. 2014) but there are several major concerns that normally restrict their utilization on large scales. One of them is their higher production cost and another is their effective dispersion in cement matrix. Moreover, acid functionalization is often used to improve the adhesion between carbon nanotubes and the cementitious matrix, leading to an increase of the toxicity of CNTs, depending on their degree of catalytic impurities and of a threshold (Figarol et al. 2014).

The literature survey indicates that little attention has been paid on the exploration of cost effective and dispersion free alternatives to improve EMI-SE of cement composites. Therefore, the current study is focused on the utilization of sub-micron-sized, carbonized agricultural residues; which includes hazelnuts and peanuts shells to enhance the EM shielding effectiveness of cement composites.

Peanut is one of the most popular and magnificently consumed dry fruit all over the world especially in China and India that are ranked as its top two producers. According to the latest survey of United States Department of Agriculture (USDA) world total production of peanuts is almost 40 million metric tons with more than 60% contributions from China and India (USDA-Foreign Agriculture Service n.d.). Hazelnuts are also getting renowned all over the world especially because of their vast usage in many chocolate and ice-cream flavors. Food and agricultural production statistics of United Nations reported that the world's hazelnuts production was about 0.91 million metric tons in year 2012, with major part coming from Turkey and Italy about 70% and 20% of its production respectively (FAOSTAT-Food and Agriculture Organization n.d.). Both hazelnuts and peanuts generate considerable amount of residues in form of their shells with little to no specific

value. Therefore it is important to look for ways to manage and utilize this bio-waste beneficially.

Peanut shell and Hazelnut shell yield high content of bio char on carbonization (Ferreira et al. 2015; Huff, Kumar, and Lee 2014; Nisamaneenate et al. 2014; E. Pu and Pu 1999). An average yield of about 35% was reported for peanut shell at a temperature of around 500^{o}C (Huff, Kumar, and Lee 2014), while in case of hazelnut shell it was found more than 40% for the same range of temperature (E. Pu and Pu 1999). The economic availability and excellent conversion efficiency of peanut shell and hazelnut shell via pyrolysis, were the two main reasons that motivated the authors to explore their use in cement composites for effective shielding against EMWs.

7.2 Mix proportions and Specimen Details

Five mix formulations were prepared including the reference one; detail mentioned in Table 7.1. Sub-micron carbonized inerts were used as an additive in two proportions i.e. 0.2 and 0.5 wt% of cement. Weight ratios of water and super plasticizer were kept constant at 35% and 1.5% by weight of cement respectively.

Table 7.1 Mix proportion

Denotations	**Weight compositions (% mass ratio of cement weight)**				
	Cement	Water	Superplasticizer	(CPS)	(CHS)
CEM	100	35	1.5	0.0	0.0
0P2CPS				0.2	0.0
0P5CPS				0.5	0.0
0P2CHS				0.0	0.2
0P5CHS				0.0	0.5

7.3 Preparation

The entire preparation consisted of two steps. First step comprises dispersion of sub-micron carbonized shells (CS) in water with the aid of surfactant and bath sonication for 15 minutes using the Sonics Vibracell 750W ultrasonic probe operated at 30% amplitude. Second step covers mixing of resultant homogeneous solution with cement using mechanical mixer operated at 440 rpm (slow mixing) for 1.5 min and at 660 rpm (fast mixing) for 2.5 min.

Mixed cement formulations were poured in associated labeled plastic molds having 6.5 cm in diameter and 1.0 cm in height. The molded specimens were kept in covered plastic box

partially filled with water for initial 24 hrs. After that the specimens were demolded and immersed in water. Curing was done at room temperature (20±2 ^{o}C) for 28 days (Bois et al. 1998). The cured specimens were dried in oven at 50±5 ^{o}C for 5 days and then stored in air tight bags. Typical cement specimen compared with one euro coin along scale is shown in Figure 7.1.

7.4 Measurement of Permittivity

Complex permittivity measurements of cement composites containing sub-micron carbonaceous fillers were performed in the frequency range 0.20-10 GHz with a commercial dielectric sensor (Agilent 85070D) and a network analyzer (E8361A; see Figure 7.2). The system was calibrated for water and air before starting measurements. Such measuring system was adopted keeping in view its feasibility to work on specimens with smaller dimensions and it also allows wide-band characterization as well. In all measurements it was tried to ensure perfect contact between sensor probe and specimen's surface. Measurements were taken at six different sites of each single specimen to ensure homogeneity and reduce error margin; reported results are the average of the six measurements.

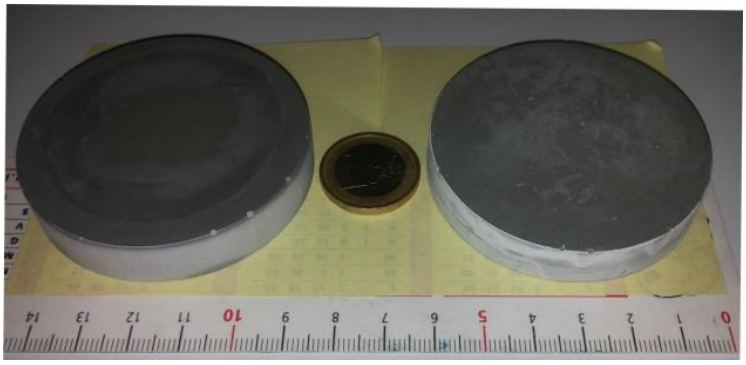

Figure 7.1 Typical sub-micron cement composite compared with one euro coin

Figure 7.2 Measurement setup. Agilent sensor (85070D) and Network Analyzer (E8361A)

7.5 Measurement of Dispersion

It was hypothesized by Nam et. al. (Nam, Kim, and Lee 2012) that better dispersion state of CNTs in the cement matrix can bring higher EMI-SE. CS were dispersed in water using ultrasonic treatment and superplasticizer. To demonstrate that a good level of dispersion was achieved a small amount of the solution (water + CS + SP) was diluted with a measured water content (1:5) in a test tube and visually inspected. The color appeared uniform even after one hour of dispersion. If CS were badly dispersed a certain quantity would have deposited at the bottom of the test tube, as in case of 0.5 wt% CNTs dispersed in water for comparison as shown in Figure 7.3.

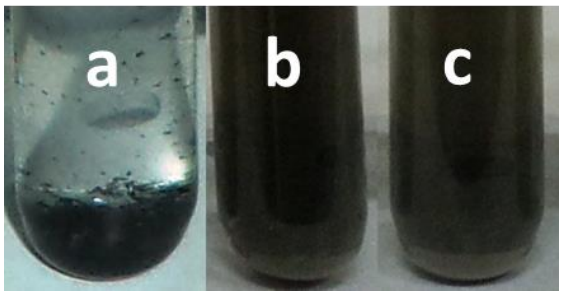

Figure 7.3 Dispersion level of 0.5wt% CNTs (a), 0p5CPS (b) and 0p5CHS (c) in water after 1hr of dispersion

FE-SEM analysis of fractured cement specimens given in Figure 7.4 showed better dispersion of CS inside cement matrix. All particles are very well distributed and no signs of agglomeration are visible. Better dispersion results in creation of more and more interfaces which ultimately enhance EMI-SE by increasing absorption loss of EMWs.

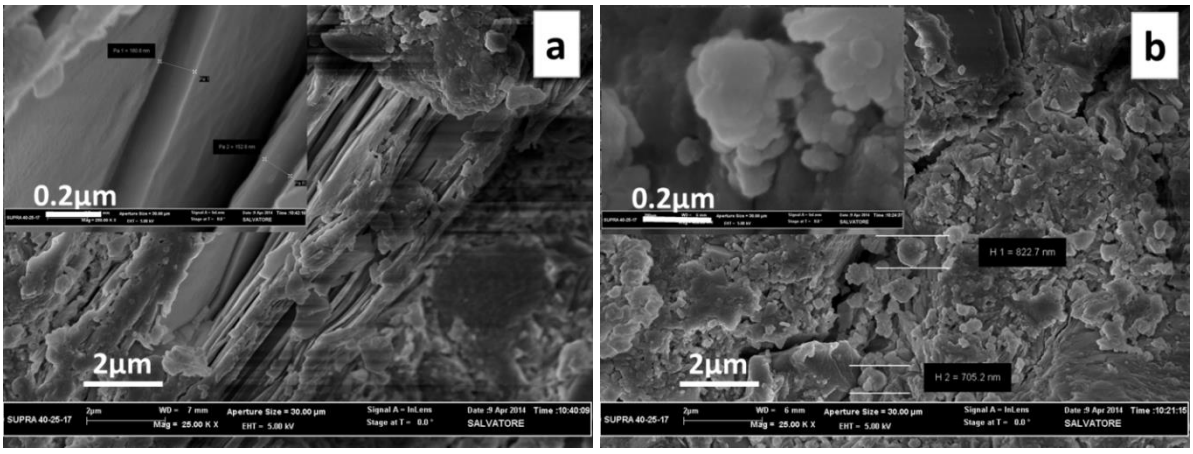

Figure 7.4 FE-SEM micrographs of 0p5CPS (a) and 0p5CHS (b) within the cement-matrix

7.6 Complex Permittivity Measurements and Analysis

The relative complex permittivity ($\varepsilon_r = \varepsilon' - j\varepsilon''$) was measured using dielectric probe sensor in 0.2-10 GHz frequency range. Figure 7.5 shows both real (ε') and imaginary (ε'') parts of permittivity as a function of frequency for cement composites with and without CS inclusions. The real part refers to the content of energy stored by material when exposed to external electric field while imaginary part is the measure of dissipated or lost energy. An appreciable increment was observed in the values of real and imaginary permittivity on induction of filler in cement matrix.

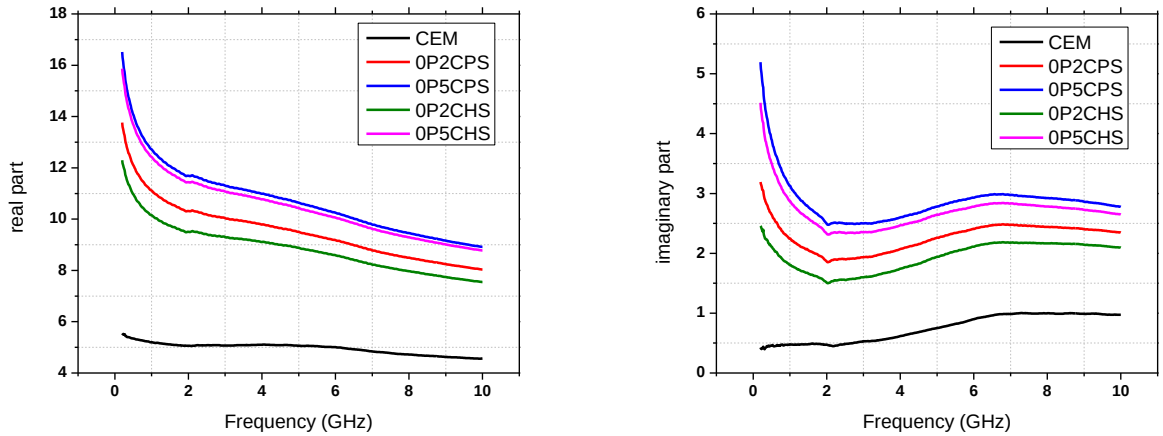

Figure 7.5 Complex permittivity of pure cement paste and cement composites with varying contents of CPS and CHS

Dielectric performance of a material depends upon its ionic, electronic, orientation and space charge polarization. Ionic polarization is inversely related to frequency of EMWs with nominal decrease observed at high frequencies. This is the reason why ε' and ε'' reduce on increase in frequency of applied EMWs. Since CS contain carbon (C > 85% see Table 5) which possesses free electrons and bound charges that account for encouraging strong orientational polarization. Inclusion of very well dispersed CS in an insulating medium like cement results in the formation of more interfaces with ultimate increase in space charge polarization. All these factors contributed to enhance both dielectric constant (ε') and dielectric loss (ε'') of cement composites containing CS; with direct relation to the added content.

7.7 EMI Shielding Effectiveness (Numerical Results)

Shielding effectiveness (SE) is defined in decibels (dB) and mathematically expressed as (Y. Dai et al. 2010):

$$SE_{dB} = R_{dB} + A_{dB} + M_{dB} \qquad Eq.\ 7.1$$

The mathematical expression of SE clearly demonstrates its dependence upon three major losses occurring while propagation of EMWs through the medium. R_{dB} is termed as reflection loss which occurs due to reflection of EMWs at the material's interfaces. A_{dB} is absorption loss of the wave as it proceeds through the barrier with strong relation to its thickness (t) and skin depth (δ). Skin depth is defined as the material's thickness which can reduce the power of EMWs by a factor of 1/e from its original power during propagation and it is given by following relation:

$$\delta = 2/\sigma\omega\mu \qquad Eq\ 7.2$$

Here σ, μ and ω are the electrical conductivity, magnetic permeability of the material and angular frequency respectively. There is some additional effect on total SE due to re-reflections and transmissions phenomena of EMWs during their propagation through the barrier; known as multiple reflection loss M_{dB} and can be neglected if SE exceeds 10 dB (Paul 1992).

Total SE along with the three major contributors i.e. R_{dB}, A_{dB} and M_{dB} was numerically evaluated in the frequency range of 0.2-10 GHz based on measured values of dielectric constant (ε') and dielectric loss (ε''). Matlab script was used considering a sample material with a thickness greater than skin depth ($t > \delta$). In the calculations conductivity, permeability and complex permittivity are given by following set of equations respectively:

$$\sigma = \varepsilon''\omega\varepsilon_o \qquad Eq.\ 7.3$$
$$\mu = \mu'\mu_o \qquad Eq.\ 7.4$$
$$\varepsilon = \varepsilon'\varepsilon_o \qquad Eq.\ 7.5$$

R_{dB}, A_{dB} and M_{dB} were calculated according to following expressions:

$$R_{dB} = 20 * log_{10}\left|\frac{(Z_O+Z_m)^2}{4*Z_O Z_m}\right| \qquad Eq.\ 7.6$$

$$A_{dB} = 20 * log_{10}\left|e^{\frac{t}{\delta}}\right| \qquad Eq.\ 7.7$$

$$M_{dB} = 20 * log_{10}\left|1 - \left[\left(\frac{Z_O-Z_m}{Z_O+Z_m}\right)^2 * e^{-\frac{2t}{\delta}} * e^{-i*2*\beta*t}\right]\right| \qquad Eq.\ 7.8$$

where Z_o and Z_m are the characteristic impedance of free space and barrier material respectively given as.

$$Z_o = \sqrt{\mu_o / \varepsilon_o} \qquad \textit{Eq. 7.9}$$

μ_o and ε_o correspond to permeability and permittivity of free space

$$Z_m = \sqrt{\frac{i*\omega*\mu}{\sigma+(i*\omega*\varepsilon)}} \qquad \textit{Eq. 7.10}$$

α and β being the propagation factors of shield are related to its propagation constant γ as:

$$\gamma = \sqrt{i\omega\mu[\sigma + (i\omega\varepsilon)]} = \alpha + i\beta \qquad \textit{Eq. 7.11}$$

Figure 7.6 shows that inclusion of both CPS and CHS in cement composites increases their SE and related losses in 0.2-10 GHz frequency range with direct proportionality to the added amount. The observed enhancement pattern of EMI-SE attained on addition of the two CS is almost similar with slightly better results observed in case of CPS; which may be associated with its relatively high specific surface area (Table 1) and defective surface morphology in comparison to CHS. Another explanation maybe also due to a higher number of particles distributed within the cementitious matrix, considering that CS additions were done in weight with respect to cement and that CPS have a slightly lower density with respect to CHS, but particles diameter are rather similar.

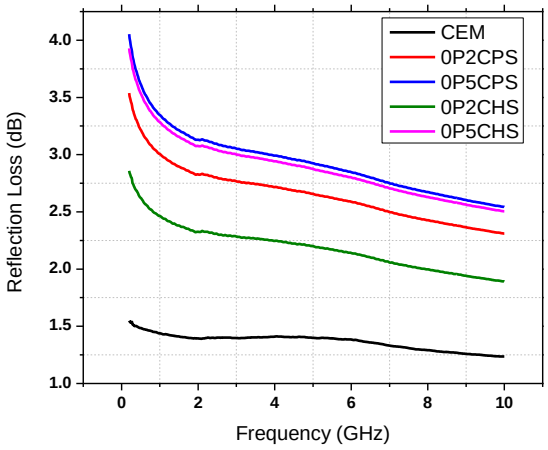

(a) EMW reflection loss of a 10mm thick cement composite sample with and without CS inclusions

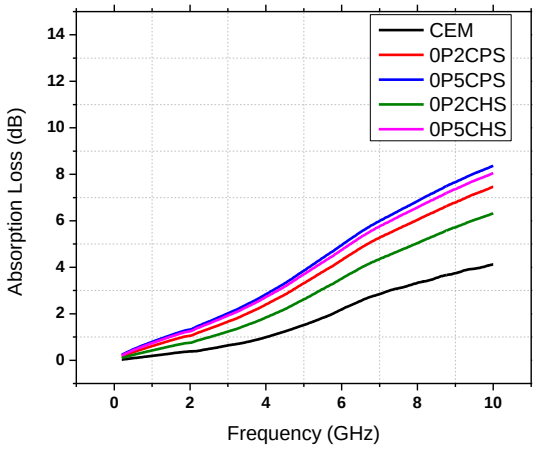

(b) EMW absorption loss of a 10mm thick cement composite sample with and without CS inclusions

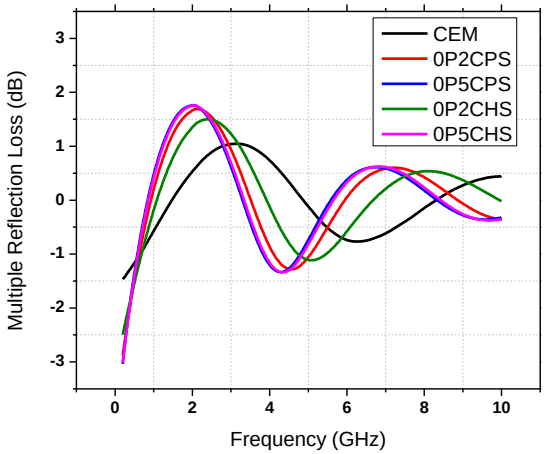

(c) EM wave multiple reflection loss of a 10mm thick cement composite sample with and without CS inclusions

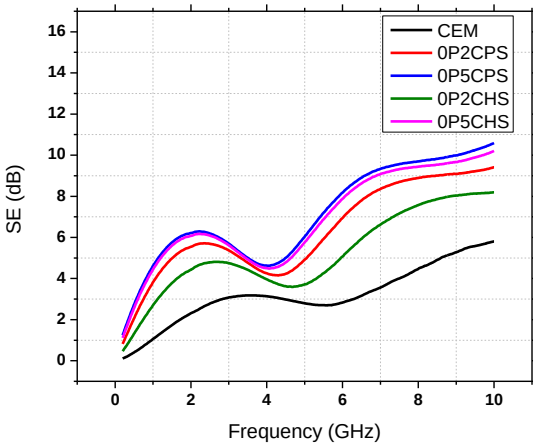

(d) Total shielding effectiveness of a 10mm thick cement composite sample with and without CS inclusions

Figure 7.6 Variation in EMWs Reflection (a), Absorption (b), Multiple reflections (c) and resultant EMI SE (d) of cement nano-composites as a function of frequency

To have a better evaluation of results, total SE of all five formulations were compared at four different frequencies of 0.94 GHz (frequency of GSM mobiles), 1.56 GHz (frequency of GPS communication devices), 2.46 GHz (frequency of microwave ovens), and 10.0

GHz (frequency of radio communication devices) as done by Nam et al (Nam, Kim, and Lee 2012). Figure 7.7 shows that maximum increase by 353% in SE of cement sub-micron composites was observed on addition of 0.5 wt% CPS at 0.9 GHz frequency. This percentage reduces to 223%, 126% and 83% as we proceed towards high frequency values of 1.56 GHz, 2.46 GHz and 10 GHz, respectively. In case of 0.5 wt % CHS inclusions, a similar patterned increase of 335%, 214%, 122% and 76% was achieved at four specified frequencies in comparison to reference specimens.

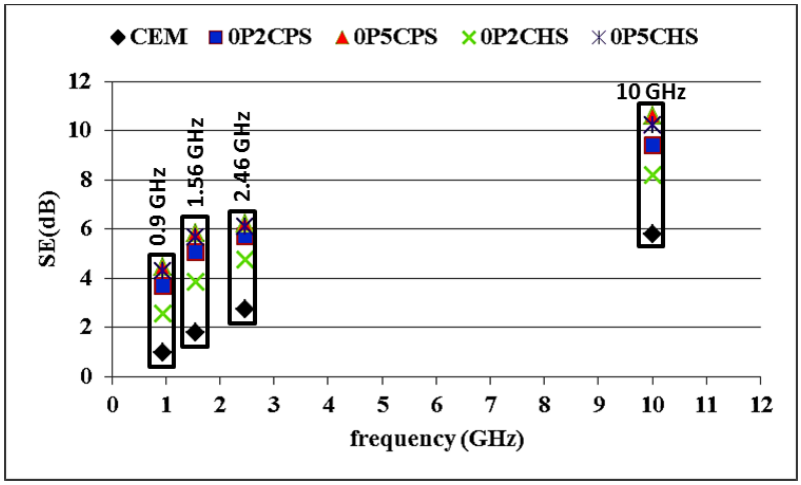

Figure 7.7 EMI SE of cement sub-micron-composites at specific frequency points with variation of CPS or CHS weight ratios added in cement matrix materials

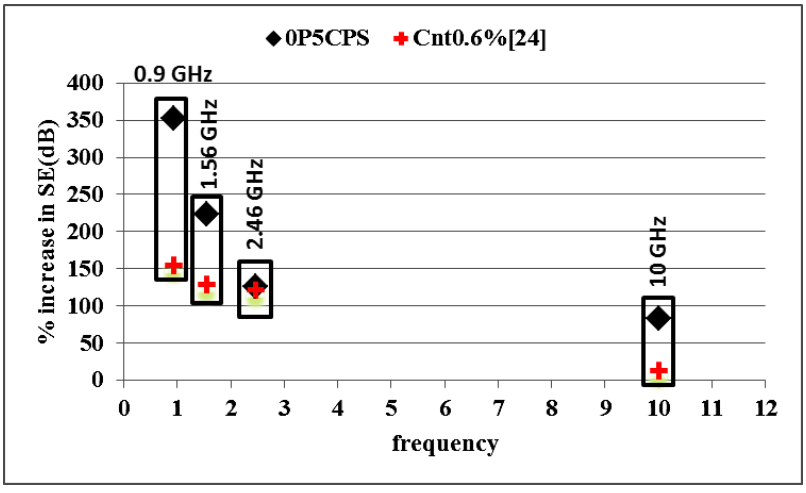

Figure 7.8 EMI SE comparison of cement sub-micron-composites containing 0p5CPS and 0.6wt% CNTs at specific frequency

Total increase in SE and associated components on adding merely 0.5 wt% CS in cement composites is much higher in comparison to the ones reported by other researcher using expensive CNTs in same content along with heavy amount of costly dispersants (Nam, Kim, and Lee 2012; Singh et al. 2013). To make the comparison more significant, percentage increase in SE of cement sub-micron composites at the four prescribed frequencies using 0.5 wt% CPS (achieved by authors) was compared with 0.6 wt% CNTs (Nam, Kim, and Lee 2012) in Figure 7.8. Comparison shows maximum enhancement on addition of 0.5 wt% CPS in cement composites due to its much better dispersion in water (Figure 7) and then in cement matrix (Figure 8). Nam et al (Nam, Kim, and Lee 2012) also reported much better results of shielding effectiveness on effectively dispersing CNTs in cement with the addition of 20 wt% silica fume.

7.8 Cost Comparison

To have an idea related to percent reduction in cost on utilizing CS instead of CNTs in preparing one cubic meter cement grout; cost analysis was performed as per the purchased price from the market (as of June 2014). Formulations containing 0.5 wt% additive fillers were selected as they attained much enhanced EMI-SE in comparison with pure cement composites. Based on Eq 12, detailed calculations of quantities and associated expenses are summarized in Table 6. After analysis, it appears that CS inclusions reduce the cost by approx. 88.5% in comparison with corresponding CNTs/cement composites.

Density of CNTs = 2.05 g/cm^3 (Grimaldi et al. 2013)
Density of SP (assuming Mapei SP1) = 1.09 g/cm^3 (Mapei n.d.)
Density of dispersant (assuming gum arabic) = 1.35 g/cm^3 ("Gum Arabic (9000-01-05), MSDS. Melting Point Boiling Point Density Storage Transport" n.d.)

$$1 = \left(\left(\frac{c}{density\ of\ c}\right) + \left(\frac{wt\ of\ water\ (0.35c)}{density\ of\ water}\right) + \left(\frac{filler\ content\ (0.005c)}{density\ of\ nano\ filler}\right) + \left(\frac{SP\ wt\ (0.015c)}{SP\ density}\right) + \left(\frac{disp\ wt\ (6*CNTs)}{disp\ density}\right)\right) + 0.02\ (air) \qquad Eq\ 7.12$$

Table 7.2 Comparison of cost analysis

Materials	**Unit Price ($)***	**CEM**		**0p5CNTs**		**0p5CPS**		**0p5CHS**	
		Quantity/ m^3	Price ($)	Quantity/ m^3	Price ($)	Quantity/ m^3	Price ($)	Quantity/ m^3	Price ($)
Cement (kg)	0.15	1359.4	203.9	1314.4	201.2	1355.1	203.3	1355.4.	203.3
CNTs (kg)	2000 ("Cheap Tubes, Multi Walled Carbon Nanotubes-MWNTs" n.d.)	-	-	6.57	13140	-	-	-	-
PS (kg)	0.01	-	-	-	-	6.78	0.07	-	-
HS (kg)	0.02	-	-	-	-	-	-	6.78	0.14
SP (kg)	100	20.4	2040	19.7	1970	20.3	2030	20.3	2030
Dispersant (kg)	110	-	-	39.4	4336	-	-	-	-
Processing cost (CS)	5.0	-	-	-	-	6.78	33.9	6.78	33.9
Total cost	-	-	2243.9	-	19647.2	-	2267.3	-	2267.4
Percent Increase (ref CEM)	-	-	100.0	-	776	-	1.08	-	1.08
Percent Reduction (ref 0p5 CNTs)				-	0.0	-	88.5	-	88.5

* $ stands for US dollars

Research Conclusions

In the recent research the effect of graphene nano platelets and synthesized nano/micro carbon particles produced from bio-waste on the overall response of high performance cementitious formulations in both paste and mortar phases was evaluated. Based on experimental observations, the following conclusions can be drawn:

1. It was determined that graphene nano-platelets can be uniformly dispersed in water as well as in the cementitious matrix without any addition of separate dispersant or surfactant or stabilizing agent.

2. It was found that even at a very low content of addition, remarkable improvements in the mechanical strength and fracture toughness can be achieved. The optimum content of addition for the grade 4 graphene nano-platelets was found as 0.08 wt% providing with a significant increase of 89% and 29% in compressive and flexure strength along with 115% improved fracture toughness.

3. It was explored that we can synthesize carbonized particles from agricultural residue and they can be effectively used in cement matrix to enhance the fracture properties and to refine microstructure. The dependence of the particle shape on toughening is critical and angular grains are needed to produce effective crack-bridging. In our case, from what observed by means of FE-SEM, we believe that carbonized particles contouring by the crack, crack pinning, crack diversion as well as the crack branching are the mechanisms which can explain the increase of toughness in the composite samples.

4. A novel cost effective material in the form of cement composites containing carbonized agricultural residue (comprising CPS and CHS) was proposed for shielding against electromagnetic waves. The investigated material was found much efficient for electromagnetic interference shielding applications, providing the advantage of better dispersion, simple manufacture at a much lower cost (cost saving > 85%) compared to the corresponding carbon nanotubes based cement composite material.

References

Abu Al-Rub, Rashid K., Ahmad I. Ashour, and Bryan M. Tyson. 2012. "On the Aspect Ratio Effect of Multi-Walled Carbon Nanotube Reinforcements on the Mechanical Properties of Cementitious Nanocomposites." *Construction and Building Materials* 35: 647–55. http://linkinghub.elsevier.com/retrieve/pii/S0950061812002887 (May 31, 2014).

Afroz, Mehar, S Irfan Sadaq, and Sameer Mohammed. 2013. "Experimental Study and the Effect of Alkali Treatment with Time on Jute Polyester Composites." *International Journal of Engineering Research* 28(2): 23–28.

Ajayan, Pulickel M., Linda S. Schadler, and Paul V. Braun. 2006. *Nanocomposite Science and Technology*. John Wiley & Sons. https://books.google.com/books?id=UpGnW8I_AvIC&pgis=1 (March 28, 2015).

Alessandro, Lopez. 2012. "'Carbon Nanotubes in Concrete' a Novel Building Material Investigation." Università di Roma.

Alkhateb, Hunain, Ahmed Al-Ostaz, Alexander H.-D. Cheng, and Xiaobing Li. 2013. "Materials Genome for Graphene-Cement Nanocomposites." *Journal of Nanomechanics and Micromechanics* 3(3): 67–77. http://ascelibrary.org/doi/abs/10.1061/(ASCE)NM.2153-5477.0000055 (June 6, 2014).

Al-Saleh, Mohammed H., Walaa H. Saadeh, and Uttandaraman Sundararaj. 2013. "EMI Shielding Effectiveness of Carbon Based Nanostructured Polymeric Materials: A Comparative Study." *Carbon* 60(2): 146–56. http://linkinghub.elsevier.com/retrieve/pii/S0008622313003011 (June 5, 2014).

Ameli, A., P.U. Jung, and C.B. Park. 2013. "Electrical Properties and Electromagnetic Interference Shielding Effectiveness of Polypropylene/carbon Fiber Composite Foams." *Carbon* 60: 379–91. http://linkinghub.elsevier.com/retrieve/pii/S0008622313003461 (June 5, 2014).

Andrews, Kurtis W., and David A. Savitz. 1999. "Accuracy of Industry and Occupation on Death Certificates of Electric Utility Workers: Implications for Epidemiologic Studies of Magnetic Fields and Cancer." *Bioelectromagnetics* 20(8): 512–18.

Andrzej, M. Brandt. 2009. *Cement-Based Composites- Materials, Mechanical Properties and Performance*. Second Edi. ed. Taylor and Francis.

Ardanuy, Mònica, Josep Claramunt, and Romildo Dias Toledo Filho. 2015. "Cellulosic Fiber Reinforced Cement-Based Composites: A Review of Recent Research." *Construction and Building Materials* 79: 115–28. http://linkinghub.elsevier.com/retrieve/pii/S0950061815000550 (January 29, 2015).

ASTM. 2004. "Annual Book of ASTM Standards Cement, Lime, Gypsum." *Standard specification for Portland cement, C150-04. ASTM International, USA*.

ASTM C 1018-02. 1998. "Standard Test Method for Flexural Toughness and First-Crack Strength of Fiber-Reinforced Concrete (Using Beam With." In , 1–8.

ASTM C 348-08. "Standard Test Method for Flexural Strength of Hydraulic-Cement Mortars 1."

Azhari, Faezeh, and Nemkumar Banthia. 2012. "Cement-Based Sensors with Carbon Fibers and Carbon Nanotubes for Piezoresistive Sensing." *Cement and Concrete Composites* 34(7): 866–73. http://linkinghub.elsevier.com/retrieve/pii/S0958946512000960 (May 31, 2014).

Bahr, Jeffrey L., and James M. Tour. 2002. "Covalent Chemistry of Single-Wall Carbon Nanotubes." *Journal of Materials Chemistry* 12(7): 1952–58. http://pubs.rsc.org/en/content/articlehtml/2002/jm/b201013p (March 29, 2015).

Bantsis, G. et al. 2012. "Comparison of Low Cost Shielding-Absorbing Cement Paste Building Materials in X-Band Frequency Range Using a Variety of Wastes." *Ceramics International* 38(5): 3683–92. http://linkinghub.elsevier.com/retrieve/pii/S0272884212000132 (May 15, 2014).

Baoyi, Li, Duan Yuping, Zhang Yuefang, and Liu Shunhua. 2011. "Electromagnetic Wave Absorption Properties of Cement-Based Composites Filled with Porous Materials." *Materials & Design* 32(5): 3017–20. http://linkinghub.elsevier.com/retrieve/pii/S0261306910007454 (May 15, 2014).

Basheerudeen, Abibasheer, and Anandan Sivakumar. 2014. "Particle Packing Approach for Designing the Mortar Phase of Self Compacting Concrete." *Engineering Journal* 18(2): 127–40.

Beall, C, E Delzell, P Cole, and I Brill. 1996. “Brain Tumors among Electronics Industry Workers.” *Epidemiology (Cambridge, Mass.)* 7(2): 125–30.

Bender, T J et al. 2007. “Cancer Incidence among Semiconductor and Electronic Storage Device Workers.” *Occupational and environmental medicine* 64(1): 30–36.

Bharj, Jyoti, Sarabjit Singh, Subhash Chander, and Rabinder Singh. 2014. “Experimental Study on Compressive Strength of Cement-CNT Composite Paste.” *Indian Journal of Pure & Applied Physics* 52(January): 35–38.

Bois, Karl J et al. 1998. “Cure-State Monitoring and Water-to-Cement Ratio Determination of Fresh Portland Cement-Based Materials Using Near-Field Microwave Techniques.” *INSTRUMENTATION AND MEASUREMENT, IEEE TRANSACTIONS* 47(3): 628–37.

Bortz, Daniel R., César Merino, and Ignacio Martin-Gullon. 2011. “Carbon Nanofibers Enhance the Fracture Toughness and Fatigue Performance of a Structural Epoxy System.” *Composites Science and Technology* 71(1): 31–38. http://linkinghub.elsevier.com/retrieve/pii/S0266353810003726 (May 31, 2014).

Brandt, A.M. 1995. *Cement-Based Composites: Materials, Mechanical Properties and Performance [Kindle Edition]*. Kindle. London: E & FN SPON. http://www.amazon.com/Cement-based-Composites-Mechanical-Properties-Performance-ebook/dp/B000Q365BY (December 8, 2014).

Buzzi-Unicem.SpA. 2014. “Buzzi Unicem.” *Buzzi Unicem Next; User Manual*.

Caneba, G T, C Dutta, V Agrawal, and M Rao. 2010. “Novel Ultrasonic Dispersion of Carbon Nanotubes.” 9(3): 165–81.

Cao, Jingyao, and D D L Chung. 2001. “Carbon Fiber Reinforced Cement Mortar Improved by Using Acrylic Dispersion as an Admixture.” *Cement and Concrete Research* 31: 1633–37.

———. 2003. “Coke Powder as an Admixture in Cement for Electromagnetic Interference Shielding.” *Carbon* 41: 2433–36.

Chafidz, Achmad, Mujtahid Kaavessina, Saeed Al-Zahrani, and Ilias Ali. 2014. “Multiwall Carbon Nanotubes Filled Polypropylene Nanocomposites: Rheological and Electrical Properties.” *Polymer Engineering & Science* 54(5): 1134–43. http://doi.wiley.com/10.1002/pen.23647 (July 26, 2014).

Chaipanich, Arnon, Thanongsak Nochaiya, Watcharapong Wongkeo, and Pincha Torkittikul. 2010. "Compressive Strength and Microstructure of Carbon Nanotubes–fly Ash Cement Composites." *Materials Science and Engineering: A* 527(4-5): 1063–67. http://linkinghub.elsevier.com/retrieve/pii/S0921509309010880 (May 30, 2014).

Chan, Lai Yin, and Bassem Andrawes. 2010. "Finite Element Analysis of Carbon Nanotube/cement Composite with Degraded Bond Strength." *Computational Materials Science* 47(4): 994–1004. http://linkinghub.elsevier.com/retrieve/pii/S0927025609004467 (March 29, 2015).

"Cheap Tubes, Multi Walled Carbon Nanotubes-MWNTs." *http://www.cheaptubes.com/MWNTs.htm#multi_walled_nanotubes-mwnts_prices [accessed on 24-06-14]*. http://www.cheaptubes.com/MWNTs.htm#multi_walled_nanotubes-mwnts_prices (June 21, 2014).

Chen, Bing, Keru Wu, and Wu Yao. 2004. "Conductivity of Carbon Fiber Reinforced Cement-Based Composites." *Cement and Concrete Composites* 26(4): 291–97. http://linkinghub.elsevier.com/retrieve/pii/S0958946502001385 (February 25, 2015).

Chen, Jun, and Chi-sun Poon. 2009. "Photocatalytic Construction and Building Materials: From Fundamentals to Applications." *Building and Environment* 44(9): 1899–1906. http://linkinghub.elsevier.com/retrieve/pii/S0360132309000134 (January 13, 2015).

Cho, Donghwan, Jin Myung Kim, In Seong Song, and Ikpyo Hong. 2011. "Effect of Alkali Pre-Treatment of Jute on the Formation of Jute-Based Carbon Fibers." *Materials Letters* 65(10): 1492–94. http://linkinghub.elsevier.com/retrieve/pii/S0167577X11001662 (November 14, 2014).

Chuah, Samuel et al. 2014. "Nano Reinforced Cement and Concrete Composites and New Perspective from Graphene Oxide." *Construction and Building Materials* 73: 113–24. http://linkinghub.elsevier.com/retrieve/pii/S0950061814010563 (December 11, 2014).

Chung, D.D.L. 2001. "Electromagnetic Interference Shielding Effectiveness of Carbon Materials." *Carbon* 39(2): 279–85. http://linkinghub.elsevier.com/retrieve/pii/S0008622300001846.

———. 2012. “Carbon Materials for Structural Self-Sensing, Electromagnetic Shielding and Thermal Interfacing.” *Carbon* 50(9): 3342–53. http://linkinghub.elsevier.com/retrieve/pii/S0008622312000620 (May 31, 2014).

Chyad, FA. 1989. “The Effects of Metastable Zirconia on the Properties of Ordinary Portland Cement.” University of Bradford, England.

Collins, Frank, John Lambert, and Wen Hui Duan. 2012a. “The Influences of Admixtures on the Dispersion, Workability, and Strength of Carbon nanotube–OPC Paste Mixtures.” *Cement and Concrete Composites* 34(2): 201–7. http://linkinghub.elsevier.com/retrieve/pii/S0958946511001703 (May 31, 2014).

———. 2012b. “The Influences of Admixtures on the Dispersion, Workability, and Strength of Carbon nanotube–OPC Paste Mixtures.” *Cement and Concrete Composites* 34(2): 201–7. http://linkinghub.elsevier.com/retrieve/pii/S0958946511001703 (November 9, 2014).

Dai, Bo et al. 2013. “Microstructure and Dielectric Properties of Biocarbon Nanofiber Composites.” *Nanoscale research letters* 8(1): 293. http://www.pubmedcentral.nih.gov/articlerender.fcgi?artid=3695796&tool=pmcentrez&rendertype=abstract (May 15, 2014).

Dai, Yawen, Mingqing Sun, Chenguo Liu, and Zhuoqiu Li. 2010. “Electromagnetic Wave Absorbing Characteristics of Carbon Black Cement-Based Composites.” *Cement and Concrete Composites* 32(7): 508–13. http://linkinghub.elsevier.com/retrieve/pii/S0958946510000582 (May 10, 2014).

Das, Chapal Kumar, Pallab Bhattacharya, and Swinderjeet Singh Kalra. 2012. “Graphene and MWCNT: Potential Candidate for Microwave Absorbing Materials.” *Journal of Materials Science Research* 1(2): 126–32. http://www.ccsenet.org/journal/index.php/jmsr/article/view/14725 (June 5, 2014).

Eswaraiah, Varrla, and Sundara Ramaprabhu. 2011. “Inorganic Nanotubes Reinforced Polyvinylidene Fluoride Composites as Low-Cost Electromagnetic Interference Shielding Materials.” *Nanoscale research letters* 6(1): 137. http://www.pubmedcentral.nih.gov/articlerender.fcgi?artid=3211184&tool=pmcentrez&rendertype=abstract (May 15, 2014).

Fan, Zhuangjun et al. 2006. "Electromagnetic and Microwave Absorbing Properties of Multi-Walled Carbon Nanotubes/polymer Composites." *Materials Science and Engineering: B* 132(1-2): 85–89. http://linkinghub.elsevier.com/retrieve/pii/S0921510706001176 (May 26, 2014).

Fang, Zhigang et al. 2007. "The Electromagnetic Characteristics of Carbon Foams." *Carbon* 45(15): 2873–79. http://linkinghub.elsevier.com/retrieve/pii/S0008622307005313 (May 26, 2014).

FAOSTAT-Food and Agriculture Organization. "Hazelnuts Area, Yield and Production." *http://faostat.fao.org/site/567/DesktopDefault.aspx?PageID=567#ancor [accessed on 06-06-14]*. http://faostat.fao.org/site/567/DesktopDefault.aspx?PageID=567#ancor (June 6, 2014).

Ferreira, Catarina I.A. et al. 2015. "Application of Pyrolysed Agricultural Biowastes as Adsorbents for Fish Anaesthetic (MS-222) Removal from Water." *Journal of Analytical and Applied Pyrolysis*: 1–12. http://linkinghub.elsevier.com/retrieve/pii/S0165237015000078 (March 2, 2015).

Ferro, G., J.M. Tulliani, P. Jagdale, and L. Restuccia. 2014. "New Concepts for Next Generation of High Performance Concretes." *Procedia Materials Science* 3: 1760–66. http://linkinghub.elsevier.com/retrieve/pii/S2211812814002855 (February 7, 2015).

Ferro, G., J.M. Tulliani, a. Lopez, and P. Jagdale. 2015. "New Cementitious Composite Building Material with Enhanced Toughness." *Theoretical and Applied Fracture Mechanics*. http://linkinghub.elsevier.com/retrieve/pii/S016784421420084X (February 8, 2015).

Ferro, Giuseppe, and Simone Musso. 2011. "Carbon Nanotubes Cement Composites." *Fracture And Structural Integrity* 1(1): 13–15.

Ferro, Giuseppe, Jean Marc Tulliani, Simone Musso, and Alberto Tagliaferro. 2008. "Cement-Carbon Nanotubes Based Composite." In *17th European Conference on Fracture 2008: Multilevel Approach to Fracture of Materials, Components and Structures*, , 1438–45.

Figarol, Agathe et al. 2014. "Biological Response to Purification and Acid Functionalization of Carbon Nanotubes." *Journal of Nanoparticle Research* 16(7): 2507.

Gao, Di, Mariel Sturm, and Y L Mo. 2009. "Electrical Resistance of Carbon-Nanofiber Concrete." *Smart Materials and Structures* 18(9). http://iopscience.iop.org/0964-1726/18/9/095039/pdf/0964-1726_18_9_095039.pdf (March 27, 2015).

Gay, Catherine, and Florence Sanchez. 2010. "Performance of Carbon Nanofiber-Cement Composites with a High-Range Water Reducer." *Journal of the Transportation Research Board* 2: 109–13. http://trb.metapress.com/content/97t0t421663417v5/?genre=article&id=doi%3a10.3141%2f2142-16 (March 29, 2015).

Gettu, Ravindra, P Balant, and Martha E Karr. 1990. "Fracture Properties and Brittleness of High-Strength Concrete." *ACI Materials Journal* (87): 608–18.

Giorcelli, M. et al. 2013. "Microwave Absorption Properties in Epoxy Resin Multi Walled Carbon Nanotubes Composites." *2013 International Conference on Electromagnetics in Advanced Applications (ICEAA)*: 1139–41. http://ieeexplore.ieee.org/lpdocs/epic03/wrapper.htm?arnumber=6632420.

Giudicianni, Paola, Giuseppe Cardone, and Raffaele Ragucci. 2013. "Cellulose, Hemicellulose and Lignin Slow Steam Pyrolysis: Thermal Decomposition of Biomass Components Mixtures." *Journal of Analytical and Applied Pyrolysis* 100: 213–22. http://linkinghub.elsevier.com/retrieve/pii/S0165237012002896 (October 21, 2014).

Gopalakrishnan, Kasthurirangan, Bjorn Birgisson, Peter Taylor, and Nii O. Attoh-Okine, eds. 2011. *Nanotechnology in Civil Infrastructure*. Berlin, Heidelberg: Springer Berlin Heidelberg. http://www.springerlink.com/index/10.1007/978-3-642-16657-0 (March 29, 2015).

Grimaldi, Claudio et al. 2013. "Electrical Conductivity of Multi-Walled Carbon Nanotubes-SU8 Epoxy Composites." *Applied Physics Letters* 102(22): 223114. http://scitation.aip.org/content/aip/journal/apl/102/22/10.1063/1.4809923 (June 23, 2014).

Grobert, Nicole. 2007. "Carbon Nanotubes - Becoming Clean." *Materialstoday* 10(1): 28–35.

Guan, Hongtao, Shunhua Liu, Yuping Duan, and Ji Cheng. 2006. "Cement Based Electromagnetic Shielding and Absorbing Building Materials." *Cement and Concrete Composites* 28(5): 468–74. http://linkinghub.elsevier.com/retrieve/pii/S0958946505001356 (May 10, 2014).

"Gum Arabic (9000-01-05), MSDS. Melting Point Boiling Point Density Storage Transport." *http://www.chemicalbook.com/ProductMSDSDetailCB1735918_EN.htm [accessed on 23-06-14]*. http://www.chemicalbook.com/ProductMSDSDetailCB1735918_EN.htm (June 23, 2014).

Habermehl-Cwirzen, K., V. Penttala, and a. Cwirzen. 2008. "Surface Decoration of Carbon Nanotubes and Mechanical Properties of Cement/carbon Nanotube Composites." *Advances in Cement Research* 20(2): 65–73. http://www.icevirtuallibrary.com/content/article/10.1680/adcr.2008.20.2.65 (June 1, 2014).

Han, Baoguo et al. 2012. "Fabrication of Piezoresistive CNT/CNF Cementitious Composites with Superplasticizer as Dispersant." *Journal of Materials in Civil Engineering* 24(6): 658–65. http://ascelibrary.org/doi/abs/10.1061/(ASCE)MT.1943-5533.0000435 (March 29, 2015).

———. 2015. "Review of Nanocarbon-Engineered Multifunctional Cementitious Composites." *Composites Part A: Applied Science and Manufacturing* 70: 69–81. http://linkinghub.elsevier.com/retrieve/pii/S1359835X14003856 (March 27, 2015).

Han, Young Hee, Seong Ok Han, Donghwan Cho, and Hyung-Il Kim. 2007. "Kenaf/polypropylene Biocomposites: Effects of Electron Beam Irradiation and Alkali Treatment on Kenaf Natural Fibers." *Composite Interfaces* 14(5-6): 559–78. http://www.tandfonline.com/doi/abs/10.1163/156855407781291272 (November 14, 2014).

Hewlett, Peter. 1998. *Lea's Chemistry of Cement and Concrete*. fourth edi. Elsevier, USA.

Hilding, Jenny, Eric A Grulke, Z George Zhang, and Fran Lockwood. 2003. "Dispersion of Carbon Nanotubes in Liquids." *journal of dispersion science and technology* 24(1): 1–41.

Huff, Matthew D, Sandeep Kumar, and James W Lee. 2014. "Comparative Analysis of Pinewood, Peanut Shell, and Bamboo Biomass Derived Biochars Produced via Hydrothermal Conversion and Pyrolysis." *Journal of environmental management* 146: 303–8. http://www.ncbi.nlm.nih.gov/pubmed/25190598 (March 5, 2015).

Hunashyal, Anand. 2014. "Experimental Investigation on the Effect of Multiwalled Carbon Nanotubes and Nano-SiO2 Addition on Mechanical Properties of Hardened Cement Paste." *Advances in Materials* 3(5): 45. http://www.sciencepublishinggroup.com/journal/paperinfo.aspx?journalid=129&doi=10.11648/j.am.20140305.13 (March 29, 2015).

Jo, Byung-Wan, Chang-Hyun Kim, Ghi-ho Tae, and Jong-Bin Park. 2007. "Characteristics of Cement Mortar with Nano-SiO2 Particles." *Construction and Building Materials* 21(6): 1351–55. http://linkinghub.elsevier.com/retrieve/pii/S095006180600136X (November 2, 2014).

Kerienė, Jadvyga et al. 2013. "The Influence of Multi-Walled Carbon Nanotubes Additive on Properties of Non-Autoclaved and Autoclaved Aerated Concretes." *Construction and Building Materials* 49: 527–35. http://linkinghub.elsevier.com/retrieve/pii/S0950061813007745 (March 29, 2015).

Kim, H.K., I.W. Nam, and H.K. Lee. 2014. "Enhanced Effect of Carbon Nanotube on Mechanical and Electrical Properties of Cement Composites by Incorporation of Silica Fume." *Composite Structures* 107: 60–69. http://linkinghub.elsevier.com/retrieve/pii/S0263822313003760 (May 31, 2014).

Kim, Jin Myung, In Seong Song, Donghwan Cho, and Ikpyo Hong. 2011. "Effect of Carbonization Temperature and Chemical Pre-Treat- Ment on the Thermal Change and Fiber Morphology of Kenaf- Based Carbon Fibers." *Carbon Letters* 12(3): 131–37.

Kok, Mustafa Versan, and Emre Özgür. 2013. "Thermal Analysis and Kinetics of Biomass Samples." *Fuel Processing Technology* 106: 739–43. http://linkinghub.elsevier.com/retrieve/pii/S0378382012003992 (November 16, 2014).

Kong, Luo et al. 2014. "Electromagnetic Wave Absorption Properties of Graphene Modified with Carbon Nanotube/poly(dimethyl Siloxane) Composites." *Carbon* 73: 185–93. http://linkinghub.elsevier.com/retrieve/pii/S000862231400195X (May 15, 2014).

Konsta-Gdoutos, Maria S., Zoi S. Metaxa, and Surendra P. Shah. 2010a. "Highly Dispersed Carbon Nanotube Reinforced Cement Based Materials." *Cement and Concrete Research* 40(7): 1052–59. http://linkinghub.elsevier.com/retrieve/pii/S0008884610000542 (May 30, 2014).

———. 2010b. "Highly Dispersed Carbon Nanotube Reinforced Cement Based Materials." *Cement and Concrete Research* 40(7): 1052–59. http://linkinghub.elsevier.com/retrieve/pii/S0008884610000542 (November 9, 2014).

———. 2010c. "Multi-Scale Mechanical and Fracture Characteristics and Early-Age Strain Capacity of High Performance Carbon Nanotube/cement Nanocomposites." *Cement and Concrete Composites* 32(2): 110–15. http://linkinghub.elsevier.com/retrieve/pii/S0958946509001632 (May 31, 2014).

Kuilla, Tapas et al. 2010. "Recent Advances in Graphene Based Polymer Composites." *Progress in Polymer Science* 35(11): 1350–75. http://linkinghub.elsevier.com/retrieve/pii/S0079670010000699 (July 11, 2014).

Kuzhir, Polina P et al. 2013. "Microwave Absorption Properties of Pyrolytic Carbon Nanofilm." *Nanoscale research letters* 8(1): 60. http://www.pubmedcentral.nih.gov/articlerender.fcgi?artid=3599098&tool=pmcentrez&rendertype=abstract.

Lee, Changgu, Xiaoding Wei, Jeffrey W Kysar, and James Hone. 2008. "Measurement of the Elastic Properties and Intrinsic Strength of Monolayer Graphene." *Science (New York, N.Y.)* 321(5887): 385–88. http://www.sciencemag.org/content/321/5887/385 (July 9, 2014).

Li, Geng Ying, Pei Ming Wang, and Xiaohua Zhao. 2005. "Mechanical Behavior and Microstructure of Cement Composites Incorporating Surface-Treated Multi-Walled Carbon Nanotubes." *Carbon* 43(6): 1239–45. http://linkinghub.elsevier.com/retrieve/pii/S0008622305000199 (May 31, 2014).

———. 2007. "Pressure-Sensitive Properties and Microstructure of Carbon Nanotube Reinforced Cement Composites." *Cement and Concrete Composites* 29(5): 377–82. http://linkinghub.elsevier.com/retrieve/pii/S095894650700008X (May 31, 2014).

Li, Jing, and Jang-Kyo Kim. 2007. "Percolation Threshold of Conducting Polymer Composites Containing 3D Randomly Distributed Graphite Nanoplatelets." *Composites Science and Technology* 67(10): 2114–20. http://linkinghub.elsevier.com/retrieve/pii/S0266353806004386 (January 4, 2015).

Li, M, J Lynch, and V.C Li. 2012. "Multifunctional Carbon Black Engineered Cementitious Composites for the Protection of Critical Infrastructure." In *High Performance Fiber Reinforced Cement Composites 6*, RILEM State of the Art Reports, eds. Gustavo J. Parra-Montesinos, Hans W. Reinhardt, and A. E. Naaman. Dordrecht: Springer Netherlands. http://www.springerlink.com/index/10.1007/978-94-007-2436-5 (March 28, 2015).

Li, M., V. Lin, J. Lynch, and V. C. Li. 2012. "Multifunctional Carbon Black Engineered Cementitious Composites for the Protection of Critical Infrastructure." *RILEM Bookseries* 2: 99–106.

Li, Yan-Huei, and Juh-Tzeng Lue. 2007. "Dielectric Constants of Single-Wall Carbon Nanotubes at Various Frequencies." *Journal of nanoscience and nanotechnology* 7(9): 3185–88. http://www.ncbi.nlm.nih.gov/pubmed/18019147 (June 6, 2014).

Liu, Qian et al. 2008. "Mechanism Study of Wood Lignin Pyrolysis by Using TG–FTIR Analysis." *Journal of Analytical and Applied Pyrolysis* 82(1): 170–77. http://linkinghub.elsevier.com/retrieve/pii/S0165237008000351 (October 14, 2014).

Liu, Qinglei et al. 2012. "High Permittivity and Microwave Absorption of Porous Graphitic Carbons Encapsulating Fe Nanoparticles." *Composites Science and Technology* 72(13): 1632–36. http://linkinghub.elsevier.com/retrieve/pii/S0266353812002576 (May 26, 2014).

Ludvig, P et al. 2009. "In-Situ Synthesis of Multiwall Carbon Nanotubes on Portland Cement Clinker." In *11th International Conference on Advanced Materials*, ICAM, 2009.

Luo, J. 2009. "Fabrication and Functional Properties of Multi-Walled Carbon Nanotube/cement Composites." Harbin Institute of Technology, Harbin, China.

Luo, Jianlin, Zhongdong Duan, and Hui Li. 2009. "The Influence of Surfactants on the Processing of Multi-Walled Carbon Nanotubes in Reinforced Cement Matrix Composites." *physica status solidi (a)*: NA–NA. http://doi.wiley.com/10.1002/pssa.200824310 (March 29, 2015).

Ma, Peng-Cheng, Naveed a. Siddiqui, Gad Marom, and Jang-Kyo Kim. 2010. "Dispersion and Functionalization of Carbon Nanotubes for Polymer-Based Nanocomposites: A Review." *Composites Part A: Applied Science and Manufacturing* 41(10): 1345–67. http://linkinghub.elsevier.com/retrieve/pii/S1359835X10002009 (July 11, 2014).

Maggio, Andrea. 2013. "Study Of Self-Monitoring Cement-Based Nanocomposite." Politecnico di Torino.

Mai, Y. W. 1979. "Strength and Fracture Properties of Asbestos-Cement Mortar Composites." *Journal of Materials Science* 14(9): 2091–2102. http://link.springer.com/10.1007/BF00688413 (March 27, 2015).

Makar, Jonathan M., and Gordon W. Chan. 2009. "Growth of Cement Hydration Products on Single-Walled Carbon Nanotubes." *Journal of the American Ceramic Society* 92(6): 1303–10. http://doi.wiley.com/10.1111/j.1551-2916.2009.03055.x (March 29, 2015).

Mapei. "Dynamon SP1 Superplasticizer Based on Acrylic Polymer." *Product manual, http://www.mapei.eu/public/COM/products/671_dynamon_sp1_gb.pdf [accessed on 23-06-14]* 1. http://www.mapei.eu/public/COM/products/671_dynamon_sp1_gb.pdf (June 23, 2014).

Metaxa, Zoi S. et al. 2012. "Highly Concentrated Carbon Nanotube Admixture for Nano-Fiber Reinforced Cementitious Materials." *Cement and Concrete Composites* 34(5): 612–17. http://linkinghub.elsevier.com/retrieve/pii/S0958946512000145 (May 31, 2014).

Mindess, Sidney, and J. Francis Young. 1981. *Concrete*. Prentice-Hall. http://books.google.com/books?id=_7tRAAAAMAAJ&pgis=1 (March 28, 2015).

Musso, Simone, Jean-Marc Tulliani, Giuseppe Ferro, and Alberto Tagliaferro. 2009. "Influence of Carbon Nanotubes Structure on the Mechanical Behavior of Cement Composites." *Composites Science and Technology* 69(11-12): 1985–90. http://linkinghub.elsevier.com/retrieve/pii/S0266353809001857 (May 31, 2014).

Naaman, Antoine E, and Hans Wolfgang Reinhardt. 2003. "Tailored Properties for Structural Performance." In *Fiber Reinforced Cement Composites (HPFRCC 4)*, RILEM Publications, 546. https://books.google.com/books?id=p5IMbceJOSsC&pgis=1 (March 26, 2015).

Nam, I.W., H.K. Kim, and H.K. Lee. 2012. "Influence of Silica Fume Additions on Electromagnetic Interference Shielding Effectiveness of Multi-Walled Carbon Nanotube/cement Composites." *Construction and Building Materials* 30: 480–87. http://linkinghub.elsevier.com/retrieve/pii/S0950061811006556 (May 15, 2014).

Nasibulin, Albert G. et al. 2013. "A Novel Approach to Composite Preparation by Direct Synthesis of Carbon Nanomaterial on Matrix or Filler Particles." *Acta Materialia* 61(6): 1862–71. http://linkinghub.elsevier.com/retrieve/pii/S1359645412008658 (March 29, 2015).

Nien, Yu-Hsun, and Chiao-li Huang. 2010. "The Mechanical Study of Acrylic Bone Cement Reinforced with Carbon Nanotube." *Materials Science and Engineering: B* 169(1-3): 134–37. http://linkinghub.elsevier.com/retrieve/pii/S0921510709004498 (May 31, 2014).

Nisamaneenate, Jurarat, Duangduen Atong, Panchaluck Sornkade, and Viboon Sricharoenchaikul. 2014. "Fuel Gas Production from Peanut Shell Waste Using a Modular Downdraft Gasifier with the Thermal Integrated Unit." *Renewable Energy*: 1–6. http://linkinghub.elsevier.com/retrieve/pii/S0960148114006119 (February 4, 2015).

Nochaiya, Thanongsak, and Arnon Chaipanich. 2011. "Behavior of Multi-Walled Carbon Nanotubes on the Porosity and Microstructure of Cement-Based Materials." *Applied Surface Science* 257(6): 1941–45. http://linkinghub.elsevier.com/retrieve/pii/S0169433210012626 (May 30, 2014).

Pan, Yongzheng, Tongfei Wu, Hongqian Bao, and Lin Li. 2011. "Green Fabrication of Chitosan Films Reinforced with Parallel Aligned Graphene Oxide." *Carbohydrate Polymers* 83(4): 1908–15. http://linkinghub.elsevier.com/retrieve/pii/S0144861710008672 (December 5, 2014).

Pandey, Ashok, Carlos R Soccol, Poonam Nigam, and Vanete T Soccol. 2000. "Biotechnological Potential of Agro-Industrial Residues . I : Sugarcane Bagasse." *Bioresource technology* 74.

Parant, Edouard, Rossi Pierre, and Fabrice Le Maou. 2007. "Durability of a Multiscale Fibre Reinforced Cement Composite in Aggressive Environment under Service Load." *Cement and Concrete Research* 37(7): 1106–14. http://linkinghub.elsevier.com/retrieve/pii/S0008884607000385 (March 26, 2015).

Park, Seung Bum, and Burtrand I Lee. 1993. "Mechanical Properties of Carbon-Fiber-Reinforced Polymer-Impregnated Cement Composites." *Cement and Concrete Composites* 15(3): 153–63.

Paul, Clayton R. 1992. *Introduction to Electromagnetic Compatibility*. http://books.google.it/books/about/Introduction_to_electromagnetic_compatib.html?hl=it&id=owRTAAAAMAAJ&pgis=1 (June 23, 2014).

Peled, Alva et al. 2008. "Influences of Textile Characteristics on the Tensile Properties of Warp Knitted Cement Based Composites." *Cement and Concrete Composites* 30(3): 174–83. http://linkinghub.elsevier.com/retrieve/pii/S0958946507001503 (March 10, 2015).

Peters, Sarah J., Todd S. Rushing, Eric N. Landis, and Toney K. Cummins. 2010. "Nanocellulose and Microcellulose Fibers for Concrete." *Transportation Research Record: Journal of the Transportation Research Board* 2142(-1): 25–28. http://trb.metapress.com/openurl.asp?genre=article&id=doi:10.3141/2142-04 (March 26, 2015).

Peyvandi, Amirpasha, Libya Ahmed Sbia, Parviz Soroushian, and Konstantin Sobolev. 2013. "Effect of the Cementitious Paste Density on the Performance Efficiency of Carbon Nanofiber in Concrete Nanocomposite." *Construction and Building Materials* 48: 265–69. http://linkinghub.elsevier.com/retrieve/pii/S0950061813006132 (May 31, 2014).

Peyvandi, Amirpasha, Parviz Soroushian, Nastran Abdol, and Anagi M. Balachandra. 2013. "Surface-Modified Graphite Nanomaterials for Improved Reinforcement Efficiency in Cementitious Paste." *Carbon* 63: 175–86. http://linkinghub.elsevier.com/retrieve/pii/S0008622313005903 (March 29, 2015).

Pretorius, Johann Christiaan, and B T Maharaj. 2013. "Improvement of Electromagnetic Wave (EMW) Shielding through Inclusion of Electrolytic Manganese Dioxide in Cement and Tile-Based Composites with Application for Indoor Wireless Communication Systems." *International Journal of Physical Sciences* 8(8): 295–301.

Promis, G., a. Gabor, G. Maddaluno, and P. Hamelin. 2010. "Behaviour of Beams Made in Textile Reinforced Mineral Matrix Composites, an Experimental Study." *Composite Structures* 92(10): 2565–72. http://linkinghub.elsevier.com/retrieve/pii/S0263822310000620 (March 27, 2015).

Pu, E, and A E Pu. 1999. "Pyrolysis of Hazelnut Shells in a Fixed-Bed Tubular Reactor : Yields and Structural Analysis of Bio-Oil." *Journal of Analytical and Applied Pyrolysis* 52: 33–49.

Pu, Nen-Wen et al. 2012. "Dispersion of Graphene in Aqueous Solutions with Different Types of Surfactants and the Production of Graphene Films by Spray or Drop Coating." *Journal of the Taiwan Institute of Chemical Engineers* 43(1): 140–46. http://linkinghub.elsevier.com/retrieve/pii/S187610701100085X (September 17, 2014).

Qian, Dong et al. 2002. "Mechanics of Carbon Nanotubes." *Applied Mechanics Reviews* 55(6): 495. http://appliedmechanicsreviews.asmedigitalcollection.asme.org/article.aspx?articleid=1397363 (July 21, 2014).

Rafiee, Mohammad A et al. 2009. "Enhanced Mechanical Properties of Nanocomposites at Low Graphene Content." *ACS nano* 3(12): 3884–90. http://pubs.acs.org/doi/pdf/10.1021/nn9010472 (December 1, 2014).

Ramachandran, V.S. 1996. *Concrete Admixtures Handbook, 2nd Ed.: Properties, Science and Technology*. Cambridge University Press. http://books.google.com/books?id=zy9l3-eQxA4C&pgis=1 (November 18, 2014).

Raza, Hassan. 2012. *Graphene Nanoelectronics - Metrology, Synthesis, Properties and Applications | Springer*. Springer. http://www.springer.com/gp/book/9783642204678 (March 26, 2015).

"Recycling Concrete." 2009. *World Business Council for Sustainable Development, The Cement Sustainability Initiative (CSI)*. www.wbcsdcement.org.

Rizwan, Syed Ali, and Thomas A Bier. 2012. "Blends of Limestone Powder and Fly-Ash Enhance the Response of Self-Compacting Mortars." *Construction and Building Materials* 27(1): 398–403. http://linkinghub.elsevier.com/retrieve/pii/S0950061811003849 (August 7, 2014).

Sáez de Ibarra, Y., J. J. Gaitero, E. Erkizia, and I. Campillo. 2006. "Atomic Force Microscopy and Nanoindentation of Cement Pastes with Nanotube Dispersions." *Physica Status Solidi (a)* 203(6): 1076–81. http://doi.wiley.com/10.1002/pssa.200566166 (November 18, 2014).

Sakthivel, S., Venkatesan V. Krishnan, and B. Pitchumani. 2008. "Influence of Suspension Stability on Wet Grinding for Production of Mineral Nanoparticles." *Particuology* 6(2): 120–24. http://linkinghub.elsevier.com/retrieve/pii/S1674200108000308 (November 14, 2014).

Sanchez, Florence, and Konstantin Sobolev. 2010. "Nanotechnology in Concrete – A Review." *Construction and Building Materials* 24(11): 2060–71. http://linkinghub.elsevier.com/retrieve/pii/S0950061810001625 (January 20, 2015).

Savi, Patrizia, Mario Miscuglio, Mauro Giorcelli, and Alberto Tagliaferro. 2014. "Analysis of Microwave Absorbing Properties of Epoxy MWCNT Composites." *Progress In Electromagnetics Research Letters* 44(October 2013): 63–69.

Shu, Xiang, Ryan K. Graham, Baoshan Huang, and Edwin G. Burdette. 2015. "Hybrid Effects of Carbon Fibers on Mechanical Properties of Portland Cement Mortar." *Materials & Design* 65: 1222–28. http://linkinghub.elsevier.com/retrieve/pii/S0261306914008024 (March 18, 2015).

Singh, Avanish Pratap et al. 2013. "Multiwalled Carbon Nanotube/cement Composites with Exceptional Electromagnetic Interference Shielding Properties." *Carbon* 56: 86–96. http://linkinghub.elsevier.com/retrieve/pii/S0008622312010482 (April 28, 2014).

Sixuan, Huang. 2012. "Multifunctional Graphite Nanoplatelets (Gnp) Reinforced Cementitious Composites." National University of Singapore.

Sobolkina, Anastasia et al. 2012. "Dispersion of Carbon Nanotubes and Its Influence on the Mechanical Properties of the Cement Matrix." *Cement and Concrete Composites* 34(10): 1104–13. http://linkinghub.elsevier.com/retrieve/pii/S095894651200162X (May 31, 2014).

Son, Seung Yong et al. 2008. "High-Quality Multiwalled Carbon Nanotubes from Catalytic Decomposition of Carboneous Materials in Gas−Solid Fluidized Beds." *Industrial & Engineering Chemistry Research* 47(7): 2166–75. http://dx.doi.org/10.1021/ie0711630 (March 8, 2015).

Syed Ali Rizwan. 2006. "High Performance Mortars and Concretes Using Secondary Raw Materials." Technischen Universitat Bergakademie Freiberg.

Thomas, T L et al. 1987. "Brain Tumor Mortality Risk among Men with Electrical and Electronics Jobs: A Case-Control Study." *Journal of the National Cancer Institute* 79(2): 233–38.

Toutanji, Houssam A, Tahar E-korchi, and R Nathan Katz. 1994. "Strength and Reliability of Carbon-Fiber-Reinforced Cement Composites." *Cement and Concrete Composites* 16(1): 15–21.

Tyson, Bryan M, Rashid K Abu Al-rub, Ardavan Yazdanbakhsh, and Zachary Grasley. 2011. "Carbon Nanotubes and Carbon Nanofibers for Enhancing the Mechanical Properties of Nanocomposite Cementitious Materials." *Journal of Material in Civil Engineering (ASCE)* (July): 1–8.

UNICA. 2014. *Sugarcane , Ethanol and Sugar Production - 2013 / 2014 Harvest Season Hydrous*. www.unica.com.br/unicadata.

USDA-Foreign Agriculture Service. "Peanuts Area, Yield and Production." *http://www.fas.usda.gov/psdonline/psdreport.aspx?hidReportRetrievalName=BVS&hidReportRetrievalID=918&hidReportRetrievalTemplateID=1#ancor, [accessed on 06-06-14]*. http://www.fas.usda.gov/psdonline/psdreport.aspx?hidReportRetrievalName=BVS&hidReportRetrievalID=918&hidReportRetrievalTemplateID=1#ancor (June 6, 2014).

Vaisman, Linda, H Daniel Wagner, and Gad Marom. 2006. "The Role of Surfactants in Dispersion of Carbon Nanotubes." *Advances in colloid and interface science* 128-130(2006): 37–46. http://www.ncbi.nlm.nih.gov/pubmed/17222381 (July 9, 2014).

Veedu, Vinod P. 2011. "Multifunctional Cementitious Nanocomposite Material and Methods of Making the Same." http://www.google.com/patents/US7875211 (March 29, 2015).

Viculis, Lisa M. et al. 2005. "Intercalation and Exfoliation Routes to Graphite Nanoplatelets." *Journal of Materials Chemistry* 15(9): 974. http://pubs.rsc.org/en/content/articlehtml/2005/jm/b413029d (December 9, 2014).

Wang, Baomin, Zhiqiang Guo, Yu Han, and Tingting Zhang. 2013. "Electromagnetic Wave Absorbing Properties of Multi-Walled Carbon Nanotube/cement Composites." *Construction and Building Materials* 46: 98–103. http://linkinghub.elsevier.com/retrieve/pii/S0950061813003140 (May 10, 2014).

Wang, Baomin, Yu Han, and Shuai Liu. 2013. "Effect of Highly Dispersed Carbon Nanotubes on the Flexural Toughness of Cement-Based Composites." *Construction and Building Materials* 46: 8–12. http://linkinghub.elsevier.com/retrieve/pii/S0950061813003310 (November 11, 2014).

Wang, Chuang et al. 2008. "Effect of Carbon Fiber Dispersion on the Mechanical Properties of Carbon Fiber-Reinforced Cement-Based Composites." *Materials Science and Engineering: A* 487(1-2): 52–57. http://linkinghub.elsevier.com/retrieve/pii/S0921509307016978 (March 27, 2015).

Wansom, S., N.J. Kidner, L.Y. Woo, and T.O. Mason. 2006. "AC-Impedance Response of Multi-Walled Carbon Nanotube/cement Composites." *Cement and Concrete Composites* 28(6): 509–19. http://linkinghub.elsevier.com/retrieve/pii/S0958946506000199 (May 31, 2014).

Wen, Sihai, and D D L Chung. 2000. "Uniaxial Tension in Carbon Fiber Reinforced Cement , Sensed by Electrical Resistivity Measurement in Longitudinal and Transverse Directions." *Cement and Concrete Research* 30: 1289–94.

———. 2001. "Effect of Carbon Fiber Grade on the Electrical Behavior of Carbon Fiber Reinforced Cement." *Carbon* 39: 369–73.

Wen, Sihai, and D.D.L. Chung. 2007a. "Double Percolation in the Electrical Conduction in Carbon Fiber Reinforced Cement-Based Materials." *Carbon* 45(2): 263–67. http://linkinghub.elsevier.com/retrieve/pii/S0008622306004970 (February 25, 2015).

———. 2007b. "Partial Replacement of Carbon Fiber by Carbon Black in Multifunctional Cement–matrix Composites." *Carbon* 45(3): 505–13. http://linkinghub.elsevier.com/retrieve/pii/S0008622306005483 (March 29, 2015).

Yakoveli, Grigorij, Jadvyga Keriene, Albinas Gailius, and Ingrida Girniene. 2006. "Cement Based Foam Concrete Reinforced by Carbon Nanotubes." *Materials Science* 12(2). http://wenku.baidu.com/view/d64f953b376baf1ffc4fad83.html (March 29, 2015).

Yang, Haiping et al. 2007. "Characteristics of Hemicellulose, Cellulose and Lignin Pyrolysis." *Fuel* 86(12-13): 1781–88. http://linkinghub.elsevier.com/retrieve/pii/S001623610600490X (July 10, 2014).

Yazdanbakhsh, Ardavan, Zachary Grasley, Bryan Tyson, and Rashid K. Abu Al-Rub. 2010. "Distribution of Carbon Nanofibers and Nanotubes in Cementitious Composites." *Transportation Research Record: Journal of the Transportation Research Board* 2142(-1): 89–95. http://trb.metapress.com/openurl.asp?genre=article&id=doi:10.3141/2142-13 (May 31, 2014).

Yu, Min-Feng, Bradley Files, Sivaram Arepalli, and Rodney Ruoff. 2000. "Tensile Loading of Ropes of Single Wall Carbon Nanotubes and Their Mechanical Properties." *Physical Review Letters* 84(24): 5552–55. http://link.aps.org/doi/10.1103/PhysRevLett.84.5552 (December 8, 2014).

Yu, W. et al. 2010. "Measurement of Mechanical Properties of Hydrated Cement Paste Using Resonant Ultrasound Spectroscopy." *American Society for Testing and Materials (ASTM)* 05. http://www.astm.org/digital_library/journals/jai/pages/jai102657.htm (December 9, 2014).

Zhang, Xiuzhi, and Wei Sun. 2010. "Microwave Absorbing Properties of Double-Layer Cementitious Composites Containing Mn–Zn Ferrite." *Cement and Concrete Composites* 32(9): 726–30. http://linkinghub.elsevier.com/retrieve/pii/S0958946510000995 (May 26, 2014).

Zhao, Naiqin et al. 2006. "Microwave Absorbing Properties of Activated Carbon-Fiber Felt Screens (vertical-Arranged Carbon Fibers)/epoxy Resin Composites." *Materials Science and Engineering: B* 127(2-3): 207–11. http://linkinghub.elsevier.com/retrieve/pii/S0921510705006872 (May 26, 2014).

List of PhD Publications

1. G. A. Ferro, S. Ahmad, **R. A. Khushnood**, L. Restuccia, J. M. Tulliani, "Improvements in self-consolidating cementitious composites by using micro carbonized aggregates," *Fracture and Structural Integrity*, vol. 30, pp. 75–83, Sep. 2014

2. **R. A. Khushnood**, S. A. Rizwan, S. A. Memon, J. M. Tulliani, G. A. Ferro, "Experimental investigation on use of wheat Straw ash and bentonite in self-compacting cementitious system," *Advances in Materials Science and Engineering*, vol. 1, pp. 1-11, 2014.

3. **R. A. Khushnood**, S. Ahmad, J. M. Tulliani, G. A. Ferro, "Improvement in electromagnetic interference shielding effectiveness of cement composites using carbonaceous nano/micro inerts", *Construction & Building Materials*, vol. 85, pp. 208-216, 2015.

4. S. Ahmad, **R. A. Khushnood**, P. Jagdale, J. M. Tulliani, G. A. Ferro, "High performance self-consolidating cementitious composites by using micro carbonized bamboo particles", *Materials & Design*, vol.76, pp. 223-229, 2015.

5. P. Jagadale, S. Ahmad, **R. A. Khushnood**, J. M. Tulliani, A. Tagliaferro, G. A. Ferro, "Bamboo based carbon material for improved mechanical properties of cement composite", *XXIII International Materials Research Congress (IMRC)*, 17-21 August-2014, Cancun, Mexico.

6. S. Musso, **R. A. Khushnood**, G. A. Ferro, M. Pavese, "Applications of carbon nanotube/cement self-sensing nano-composite for monitoring stress and strain down-hole", *Challenges in Nano-Science (ISACS 15)*, 17-20 August 2014, San Diego, USA.

7. S. Ahmad, **R. A. Khushnood**, P. Savi, M. Giorcelli, G. A. Ferro, A. Tagliaferro, "Effects of multiwalled carbon nanotubes on the complex permittivity of cement composites", *Proceeding of IET Brunei International Conference on Engineering and Technology (BICET)*, Institut Teknologi Brunei, Brunei Darussalam, November 1-3, 2014.

Appendix A Particle Size Distribution (PSD) Curves of Nano/Micro Carbonized Particles

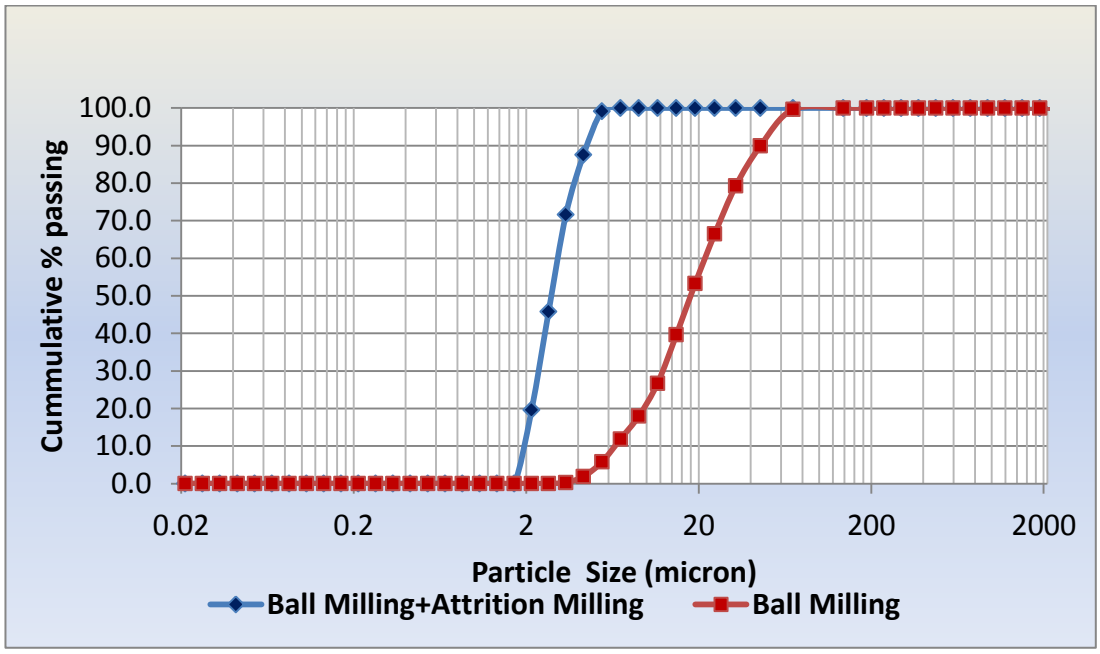

Figure A.1 PSD of CBF particles

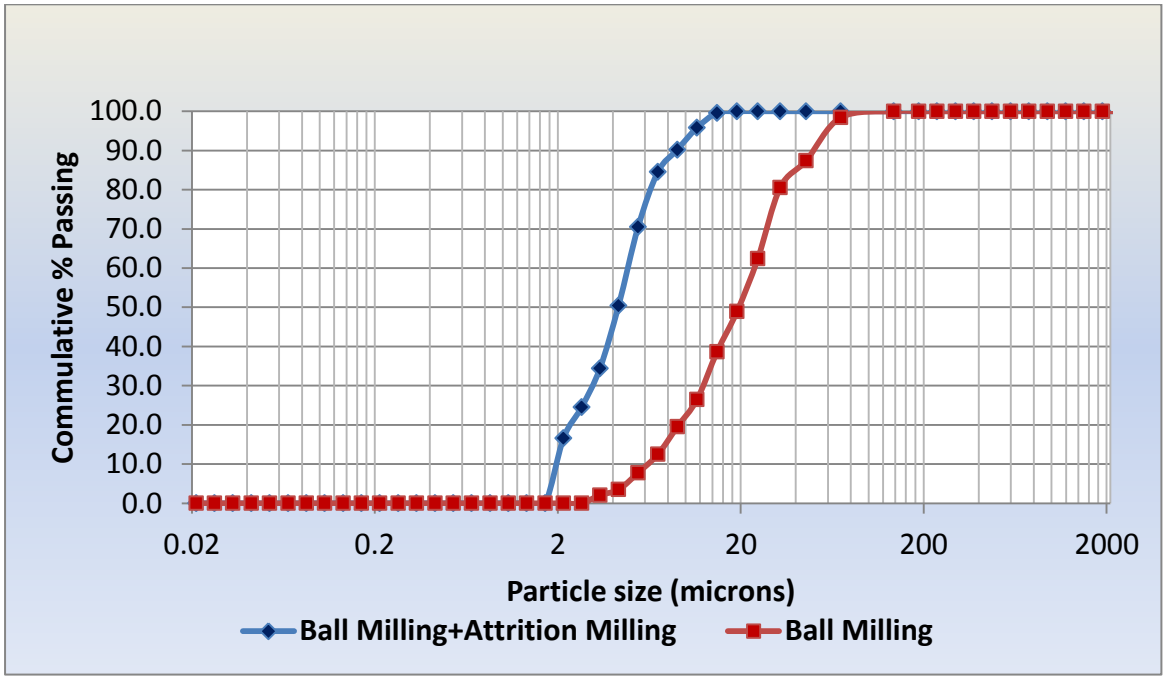

Figure A.2 PSD of CHS particles

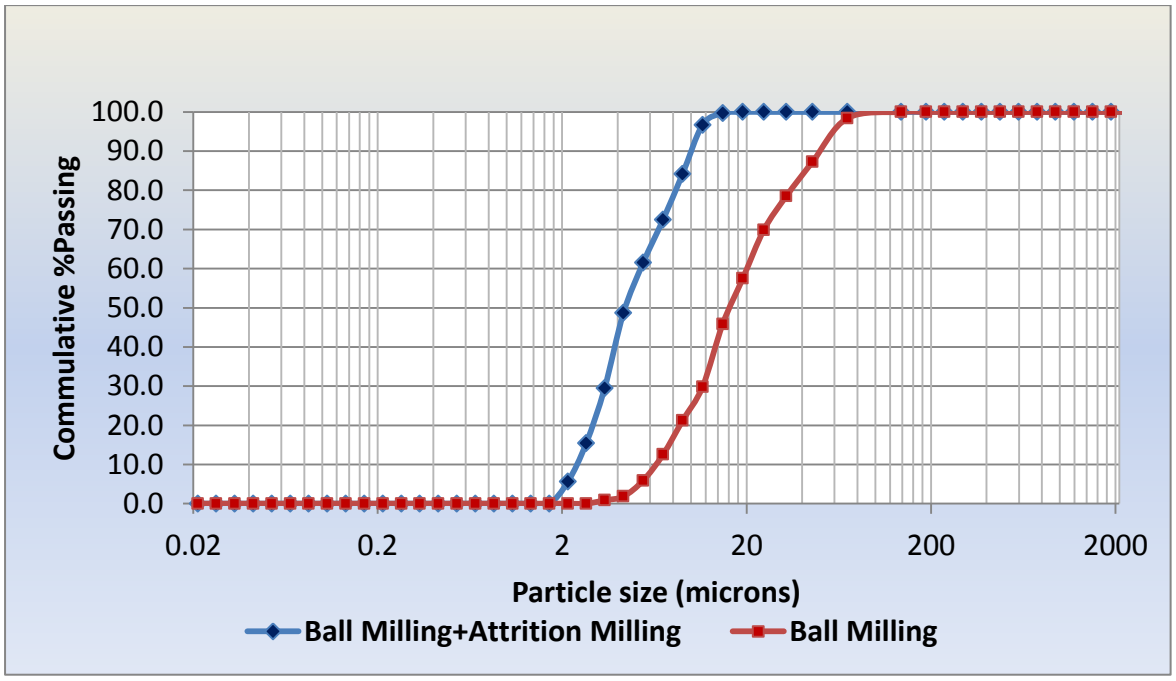

Figure A.3 PSD of CPS particles

Appendix B Energy Dispersive X-Ray (EDX) Spectroscopy of NMCPs

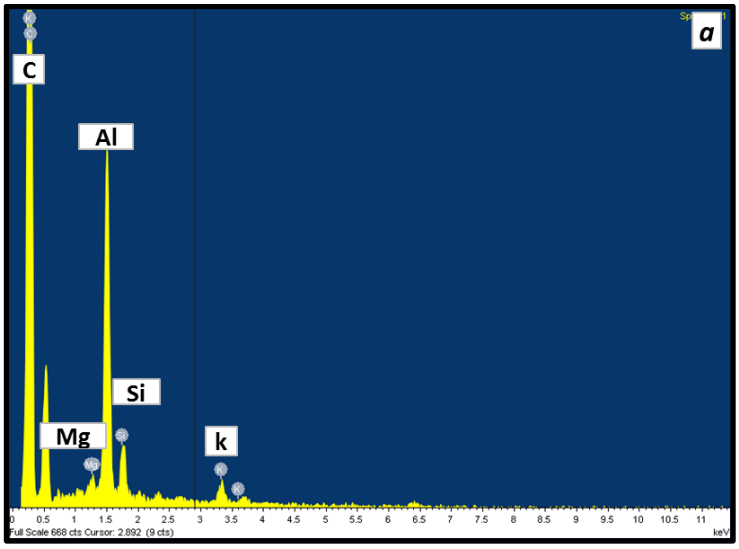

Figure B.1 EDX of CBF spectroscopy particles

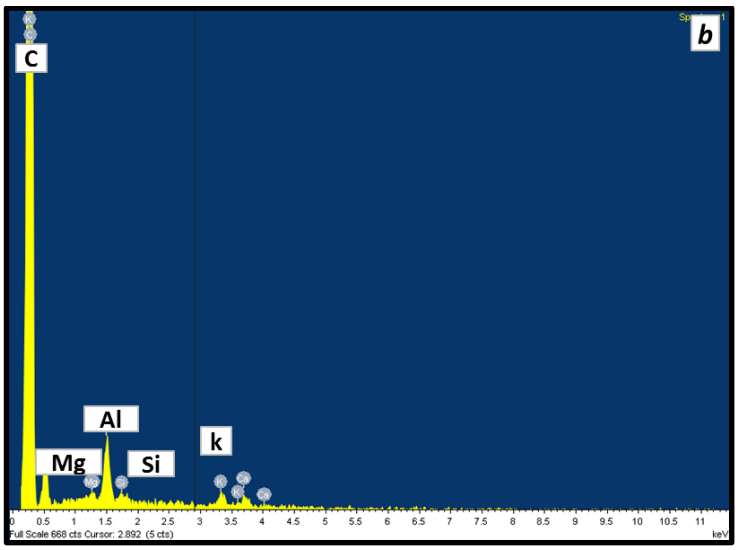

Figure B.2 EDX of CHS spectroscopy particles

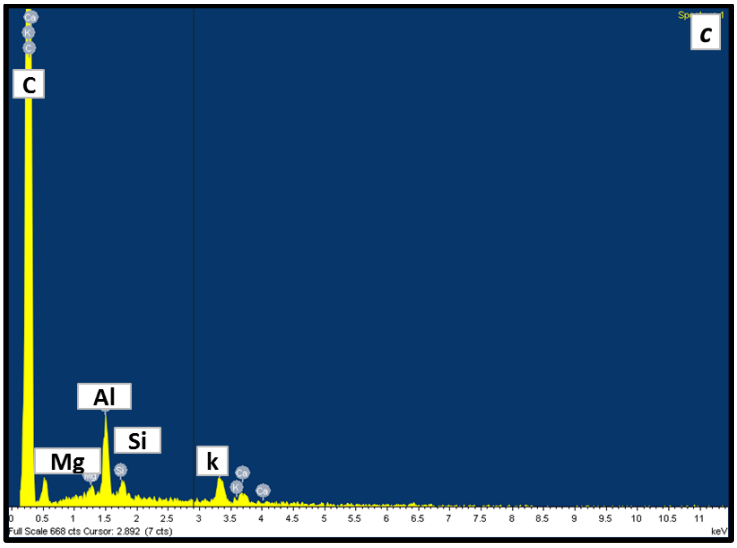

Figure B.3 EDX spectroscopy of CPS particles

Appendix C Mechanical Performance of Plain and Nano/Micro Reinforced HPCC

Table C.1 Mechanical strength of plain and GNP_3 reinforced HPCC

Sample name	Avg Compressive Strength (N*mm^-2)	Avg. Modulus of Rupture (N*mm^-2)	weight efficiency factor
CEM	49.91	2.70	0.00
0,025_GNPs_3	70.05	2.46	-361.24
0,05_GNPs_3	77.52	2.55	-111.89
0,08_GNPs_3	92.27	2.87	79.36
0,2_GNPs_3	94.37	3.33	116.64
0,5_GNPs_3	87.30	2.45	-18.77
1,0_GNPs_3	88.71	2.57	-4.76

Table C.2 Mechanical strength of plain and GNP_4 reinforced HPCC

Sample name	Avg Compressive Strength (N*mm^-2)	Avg. Modulus of Rupture (N*mm^-2)	weight efficiency factor
CEM	49.91	2.70	0.00
0,025_GNPs_4	71.38	2.78	125.34
0,05_GNPs_4	92.12	3.06	270.23
0,08_GNPs_4	105.51	3.50	369.26
0,2_GNPs_4	93.48	2.97	50.28
0,5_GNPs_4	85.28	2.75	3.46
1,0_GNPs_4	84.78	2.67	-1.06

Table C.3 Mechanical strength of plain and CBF reinforced HPCC

Sample name	Avg Compressive Strength (N*mm^-2)	Avg. Modulus of Rupture (N*mm^-2)
CEM	49.91	2.96
CBF_0,025	60.80	3.54
CBF_0,05	71.95	3.84
CBF_0.08	76.58	4.12
CBF_0.2	92.11	4.26
CBF_0.5	68.99	2.70
CBF_1.0	67.02	3.24

Table C.4 Mechanical strength of plain and CHS reinforced HPCC

Sample name	Avg Compressive Strength (N*mm^-2)	Avg. Modulus of Rupture (N*mm^-2)
CEM	49.91	2.96
CHS_0,025	74.94	3.44
CHS_0,05	98.73	3.91
CHS_0.08	108.86	5.33
CHS_0.2	101.65	5.44
CHS_0.5	90.18	5.19
CHS_1.0	85.25	4.21

Table C.5 Mechanical strength of plain and CPS reinforced HPCC

Sample name	Avg Compressive Strength (N*mm^-2)	Avg. Modulus of Rupture (N*mm^-2)	weight efficiency factor
CEM	49.91	2.96	0.00
CPS_0,025	93.63	3.15	265.94
CPS_0,05	92.92	3.88	623.02
CPS_0.08	103.62	4.30	569.73
CPS_0.2	119.48	5.43	417.45
CPS_0.5	99.35	3.61	44.26
CPS_1.0	98.15	2.77	-6.26

Table C.6 Fracture toughness of plain and GNP_3 reinforced HPCC

Sample name	Avg.First Crack Toughness *10^-3 (N.m)	Avg.Fracture Toughness *10^-3 (N.m)	T.I (I5)	T.I (I10)	T.I (I20)
CEM	1.27	2.79	2.16	2.26	2.26
0,025_GNPs_3	1.27	3.51	2.43	2.75	2.75
0,05_GNPs_3	1.45	4.92	3.05	3.39	3.39
0,08_GNPs_3	1.60	5.30	2.77	3.27	3.27
0,2_GNPs_3	1.64	6.00	2.69	3.45	3.64
0,5_GNPs_3	1.14	4.07	2.96	3.60	3.87
1,0_GNPs_3	1.14	3.15	2.69	2.76	2.76

Table C.7 Fracture toughness of plain and GNP_4 reinforced HPCC

Sample name	Avg.First Crack Toughness *10^-3 (N.m)	Avg.Fracture Toughness *10^-3 (N.m)	T.I (I5)	T.I (I10)	T.I (I20)
CEM	1.27	2.79	2.16	2.26	2.26
0,025_GNPs_4	1.36	3.27	2.38	2.67	2.67
0,05_GNPs_4	1.50	4.70	3.28	3.83	3.83
0,08_GNPs_4	1.71	5.17	2.71	3.13	3.24
0,2_GNPs_4	1.46	5.77	2.90	3.33	3.33
0,5_GNPs_4	1.24	4.82	2.86	3.50	3.57
1,0_GNPs_4	1.15	3.54	2.76	2.90	2.93

Table C.8 Fracture toughness of plain and CBF reinforced HPCC

Sample name	Avg.First Crack Toughness *10^-3 (N.m)	Avg.Fracture Toughness *10^-3 (N.m)	T.I (I5)	T.I (I10)	T.I (I20)
CEM	1.18	3.13	2.54	2.64	2.64
CBF_0,025	1.41	3.93	2.42	2.48	2.48
CBF_0,05	1.71	4.26	2.54	2.61	2.61
CBF_0.08	1.53	3.97	2.53	2.72	2.72
CBF_0.2	1.19	3.44	2.81	2.89	2.89
CBF_0.5	1.53	3.86	2.50	2.57	2.57
CBF_1.0	2.08	4.97	2.37	2.39	2.39

Table C.9 Fracture toughness of plain and CHS reinforced HPCC

Sample name	Avg.First Crack Toughness *10^-3 (N.m)	Avg.Fracture Toughness *10^-3 (N.m)	T.I (I5)	T.I (I10)	T.I (I20)
CEM	1.18	3.13	2.54	2.64	2.64
CHS_0,025	1.21	3.48	2.66	2.83	2.83
CHS_0,05	1.16	3.22	2.57	2.76	2.76
CHS_0.08	1.31	3.83	2.64	2.85	2.85
CHS_0.2	1.46	4.43	2.72	3.04	3.04
CHS_0.5	1.81	5.15	2.55	2.88	2.88
CHS_1.0	1.59	4.24	2.53	2.66	2.66

Table C.10 Fracture toughness of plain and CPS reinforced HPCC

Sample name	Avg.First Crack Toughness *10^-3 (N.m)	Avg.Fracture Toughness *10^-3 (N.m)	T.I (I5)	T.I (I10)	T.I (I20)
CEM	1.18	3.13	2.54	2.64	2.64
CPS_0,025	1.21	3.56	2.78	2.94	2.94
CPS_0,05	1.28	3.66	2.86	3.00	3.00
CPS_0.08	1.75	5.28	2.70	2.93	2.93
CPS_0.2	1.10	3.58	2.83	3.25	3.25
CPS_0.5	1.44	4.54	2.79	3.10	3.10
CPS_1.0	1.05	3.44	2.72	2.88	2.88

Appendix D Mechanical Performance of Plain and Nano/Micro Reinforced HPMC

Table D.1 Mechanical strength of plain and nano/micro reinforced HPMC

Sample name	Avg. Modulus of Rupture (N*mm^-2)	weight efficiency factor
CEM	5.61	0
GNPs_3	6.91	115.58
GNPs_4	6.86	278.16
CBF	6.13	46.44
CHS	6.55	83.52
CPS	6.30	61.25

Table D.2 Fracture properties of plain and nano/micro reinforced HPMC

Sample name	Avg.First Crack Toughness *10^-3 (N.m)	Avg.Fracture Toughness *10^-3 (N.m)	T.I (I5)	T.I (I10)	T.I (I20)
CEM	9.98	60.86	3.19	4.33	5.17
GNPs_3	12.11	72.62	3.41	4.85	6.08
GNPs_4	14.52	91.64	3.39	4.86	6.15
CBF	15.29	93.43	3.22	4.71	5.98
CHS	12.56	86.02	3.51	5.25	7.06
CPS	12.11	72.62	3.36	4.81	6.08